Mechanisms of Resistance to BCG Immunotherapy in Bladder Cancer

Mathieu Rouanne

université PARIS-SACLAY

NNT : 2019SACLS342

Thèse de doctorat

UNIVERSITÉ PARIS SUD
Comprendre le monde, construire l'avenir

Mechanisms of resistance to BCG immunotherapy in bladder cancer

Thèse de doctorat de l'Université Paris-Saclay
préparée à Gustave Roussy INSERM U1015

École doctorale n°582 Cancérologie : Biologie - Médecine - Santé
Spécialité de doctorat: Aspects moléculaires et cellulaires de la biologie

Thèse présentée et soutenue à Villejuif, le 23 octobre 2019, par

Mathieu Rouanne

Composition du Jury:

Jean-Charles Soria Professeur des Universités - Praticien Hospitalier Université Paris-Saclay	Président
Eric Tartour Professeur des Universités - Praticien Hospitalier Responsable d'Equipe, INSERM U970 Université Sorbonne Paris Cité, HEGP, Paris	Rapporteur
Christine Gilles Responsable d'Equipe, GIGA-Cancer Université de Liège, CHU Sart-Tilman, Liège	Rapporteur
Thierry Lebret Professeur des Universités - Praticien Hospitalier Université Paris-Saclay, Hôpital Foch, Suresnes	Examinateur
Hélène Salmon Responsable d'Equipe, INSERM U932 Institut Curie, Paris Icahn School of Medicine, Mount Sinai, New York	Examinateur
Aurélien Marabelle Praticien Spécialiste de CLCC Responsable d'Equipe, INSERM U1015 Université Paris-Saclay, Gustave Roussy, Villejuif	Directeur de thèse

Remerciements

Je remercie tout d'abord mon directeur de thèse, le Docteur Aurélien Marabelle, pour sa confiance, la liberté et l'autonomie accordées tout au long de ce projet. Merci du soin que tu prends à partager tes connaissances avec tous. Merci pour tes conseils sur le *deep work*, pour ton enthousiasme et ta façon de penser *out of the box*.

Je remercie particulièrement le Professeur Jean-Charles Soria pour son soutien constant depuis plus de 8 ans. Merci de porter cette vision sur la recherche translationnelle, interface singulière entre la clinique et la recherche, qui a été pour moi un fil conducteur depuis mon expérience au sein du Département d'Innovation Thérapeutique et Essais Précoces à Gustave Roussy. Merci de m'avoir encadré au début de ce projet et de m'avoir encouragé à sortir de ma *comfort zone*.

Merci vivement au Professeur Thierry Lebret, pour m'avoir permis d'effectuer ce projet de recherche dans des conditions très favorables, merci de votre soutien constant au sein de l'Hôpital et de la Fondation Foch, ainsi qu'au niveau de l'Association Française d'Urologie.

Je souhaite également remercier le Professeur Laurence Zitvogel, et le Docteur Jean-Paul Thierry, qui par leur exigence, leur rigueur scientifique et leurs conseils éclairés, m'ont amené à aller plus loin dans l'analyse de mes données.

Je remercie chaleureusement le Docteur Camélia Radulescu et le Docteur Julien Adam, sans qui ce travail n'aurait pu se concrétiser. Merci Camélia pour ton analyse uro-pathologique et ton enthousiasme, tu as été le lien indispensable entre Foch et Gustave Roussy. Merci Julien de m'avoir fait bénéficier de ton expérience étendue des biomarqueurs tissulaires en immuno-oncologie. J'ai particulièrement apprécié nos échanges amicaux tout au long de ce projet.

J'adresse également mes remerciements les plus chaleureux à Séverine Mouraud, ingénieure de recherche, et Delphine Bredel, technicienne de recherche. Votre accompagnement dans la réalisation des manips et dans l'analyse des données a été essentielle au début de ce projet. Grâce à vous, je peux enfin apprécier tous les apports et les limites de la cytométrie de flux.

Merci à Amélie Bigorgne et à Michaël Dussiot de m'avoir ouvert les portes de l'Institut Imagine, et de m'avoir permis d'utiliser cette technologie innovante *ImageStream*.

Merci à toute l'équipe du LRTI, Sandrine, François-Xavier, Lambros, Thomas et à nos collègues de l'U1015, Jean-Eudes, Anne-Gaëlle, Mélodie, Agathe,… pour les discussions et partages d'expérience autour de nos projets respectifs.

Enfin, je tiens particulièrement à remercier chacun des membres du Jury d'avoir accepté d'évaluer et d'enrichir ce travail de leur avis d'expert en immunologie des tumeurs et biologie du cancer. Je remercie les rapporteurs de cette thèse, le Professeur Eric Tartour, et le Docteur Christine Gilles, ainsi que le Docteur Hélène Salmon, pour avoir accepté d'examiner ce travail.

A Aurélie,

Merci de partager avec moi ton regard, lucide et plein de vie, sur le monde qui nous entoure.

Abstract

The origin of the bacillus Calmette-Guérin (BCG), trace back to the determined and perseverant work of Albert Calmette and Camille Guérin, who developed an attenuated form of live Mycobacterium Bovis after 13 years of culture and 231 passages. BCG is still today the only available vaccine against tuberculosis and one of the most successful cancer immunotherapy as a standard treatment for high-risk non muscle-invasive bladder cancers (NMIBC). High-risk NMIBC, which include carcinoma *in situ*, high-grade Ta and T1, are potentially lethal diseases that frequently relapse after standard BCG immunotherapy. Although BCG induces potent immune responses after intravesical instillations, mechanisms of tumor resistance remain elusive.

To address this, we developed an *ex vivo* BCG stimulation assay, using fresh human bladder tumors. We demonstrated that a subset of cancer cells acquire HLA-class I downregulation and mesenchymal properties following co-incubation with BCG. *In vitro* data confirmed that BCG intracellular infection induced immune evasion and epithelial-to-mesenchymal transition in a subset of cancer cells. *In situ* analyses in a clinical cohort of patients with BCG-resistant tumors support our preclinical finding. HLA-class I deficiency acquired by a subset of cancer cells after BCG immunotherapy, led to a myeloid suppressive microenvironment. HLA-I deficient tumors displayed intrinsic characteristics that promoted local invasion and metastatic disease. Taken together, these data emphasize that live attenuated BCG may directly induce immune evasion by infecting a subset of cancer cells and further promote tumor resistance and metastasis.

Table of contents

REMERCIEMENTS **1**

ABSTRACT **3**

TABLE OF CONTENTS **5**

CHAPTER I. GENERAL INTRODUCTION **7**

A brief history of BCG **7**

What differentiates BCG from Mycobacterium bovis **8**

Immune responses against Mycobacteria infection **9**

Balancing immunity and immune evasion 9

Toll-like receptors and pathogen recognition receptors. 10

Consequences of TLR signaling 12

The infected APC as a niche for immune evasion 13

IFNγ, a critical mediator of host defense against M. tuberculosis. 14

Type I IFN: foe and occasionally friend 16

Trained innate immunity: off-target effect of BCG? **18**

From a vaccine to a cancer immunotherapy **19**

Bladder cancers are immune-sensitive tumors **21**

Are there resident immune cells in the bladder mucosa? **23**

How does BCG immunotherapy work? **25**

BCG unresponsive tumors: what do we know so far? **26**

AIMS OF THIS PHD PROJECT **46**

CHAPTER II. RESULTS **47**

HLA-I downregulation together with epithelial-mesenchymal transition is a mechanism of tumor escape to intravesical BCG immunotherapy in non-muscle invasive bladder cancers. **47**

CHAPTER III. GENERAL DISCUSSION AND PERSPECTIVES **84**

CHAPTER IV. PUBLICATIONS RELATED TO MY PHD RESEARCH 90

Original articles 90

Contribution to other original articles 109

Review article 111

Letters to the Editor. 125

Poster presentations 130

Manuscripts in preparation 131

Translational research projects 132

Chapter I. General Introduction

A brief history of BCG

In December 2018 at the Pasteur Institute of Lille, an international scientific symposium celebrated the 110th anniversary of the first sub-culture of the « lait de Nocard », the Mycobacterium bovis strain that eventually led to the Bacillus Calmette - Guérin (BCG).

In 1908, Albert Calmette, a bacteriologist, and Camille Guérin, a veterinarian at the Pasteur Institute of Lille, started what would become a lifelong quest to develop a vaccine against Tuberculosis (TB) (Calmette, 1927). They cultured and serially passaged a Mycobacterium bovis (M. bovis) virulent strain highly related to the human pathogen Mycobacterium tuberculosis, isolated from cow's milk. Thirteen years and 231 passages later, the two researchers were able to show that the strain was protective in animal models and no longer caused disease(Norazmi Mohd Nor, Acosta and Sarmiento, no date). The virulence was lost and the M. bovis strain became what is today referred as Bacille de Calmette et Guérin (BCG). Indeed, when Calmette and Guérin grew the progenitor M. bovis strain on glycerinated potato slices, they unknowingly imposed selective pressure for genetic alterations to this natural mutant for glycerol metabolism, so that glycerol could be used as a carbon and energy source (Behr *et al.*, 1999; Fine *et al.*, 1999; Gordon *et al.*, 1999; Mostowy *et al.*, 2003; Belley *et al.*, 2004). Tested for the first time in humans in 1921, BCG is considered to be the world's most widely used vaccine and still today the only vaccine available against TB- although its ability to prevent active tuberculosis in studies has been inconsistent (Behr *et al.*, 2002) . Once safety had been confirmed, BCG was disseminated in different laboratories around the world. Daughter strains were maintained by passaging, until the introduction of archival seed lots in the 1960s. Since then, it has been recommended that vaccine preparations undergo no more than 12 passages from each seed lot.

What differentiates BCG from Mycobacterium bovis

Recently, the various daughter strains have been studied by comparative genomics and this uncovered regions of difference (RD) such as deletions and insertions, plus some SNPs. BCG vaccines were thus divided into the early strains, represented by BCGs Japan, Birkhaug, Sweden, and Russia and the late strains, including BCGs Pasteur, Danish, Glaxo, and Prague (Cole *et al.*, 2005) . The most obvious reason for the attenuation of BCG was the loss of the protein secretion system ESX-1, absent from all strains, due to deletion of RD1 (Mahairas *et al.*, 1996; Pym *et al.*, 2002; Hsu *et al.*, 2003; Lewis *et al.*, 2003; Stanley *et al.*, 2003; Guinn *et al.*, 2004) . Comparative genome and transcriptome analysis of M. bovis BCG Pasteur (passage 1173P2) identified 58 protein-coding genes present in two copies as a result of two independent tandem duplications, DU1 and DU2. DU1 is restricted to BCG Pasteur, although four forms of DU2 exist. All these genetic differences affect gene expression levels, immunogenicity, and, possibly, protection against TB, with early BCG vaccines (DU2 Group I) may even be superior to the later ones that are more widely used (Brosch *et al.*, 2007) .

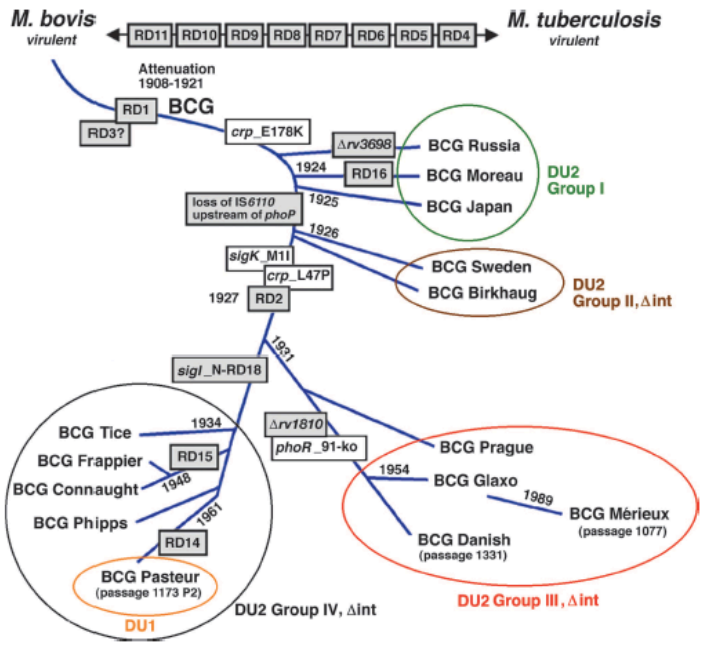

Fig. 1. Comparative genomics helped to define BCG phylogeny (from Brosch et al., PNAS 2007).

Immune responses against Mycobacteria infection

Understanding the immune responses against mycobacteria infection has been an important step during my PhD. I summarized below the key points that provided new insights to interpret my data and setb up my experiments.

Balancing immunity and immune evasion

Mycobacterium tuberculosis is an intracellular pathogen that infects antigen-presenting cells (APCs) in the lung, including lung macrophages and dendritic cells (DCs), and survives in phagosomes. Infected APCs migrate to regional lymphoid tissues, where adaptive immunity develops through antigen presentation to naive T cells. APCs process M. tuberculosis antigens by intravacuolar proteolysis to produce peptides that bind to major histocompatibility complex (MHC) class II molecules, which then translocate to the cell surface to mediate presentation of M. tuberculosis peptides to CD4+ T cells. M. tuberculosis peptides are also presented by MHC class I molecules to CD8+ T cells. Effector and memory T cells migrate back to sites of infection to control M. tuberculosis growth. Granulomas develop through the secretion of tumor necrosis factor and other effector cytokines (Harding et al., 2010).

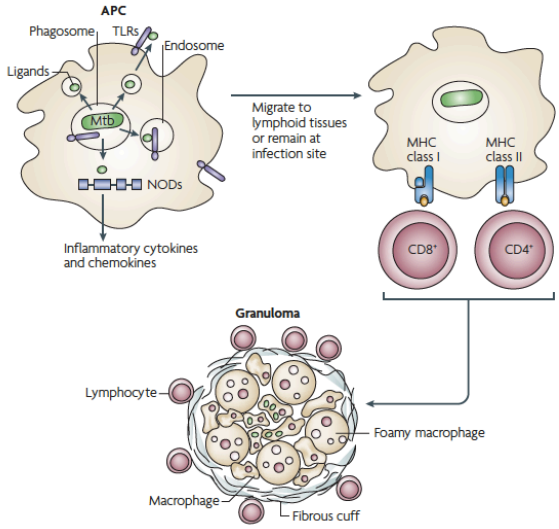

Fig. 2. Host immune response to M. tuberculosis infection (from Harding et al., Nat Rev Microbiol 2010).

However, multiple mechanisms contribute to the ability of M. tuberculosis to survive in the host. In APCs, M. tuberculosis survives in modified phagosomes and uses multiple mechanisms to evade both innate and adaptive host immunity, including inhibition of phagosome maturation, resistance to innate microbicidal mechanisms and cytokine-mediated host defenses, and, inhibition of antigen presentation.

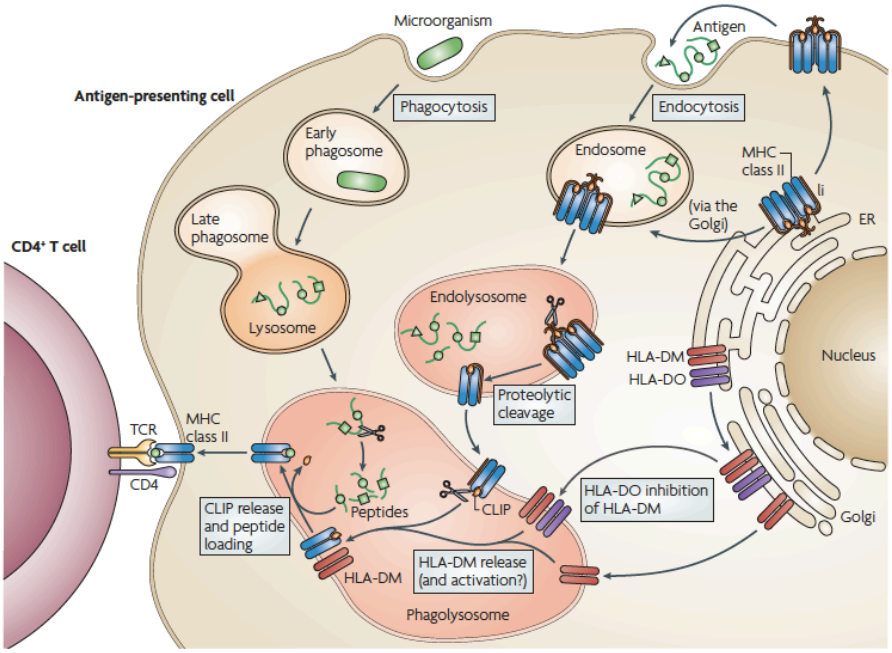

Fig. 3. Major histocompatibility complex (MHC) class II synthesis and functions. (CLIP class II associated Ii peptide; ER endoplasmic reticulum) *(from Harding et al., Nat Rev Microbiol 2010).*

Toll-like receptors and pathogen recognition receptors.

M. tuberculosis cell wall is rich in molecules with adjuvant activity that readily induce immune responses in animal models and in humans. M. tuberculosis ligands, including lipoproteins and glycolipids, are recognized in APCs by Toll-like receptors (TLRs) and nucleotide-binding oligomerization domain (NOD) proteins, resulting in the secretion of pro-inflammatory cytokines and chemokines (Krutzik and Modlin, 2004; Ferwerda *et al.*, 2005; Coulombe *et al.*, 2009). TLRs are a family of receptors that detect a wide range of microbial

molecules known as pathogen-associated molecular patterns (PAMPs) to activate innate immunity and enhance adaptive immunity. Among the TLRs, TLR2, TLR9 and, possibly, TLR4 are responsible for recognizing M. tuberculosis and are therefore largely responsible for the unique adjuvant activity of M. tuberculosis. Although macrophages and dendritic cells (DCs) both secrete cytokines and produce antimicrobials (such as reactive oxygen species (ROS) and reactive oxygen intermediates (ROI) in response to Toll-like receptor (TLR) signaling, these cell types differ in how their major histocompatibility complex (MHC) class II antigen presentation function is regulated by TLR signaling. DCs present antigen in lymph nodes to activate naive T cells, whereas macrophages present antigens to effector T cells at sites of infection, which produces inflammatory responses that can damage host tissues if they are not controlled.

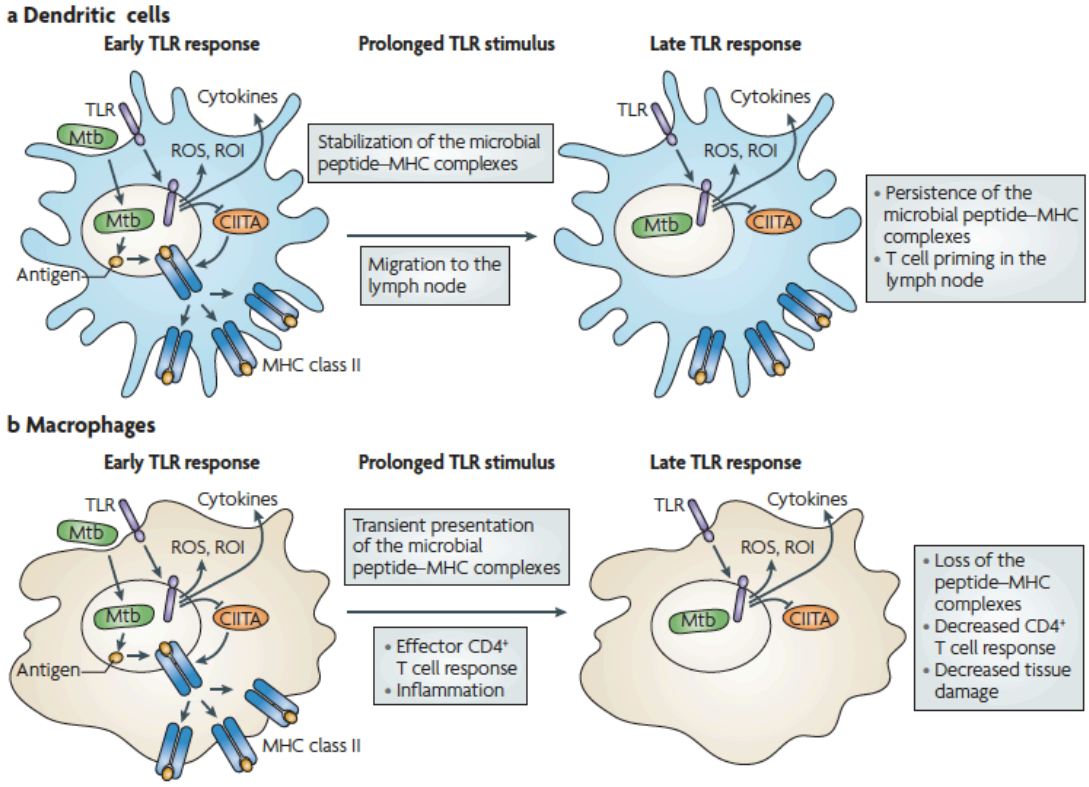

Fig. 4 The different responses of macrophages and dendritic cells to Toll-like receptor signaling. CIITA, MHC class II transactivator; Mtb, Mycobacterium tuberculosis (from Harding et al., Nat Rev Microbiol 2010).

This model proposes that macrophages decrease antigen presentation after prolonged TLR stimulation as a means of homeostatic negative-feedback regulation to limit tissue damage from excessive activation of effector T cells.

Consequences of TLR signaling

In macrophages, major histocompatibility complex (MHC) class II expression is induced by interferon-γ (IFNγ), which signals through its receptor to activate Janus kinase–signal transducer and activator of transcription (JAK–STAT) signaling, resulting in STAT1α phosphorylation and dimerization. STAT1α dimers translocate into the nucleus and bind to interferon-γ-activated sequence (GAS) sites in promoters, resulting in the induction of genes, including the gene encoding MHC class II transactivator (CIITA). CIITA assembles with other transcription factors to bind to the promoters of MHC class II genes and other genes related to antigen processing (for example, the human leukocyte antigen gene HLA-DM), driving their expression. The resulting MHC class II molecules participate in antigen processing and presentation. Most studies suggest that Mycobacterium tuberculosis infection and Toll-like receptor (TLR) signaling do not interfere with the proximal steps of IFNγ signaling that lead to activation of STAT1α. M. tuberculosis inhibits the induction of a subset of IFNγ-induced molecules, including molecules that contribute to antigen presentation, providing a mechanism for evasion of immune surveillance (Pai *et al.*, 2004). TLR signaling occurs through the adaptor molecule myeloid differentiation primary response protein 88 (MYD88) and downstream signaling pathways that result in the activation of nuclear factor-κB (NF-κB) and mitogen-activated protein kinases (MAPKs) and the induction of expression of many genes. CCAATT/ enhancer-binding protein-β (C/EBPβ) and C/EBPδ are induced by TLR2 signaling and bind to CIITA (MHC class II trans activator) promoters, contributing to the

inhibition of CIITA, which results in decreased MHC class II molecule expression and inhibition of antigen presentation (Pennini *et al.*, 2007).

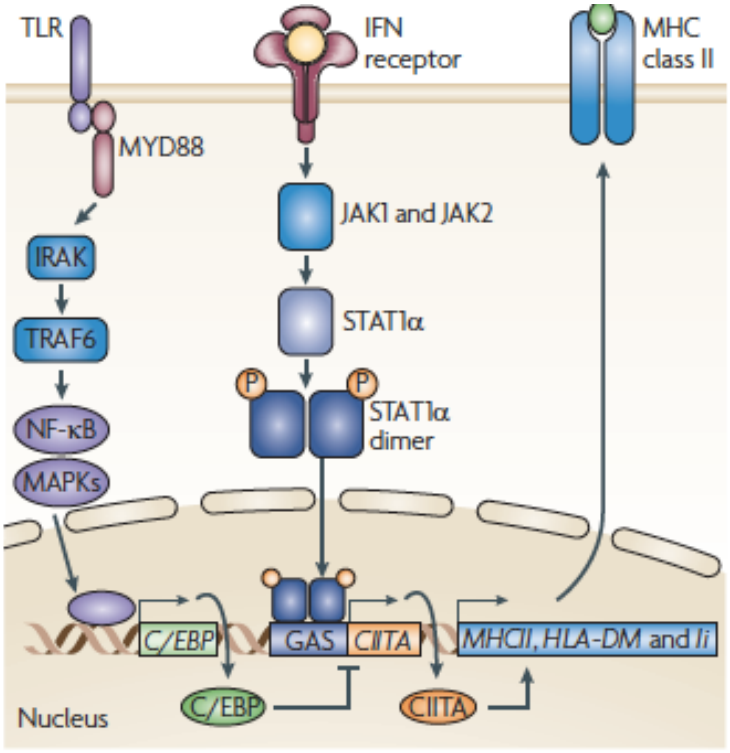

Fig. 5. Inhibition of major histocompatibility complex class II by Mycobacterium tuberculosis through Toll-like receptor signalling. Ii, invariant chain; IRAK, interleukin-1 receptor-associated kinase; TRAF6, tumour necrosis factor receptor-associated factor 6. (from Harding et al., Nat Rev Microbiol 2010).

The infected APC as a niche for immune evasion

Despite the proposal that TLR stimulation increases DC antigen presentation, mycobacterial infection might interfere with MHC class II antigen processing and the presentation of M. tuberculosis antigens by DCs. Some in vitro studies indicate that infection of DCs with M. bovis BCG ultimately leads to loss of MHC class II molecules on DCs, as observed in macrophages, making DCs another possible niche for immune evasion by mycobacteria(Jiao *et al.*, 2002). The ability of M. tuberculosis to inhibit MHC class II antigen presentation through prolonged stimulation of TLR2, thereby directly inhibiting its recognition by CD4+ T

cells, is an additional means of immune evasion. This mechanism takes advantage of a natural regulatory mechanism of macrophages to decrease MHC class II molecule expression and antigen presentation in order to down-modulate the excessive inflammation that would be induced by prolonged stimulation of the innate immune system.

This mechanism could be especially relevant during the chronic phase of infection, when few organisms are present and immune surveillance is focused on macrophages. In this way, M. tuberculosis is able to turn a liability (namely, a cell wall that is rich in TLR agonists) into a survival mechanism that relies on inhibition of macrophage-mediated presentation of M. tuberculosis antigens and induction of effector T cell responses.

IFNγ, a critical mediator of host defense against M. tuberculosis.

The interactions between M. tuberculosis and innate and adaptive immune cells result in the secretion of chemokines and cytokines, of which IFNγ and tumor necrosis factor (TNF) are particularly important in TB. IFNγ has a key role in humans, as defects in the genes encoding IFNγ or the IFNγ receptor predispose the host to serious mycobacterial infections (Ottenhoff, Kumararatne and Casanova, 1998). Among its many effects, IFNγ has an important role in activating macrophages and enhancing their expression of MHC class II molecules, resulting in enhanced antigen presentation to T cells (as presented above). IFN-γ activates macrophage to produce TNF-α and other protective cytokines, promoting intracellular killing of the pathogen through the production of reactive oxygen and nitrogen species (Flynn *et al.*, 2001; North *et al.,* 2004; Cooper, 2009; O'Garra *et al.*, 2013). IFNγ also induces molecules that contribute to innate antimicrobial mechanisms such as inducible nitric oxide synthase (NOS2) (Cooper et al., 1993; Dalton et al., 1993; Flynn et al., 1993; Kaufmann, 2010).

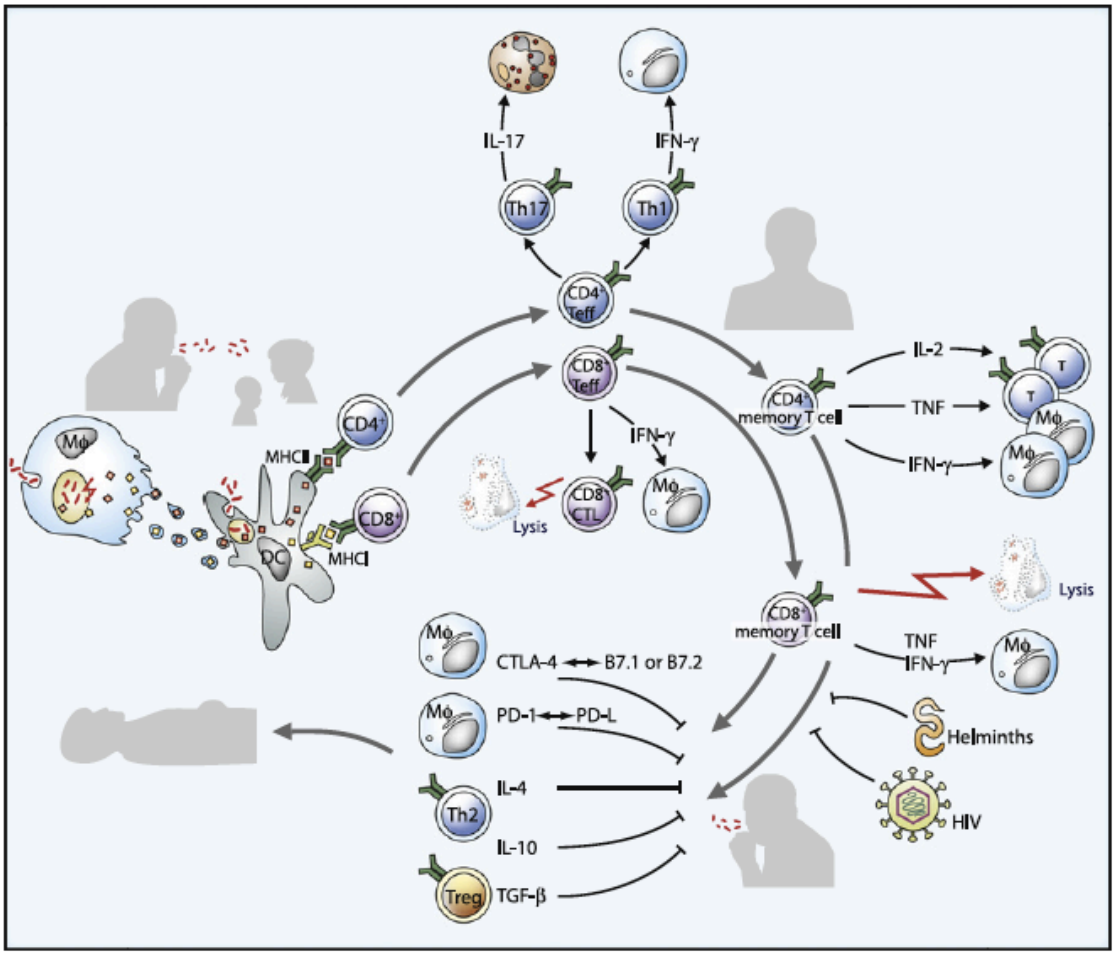

Fig. 6. The pathologic and cellular basis of the host immune response in TB (from Kaufman et al. Immunity 2010).

Antigen-specific CD4 + T cells have long been regarded as the main producer of IFNγ in TB and CD4+ T cell immunity is the main target of current TB vaccine candidates (Kupz *et al.*, 2016). However, unconventional T cells, γδ T cells, mucosal-associated invariant T (MAIT) cells, invariant NK T (iNKT) cells, and CD1-restricted T cells, also participate in a protective immune response against M. tuberculosis, and have a broad range of effector functions including cytotoxicity activity and IFNγ secretion (Kaufmann *et al.*, 2015). More recently, noncognate source of IFN-γ production by M. tuberculosis antigen–independent memory CD8+ T cells and NK cells (IL18 dependant) have been related to protective immunity during M. tuberculosis infection in a mice model (Kupz *et al.*, 2016). Indeed, we do not exactly know

which types of T cells are needed for containment of M. tuberculosis: Teff, because ‘‘trench warfare’’ takes place, or memory T cells, because long-term immunity is required. Among Teff, do we need CD4+ Th1 cells, CD4+ Th17 cells, CD8+ CTL, or all of them, with additional help from unconventional CD1-restricted T cells and γδ T cells? Among memory T cells, do we need Tem cells, which are active at the site of M. tuberculosis containment, i.e., solid granulomas in the lung, or Tcm cells, residing in draining lymph nodes that constantly generate Teff cell progeny (Brigl *et al.*, 2004; Scotet *et al.*, 2008; Cooper, 2009; O’Shea *et al.*, 2010)?

Type I IFN: foe and occasionally friend

In contrast to the now well-established protective function of IFNγ, the pathogenic role of type I IFN in tuberculosis has only recently been appreciated. Blood transcriptomic profiling has provided an unbiased analysis and comprehensive overview of the host factors that are perturbed after infection and during active TB in humans. Patients with active tuberculosis have a blood transcriptional gene signature dominated by type I IFN–related genes that is correlated with disease severity and is down-regulated following successful treatment (Singhania *et al.*, 2018). Overexpression of IFN response genes, including STAT1, IFITs, GBPs, MX1, OAS1, IRF1, and other genes, were also detected early in tuberculosis contacts who progressed to active disease (Zak *et al.*, 2016; Scriba *et al.*, 2017; Esmail *et al.*, 2018), suggesting that peripheral activation of the type I IFN response precedes the onset of active disease and clinical manifestations of tuberculosis. Studies performed in patients and mouse models of infection collectively point to a harmful role of high and sustained type I IFN in tuberculosis.

However, the mechanisms by which type I IFN signaling exacerbates M. tuberculosis infection are not yet fully understood (Mayer-Barber and Sher, 2015; McNab *et al.*, 2015;

Donovan *et al.*, 2017; Sabir *et al.*, 2017). Several mechanisms underlying the pathogenic role of type I IFN in tuberculosis have been described, including induction of IL-10 and negative regulation of the IL-12/IFN-γ and IL-1β/PGE2 host-protective responses. However, there is also evidence that type I IFN may play a friendly role in certain contexts, highlighting the complex role of type I IFN in tuberculosis (Fig. 7 & 8).

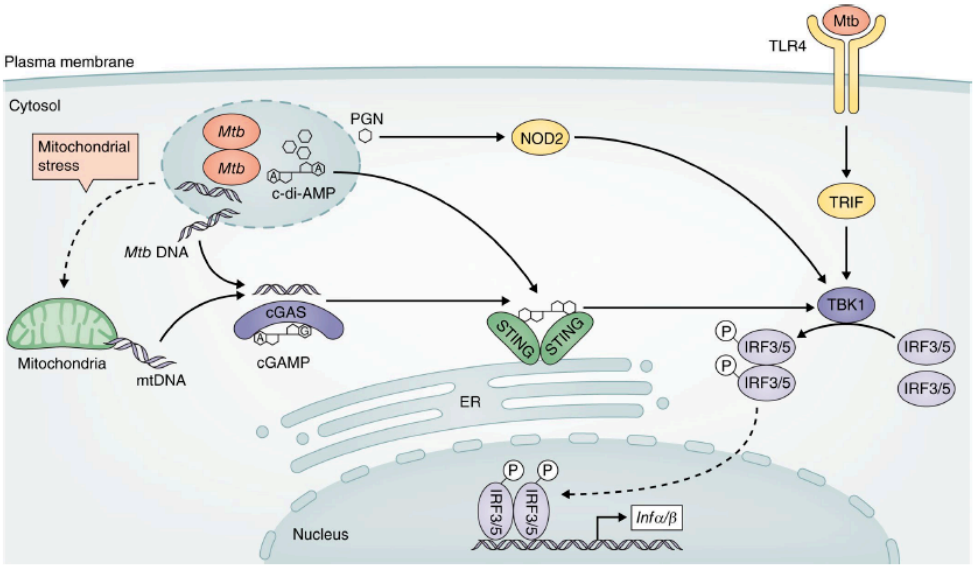

Fig. 7. Alternative pathways of type I IFN induction during M. tuberculosis infection *(from Moreira-Teixeira et al., J Exp Med 2018).*

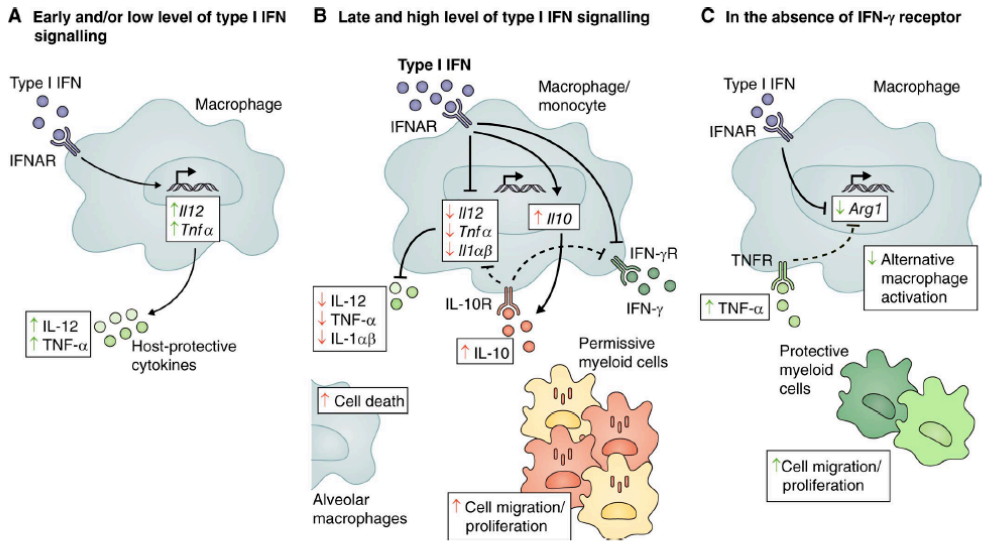

Fig. 8. Foe- and friendly-like effects of type I IFN during M. tuberculosis infection (from Moreira-Teixeira et al., J Exp Med 2018)

Trained innate immunity: off-target effect of BCG?

There is no doubt that BCG vaccine is immunogenic as clear-cut T-cell immune responses are induced by BCG vaccination in humans. However, the direct evidence of protective T cells in current human vaccines is minimal (Divangahi *et al.*, 2018). This affirmation is consistent with the clinical observation that in BCG trials there was no correlation between the proportion of subjects who converted their TST and subsequent protection against TB (Comstock *et al.*, 1996; Mittrücker *et al.*, 2007; Kagina *et al.*, 2010). The concept of innate immune memory, also termed trained innate immunity, has been developed in plants and invertebrates (who lack T and B cells) and more recently in humans. Innate immune cells, like monocytes/macrophages, may develop a fast and robust immune response on secondary infection by the same organism or even an unrelated pathogen(Netea *et al.*, 2016). Impressively, this immune memory can be transmitted to the next generation. This innate immune memory is considered independent of adaptive immunity and mainly driven epigenetically at the level of histone and chromatin modifications that influence gene expression (Tribouley, Tribouley-Duret *et al.*, 1978; Kleinnijenhuis *et al.*, 2012; Saeed *et al.*, 2014). The concept of trained immunity in vertebrates is supported by BCG immunization of T-cell–deficient mice (e.g., athymic or nude mice) that led to protection against secondary infection with Candida albicans or Schistosoma mansoni, with this protection dependent on macrophages (Tribouley *et al.*, 1978; Bistoni *et al.*, 1986; van 't Wout, Poell *et al.*, 1992).

Very recently, Kaufmann and colleagues have also shown that BCG reprogramming of hematopoietic stem cells (HSCs) in murine model of TB generates enhanced protection via trained monocytes/macrophages (Kaufmann *et al.*, 2018). This study and others support the paradigm of BCG-induced HSC-mediated protection and push scientists beyond the dogma of M. tuberculosis antigen–specific T-cell–mediated immunity in TB vaccines. Trained immunity is a de facto immune memory of the innate immune system and involves the

epigenetic programming of myeloid lineage cells, which results in changes in their metabolic and phenotypical behaviour that enable a stronger immune response to secondary stimuli. Importantly, the heterologous effects of BCG vaccination also served as the basis for the discovery of 'trained immunity'. Interestingly, Buffen and colleagues identified trained immunity to be the therapeutic mechanism by which BCG exerts its protective effects in bladder cancer (Buffen *et al.*, 2014).

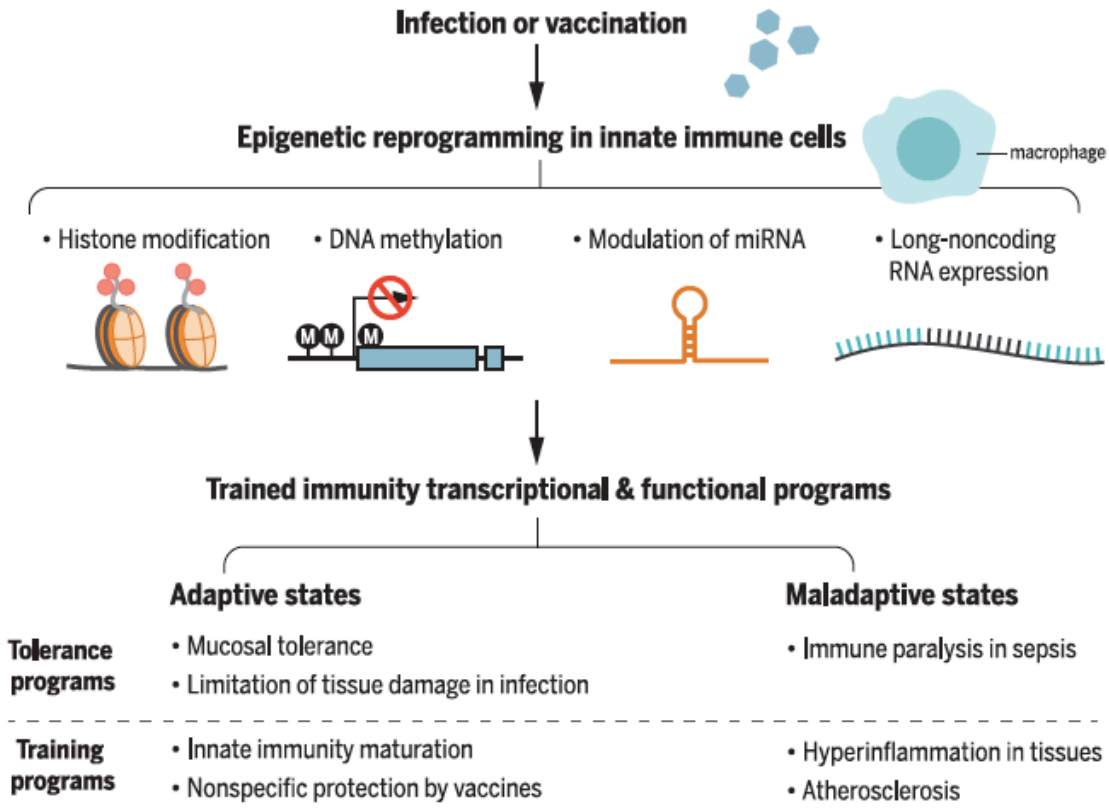

Fig. 9. Trained innate immunity concept (Netea et al., Science 2016).

From a vaccine to a cancer immunotherapy

The origins of cancer immunotherapy trace back to the pioneering work of William Coley, a bone surgeon at New York Cancer Hospital in the late 19th century. He observed tumor clearance in some patients that received intra tumor injections of streptococcal bacteria (Coley, 1891)_a result that has now been attributed to the recruitment and activation of the immune system (Berendt, *et al.*1978; Tsung *et al.* 2006; Mellman, *et al.* 2011). Although

Coley successfully treated several patients, his work was met with a lot of criticism and scepticism because of the unpredictability of the approach. Coley's immunotherapeutic method quickly fell out of fashion after the introduction of radiotherapy and chemotherapy, modalities with much more predictable and consistent outcomes. After performing over 1,600 autopsies, Raymond Pearl identified an inverse relationship between cancer and tuberculosis, leading to the idea of tuberculin as a therapy for cancer (Pearl *et al.*, 1928). In 1959, Lloyd Old and colleagues reported the use of the BCG vaccine as an immunotherapeutic to treat cancer. They challenged mice with tumour cells at specific intervals following BCG administration and observed that mice receiving BCG at least 7 days before tumour challenge were protected from developing cancer (Old *et al.*, 1959). In addition, Mathé in 1969 showed that BCG has an effect against human leukaemia (Mathé *et al.*, 1969). Then, Morton in 1970 demonstrated that intralesional BCG has an effect against human melanoma (Morton *et al.*, 1970). Zbar et al described the principal rules for adequate BCG immunotherapy (Zbar *et al.*, 1970; Zbar, *et al.*, 1973):

a) Tumour burden must be small.

b) Direct contact between BCG and tumour is essential.

c) The dose of the immunising agent must be adequate.

d) Tumours respond better when confined to the parent organ or, in case of metastases, when only in regional lymph nodes.

Based on these preliminary data, Alvaro Morales evaluated the use of BCGintravesical instillation, in which 7/10 patients with recurrent non-muscle invasive bladder cancer (NMIBC) were tumor-free at follow-up (Morales, *et al.*1976). Today, the BCG vaccine is a US Food and Drug Administration-approved treatment modality for bladder cancer, and other malignancies such as lymphoma and melanoma also reportedly respond to the BCG vaccine (Lamm *et al.*, 1991).

Bladder cancers are immune-sensitive tumors.

Bladder cancer (BC) has become a common cancer globally, with an estimated 430 000 new cases diagnosed in 2012 (Antoni *et al.*, 2017). It also leads to the highest cancer-related cost per patient among cancer types from diagnosis to death(Hong and Loughlin, 2008; Leal *et al.*, 2016). Approximately 75% of patients with BC present with a disease that is confined to the mucosa (stage Ta, CIS) or submucosa (stage T1). These categories are grouped as non-muscle-invasive bladder tumors (NMIBC). In order to separately predict the short-term and long-term risks of recurrence and progression in individual patients, the European Organization for Research and Treatment of Cancer (EORTC) Genitourinary (GU) group has developed a scoring system and risk tables. According to European Association of Urology guidelines, high-risk tumors are defined by the presence of any T1 tumor and/or high-grade tumor and/or presence of CIS (Babjuk *et al.*, 2019). It is therefore necessary to consider adjuvant therapy in all patients, shortly after initial trans-urethral resection (TUR). Five meta-analyses have confirmed that intra-vesical Mycobacterium bovis bacillus Calmette-Guérin (BCG) after TUR is superior to TUR alone or TUR and intra-vesical chemotherapy for prevention of recurrence of high risk NMIBC (Malmström *et al.*, 2009). In 2016-2018, the FDA approval of 5 immune-checkpoint inhibitors has revolutionized bladder cancer treatment in the second-line setting of advanced bladder cancer (Rouanne *et al.*, 2018). In addition, combination trial evaluating α-CTLA4 plus α-PD1 antibodies recently highlighted better tumor responses in the group of patients who received the highest dose of ipilimumab. This data may suggest the presence of immunosuppressive activated TReg in previously treated metastatic urothelial carcinoma.

Immunological and molecular correlates of responses to anti-PD(L)1 inhibitors include high levels of intra-tumoral CD8+ T cells, IFNγ signature, PDL1 expression in immune and/or tumor cells, and higher tumor mutational burden, although no predictive biomarker has

been identified so far. Also, TGFβ signature has been related to immune desert and potential resistance to anti-PDL1 inhibitors in the advanced metastatic setting (Mariathasan *et al.*, 2018). Recently, FDA has limited the use of α-PD(L)1 inhibitors in the first-line setting of metastatic bladder cancer for patients with PD-L1 high expression on immune cells (or combined positive score) (*FDA limits the use of Tecentriq and Keytruda for some urothelial cancer patients, 2018*).

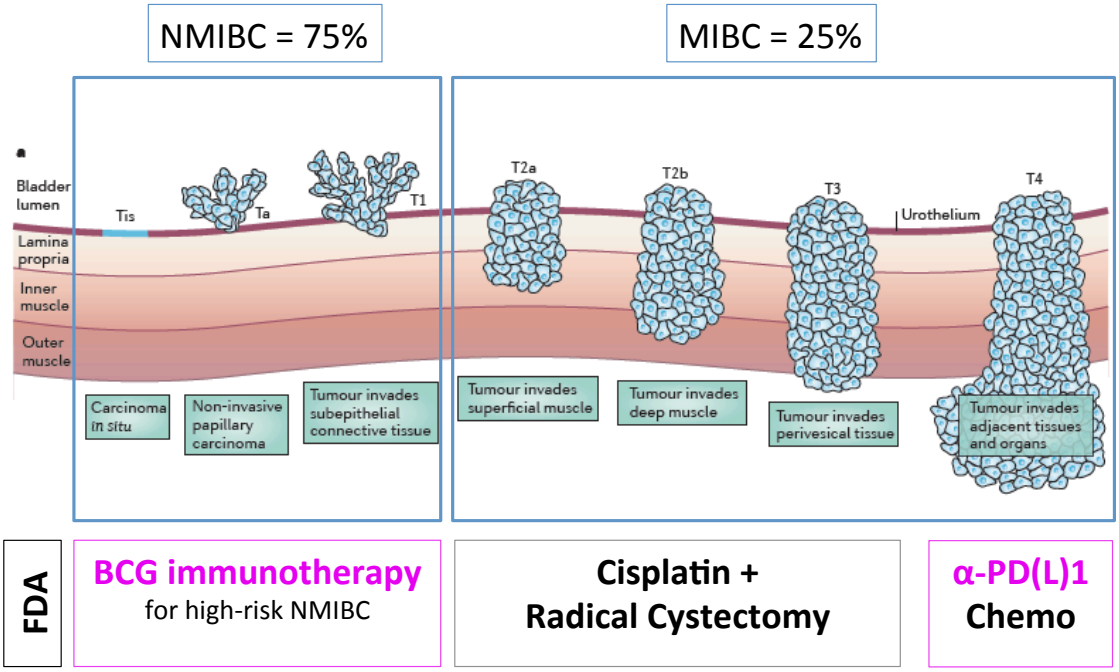

Fig. 10. Treatment strategy in bladder cancer is based on pathological staging (adapted from Knowles et al. Nat Rev Cancer 2015)

In 2018, two phase II trials, Pure Study-001 and Abacus, evaluating monoclonal antibodies α-PD1 and α-PDL1 showed antitumor efficacy of muscle-invasive tumors in the neoadjuvant setting before radical cystectomy (Necchi *et al.*, 2018; Powles *et al.*, 2018). In "superficial" high-risk non muscle-invasive bladder cancer (i.e. Cis, T1, high-grade Ta), preliminary results of anti-PD1 antibody in BCG unresponsive tumors showed potential benefit with 40% of patients without relapse after 3-months treatment. These results have to be confirmed with longer follow-up (Balar *et al.*, 2019). Other immunostimulatory molecules are currently

evaluating in BCG unresponsive tumors including α-PD1 (± BCG ±IDO1 inhibitors), IFNα-expressing adenovirus, and STING agonists. Improved understanding of resident immune cells in the bladder mucosa, including characterization of the urinary microbiome, may help both scientists, and researchers to develop novel therapeutic strategies in this heterogenous disease.

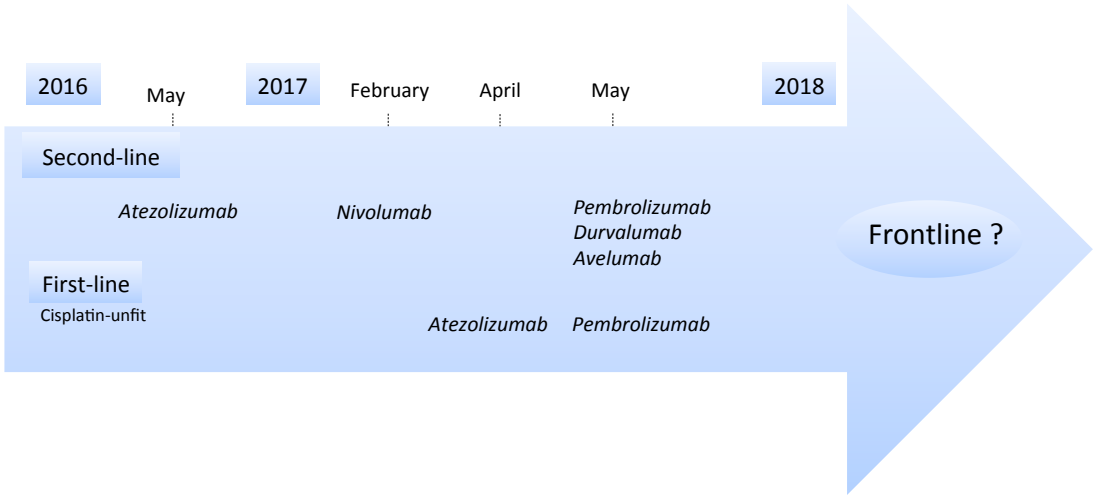

Fig. 11. Recent FDA approval of ICIs in advanced bladder cancer (from Rouanne et al., World J Urol 2018).

Are there resident immune cells in the bladder mucosa?

Currently, predictions regarding steady-state immune cell populations in the bladder can only be extrapolated from more detailed descriptions of resident cells of other mucosal surfaces such as the gut or lung. Ultimately, to define the immune cell populations of the steady-state bladder, an extensive and detailed study must be undertaken(Ingersoll *et al.*, 2013). In humans, the bladder urothelium is a pseudo-stratified epithelioma, meaning that all the epithelial cells are in contact with the basal membrane. This is different from what is observed in mice for whom the bladder urothelium is composed of 3-6 urothelial cell layers. Urothelial stem cells can be found in the basal layer where they have the capacity to differentiate into the other urothelial layers of the bladder (Shin *et al.*, 2011). Historically,

the bladder has been considered to lack colonizing microflora (Zasloff *et al.*, 2007) but more recent evidence suggests that similar to the gut or skin, commensal bacteria populate the bladder mucosal surface (Anderson *et al.*, 2004; Siddiqui *et al.*, 2011; Fouts *et al.*, 2012). As in most tissues, the bladder contains resident immune cells poised for encounter with invading microorganisms. Data suggest that both macrophages and dendritic cells reside in the naive bladder (Gautiar *et al.*, 2012; Miller *et al.*, 2012). Notably, little is known about the frequency, phenotype, or role of resident antigen-presenting cells in the bladder mucosa. In addition to antigen-presenting cells, the bladder contains resident αβ and γδ T cells, that may contribute to the innate defenses against infection in bladder cancer (Christmas *et al.*, 1994). Additional innate lymphocytes, such as innate lymphoid cells or mucosal-associated invariant T cells, reside in other mucosal tissues and play an important role in the maintenance of colonizing microbiota and the defense against infection (Porcelli *et al.*, 1993; Tilloy *et al.*, 1999; Treiner *et al.*, 2003; Zheng *et al.*, 2008); thus, it is reasonable to hypothesize that they play a critical role in the bladder, although this possibility has not been explored.

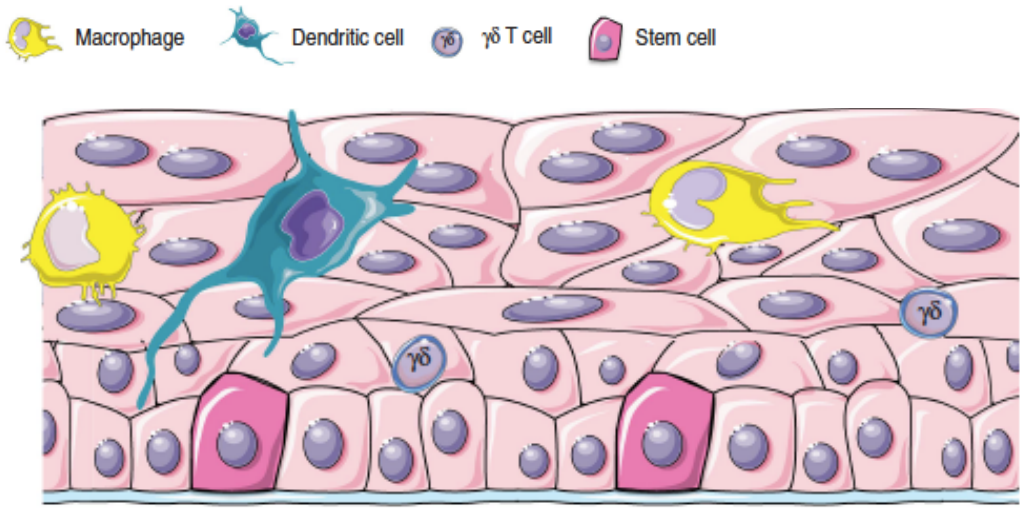

Fig. 12. Schematic representation of resident immune cells in bladder mucosa (from Ingersoll MA et al., Mucosal Immunol 2013).

How does BCG immunotherapy work?

It is worth noting that all vaccines present as a lyophilized stock (Behr, 2002), which is resuspended in saline before inoculation. As such, the inoculated preparation contains considerable amounts of dead material, in a proportion that used to vary greatly from one preparation to the other (Gheorghiu and Lagrange, 1983). Nowadays, most preparations contain only 5-10% live material (Behr, 2002). The importance of the ratio of live versus dead has not been formally assessed; however, killed mycobacterial preparations have been reported not to be an effective vaccine against TB (Orme, 1988). Interestingly, Biot et al confirmed in a mice model that T-cell recruitment was indeed dependent of live bacilli, as heat-killed BCG did not generate T-cell infiltration into the bladder. Intravesical instillation of Bacillus Calmette-Guérin (BCG) has been used as the gold-standard treatment for non-muscle invasive bladder cancer (NMIBC) since 1990 (68). Despite many unknowns regarding its mechanism of action, the role of the immune system in the BCG therapeutic effect is undoubtedly crucial.

Briefly, the different steps following intravesical BCG instillation can be summarized as below (Fig. 13) (Redelman-Sidi, *et al.*, 2014). BCG first needs to attach to the urothelium through fibronectin and integrins (Zlotta *et al.*, 1997). BCG is then internalized by urothelial cells and captured by the first line of innate immune response cells. Antigen presentation and cytokine release result in major histocompatibility complex (MHC) II upregulation and of IL-6, Il-8 and granulocyte-macrophage colony-stimulating factor (GM-CSF). Immune cells are then recruited to the 'war zone,' including granulocytes, CD4 and CD8 T cells, natural killer (NK) cells and macrophages. A torrent of mainly Th-1 cytokines, including Interferon gamma, IL-1, IL-12, IL-18, IL-23 and tumor necrosis factor-alpha are produced by these immune cells. This response is mainly non-specific. Local immune responses are exemplified by the granulomas, which can be observed in the bladder wall of patients treated with BCG. Bladder tumor cell

killing involves an immune-mediated cytotoxicity, including NK cells, NK T cells, CD8+ T cells, macrophages and TRAIL (granulocytes) among many others. Numerous BCG subcomponents, including BCG cell wall, plasma membrane, cytosol, purified polysaccharides as glucan or arabinomannan, purified native proteins from BCG culture filtrate, phosphate transporter PstS-2 and -3 proteins also provide positive stimuli for Th1 cell differentiation and enhance the cytotoxicity against bladder tumour cells (Zlotta *et al.*, 2000).

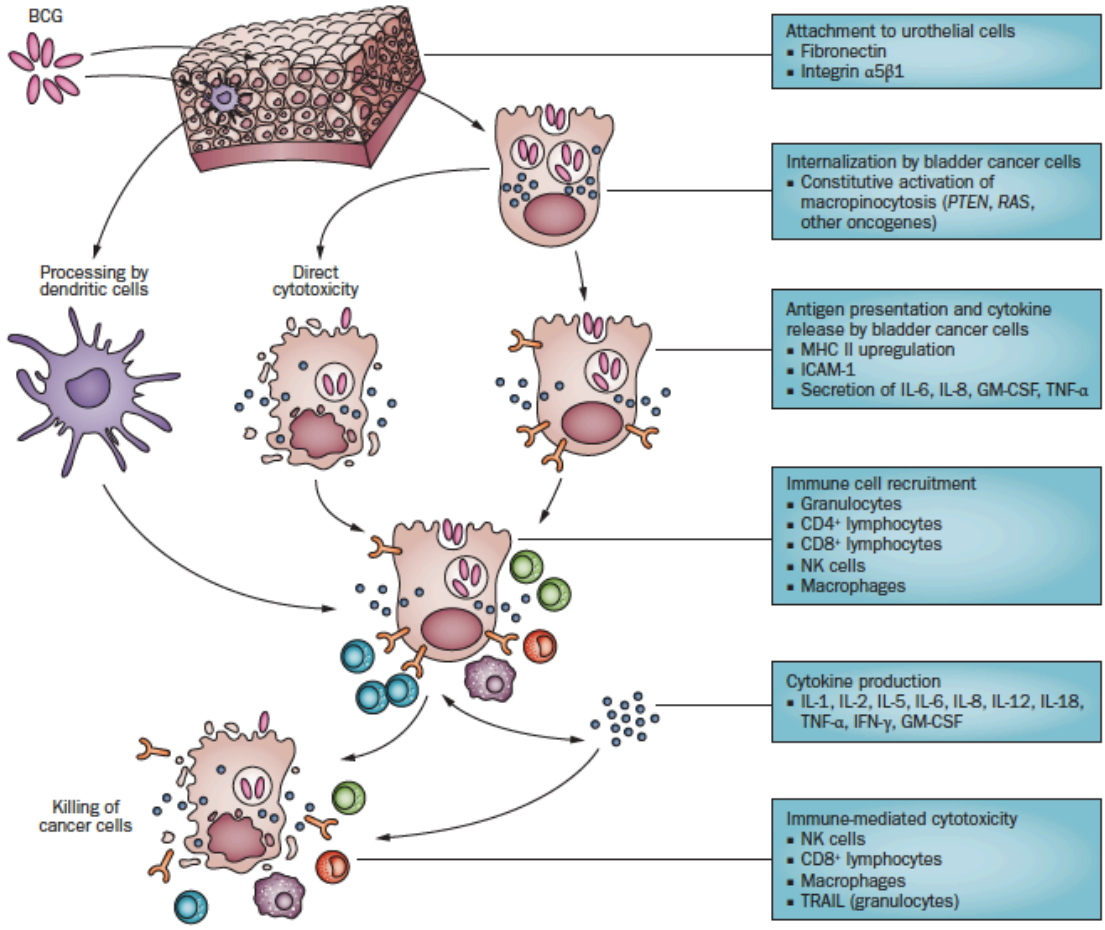

Fig. 13. Tentative model of the mechanism of action of BCG in bladder cancer (from Redelman-Sidi et al. Nat Rev Urol 2013).

BCG unresponsive tumors: what do we know so far?

Despite gold standard BCG immunotherapy, half of the patients experience tumor recurrence, and 20–30% of patients will progress to muscle-invasive bladder cancer (MIBC)

within 5-yr. Although they eventually undergo radical cystectomy, 10-15% ultimately die of bladder cancer (Van Den Bosch *et al.*, 2011; Chamie *et al.*, 2013). Based on our recent meta-cohort analysis of publicly available RNA-seq databases of urothelial bladder tumors, we found that 20% of NMIBC harbor the molecular portrait of MIBC(Tan *et al.*, 2019). However, no predictive biomarker has yet been identified. The lack of prognostic and predictive biomarkers is also a major drawback to rationally design innovative early phase clinical trials in this challenging-to-treat patient population (Ashish M. Kamat *et al.*, 2016). So far, immune escape from intravesical BCG therapy has not been fully understood. This gap in knowledge has catastrophic outcomes for patients with high-risk NMIBC, as escaped cancer cells spread locally and to distant sites.

The current working paradigm indicates tumor escape occurs in the context of immune exhaustion, and/or when the pre-existing immune response no longer recognizes tumor-derived antigens (eg due to tumor clonal mutations or loss of antigen presentation molecules). Additionally, immune parameters that may impact clinical response to BCG include cytokines released locally (Kamat *et al.*, 2018), the existence of preexisting immunity to BCG(Biot, 2013), the Th1 versus Th2 milieu (Pichler *et al.*, 2017), as well as the local balance between T lymphocytes and myeloid suppressor cells (Chevalier, Bohner, *et al.*, 2017). How BCG stimulates an antitumour response, and whether this response is specifically targeted against tumor cells or a positive side effect of a global intravesical inflammatory response, is still unknown(Pettenati and Ingersoll, 2018). Altogether, this highlights the crucial need to better understand the regulation of immune responses and tumor escape mechanisms after BCG immunotherapy in order to identify new targetable pathways.

References

1. van ’t Wout, J. W., Poell, R. and van Furth, R. (1992) ‘The role of BCG/PPD-activated macrophages in resistance against systemic candidiasis in mice.’, *Scandinavian journal of immunology*, 36(5), pp. 713–9. doi: 10.1111/j.1365-3083.1992.tb03132.x.

2. Advani, R. *et al.* (2018) ‘CD47 Blockade by Hu5F9-G4 and Rituximab in Non-Hodgkin’s Lymphoma.’, *The New England journal of medicine*, 379(18), pp. 1711–1721. doi: 10.1056/NEJMoa1807315.

3. Agudo, J. *et al.* (2018) ‘Quiescent Tissue Stem Cells Evade Immune Surveillance’, *Immunity*. Elsevier Inc., 48(2), pp. 271-285.e5. doi: 10.1016/j.immuni.2018.02.001.

4. Aleynick, M. *et al.* (2019) ‘Pathogen Molecular Pattern Receptor Agonists: Treating Cancer by Mimicking Infection’, *Clinical Cancer Research*. American Association for Cancer Research (AACR). doi: 10.1158/1078-0432.ccr-18-1800.

5. Anderson, M. *et al.* (2004) ‘Viable but nonculturable bacteria are present in mouse and human urine specimens.’, *Journal of clinical microbiology*, 42(2), pp. 753–8. doi: 10.1128/jcm.42.2.753-758.2004.

6. Annels, N. E. *et al.* (2019) ‘Viral Targeting of Non-Muscle-Invasive Bladder Cancer and Priming of Antitumor Immunity Following Intravesical Coxsackievirus A21.’, *Clinical cancer research : an official journal of the American Association for Cancer Research*. doi: 10.1158/1078-0432.CCR-18-4022.

7. Antoni, S. *et al.* (2017) ‘Bladder Cancer Incidence and Mortality: A Global Overview and Recent Trends’, *European Urology*. Elsevier B.V., pp. 96–108. doi: 10.1016/j.eururo.2016.06.010.

8. Babjuk, M. *et al.* (2019) ‘European Association of Urology Guidelines on Non-muscle-invasive Bladder Cancer (TaT1 and Carcinoma In Situ) - 2019 Update.’, *European urology*. doi: 10.1016/j.eururo.2019.08.016.

9. Balar, A. V. *et al.* (2019) 'Keynote 057: Phase II trial of Pembrolizumab (pembro) for patients (pts) with high-risk (HR) nonmuscle invasive bladder cancer (NMIBC) unresponsive to bacillus calmette-guérin (BCG).', *Journal of Clinical Oncology*. American Society of Clinical Oncology (ASCO), 37(7_suppl), pp. 350–350. doi: 10.1200/jco.2019.37.7_suppl.350.

10. Behr, M. A. *et al.* (1999) 'Comparative genomics of BCG vaccines by whole-genome DNA microarray.', *Science (New York, N.Y.)*, 284(5419), pp. 1520–3. doi: 10.1126/science.284.5419.1520.

11. Behr, M. A. (2002) 'BCG--different strains, different vaccines?', *The Lancet. Infectious diseases*, 2(2), pp. 86–92.

12. Belley, A. *et al.* (2004) 'Impact of Methoxymycolic Acid Production by Mycobacterium bovis BCG Vaccines', *Infection and Immunity*, 72(5), pp. 2803–2809. doi: 10.1128/IAI.72.5.2803-2809.2004.

13. Benci, J. L. *et al.* (2016) 'Tumor Interferon Signaling Regulates a Multigenic Resistance Program to Immune Checkpoint Blockade.', *Cell*, 167(6), pp. 1540-1554.e12. doi: 10.1016/j.cell.2016.11.022.

14. Berendt, M. J., North, R. J. and Kirstein, D. P. (1978) 'The immunological basis of endotoxin-induced tumor regression. Requirement for T-cell-mediated immunity.', *The Journal of experimental medicine*, 148(6), pp. 1550–9. doi: 10.1084/jem.148.6.1550.

15. Biot, C. (2013) 'BCG immunotherapy for bladder cancer : characterization and modeling of the bladder immune response to BCG identify strategies for improving anti-tumor activity'.

16. Bistoni, F. *et al.* (1986) 'Evidence for macrophage-mediated protection against lethal Candida albicans infection.', *Infection and immunity*, 51(2), pp. 668–74.

17. Van Den Bosch, S. and Witjes, J. A. (2011) 'Long-term cancer-specific survival in patients with high-risk, non-muscle-invasive bladder cancer and tumour progression: A systematic review', *European Urology*, pp. 493–500. doi: 10.1016/j.eururo.2011.05.045.

18. Brigl, M. and Brenner, M. B. (2004) 'CD1: Antigen Presentation and T Cell Function', *Annual Review of Immunology*. Annual Reviews, 22(1), pp. 817–890. doi: 10.1146/annurev.immunol.22.012703.104608.

19. Brosch, R. *et al.* (2007) 'Genome plasticity of BCG and impact on vaccine efficacy', *Proceedings of the National Academy of Sciences of the United States of America*, 104(13), pp. 5596–5601. doi: 10.1073/pnas.0700869104.

20. Calmette, A. (1927) *La Vaccination préventive contre la tuberculose par le "BCG, "*. Paris : Masson et cie.

21. Carretero, R. *et al.* (2011) 'Bacillus Calmette-Guerin immunotherapy of bladder cancer induces selection of human leukocyte antigen class I-deficient tumor cells', *International Journal of Cancer*, 129(4), pp. 839–846. doi: 10.1002/ijc.25733.

22. Chamie, K. *et al.* (2013) 'Recurrence of high-risk bladder cancer: A population-based analysis', *Cancer*, 119(17), pp. 3219–3227. doi: 10.1002/cncr.28147.

23. Chevalier, M. F., Trabanelli, S., *et al.* (2017) 'ILC2-modulated T cell-to-MDSC balance is associated with bladder cancer recurrence', *Journal of Clinical Investigation*, 127(8), pp. 2916–2929. doi: 10.1172/JCI89717.

24. Chevalier, M. F., Bohner, P., *et al.* (2017) 'Immunoregulation of Dendritic Cell Subsets by Inhibitory Receptors in Urothelial Cancer', *European Urology*, 71(6), pp. 854–857. doi: 10.1016/j.eururo.2016.10.009.

25. Chevalier, M. F. *et al.* (2018) 'Conventional and PD-L1-expressing Regulatory T Cells are Enriched During BCG Therapy and may Limit its Efficacy', *European Urology*, 74(5), pp. 540–544. doi: 10.1016/j.eururo.2018.06.045.

26. Chowdhury, S. *et al.* (2019) 'Programmable bacteria induce durable tumor regression and systemic antitumor immunity. *Nature medicine*, 25(7), pp. 1057–1063. doi: 10.1038/s41591-019-0498-z.

27. Christmas, T. J. (1994) 'Lymphocyte sub-populations in the bladder wall in normal bladder, bacterial cystitis and interstitial cystitis.', *British journal of urology*, 73(5), pp. 508–15. doi: 10.1111/j.1464-410x.1994.tb07635.x.

28. Cole, S. T. (2005) *Tuberculosis and the tubercle bacillus*. ASM Press.

29. Coley W. B. (1891) 'Contrivution to the knowledge of sarcoma', *Annals of Surgery*. Ovid Technologies (Wolters Kluwer Health), 14, pp. 199–220. doi: 10.1097/00000658-189112000-00015.

30. Comstock, G. W. (1996) 'Does the protective effect of neonatal BCG vaccination correlate with vaccine-induced tuberculin reactions? [letter; comment]', *Am J Respir Crit Care Med*, 154(1), pp. 263–264.

31. Cooper, A. M. *et al.* (1993) 'Disseminated tuberculosis in interferon gamma gene-disrupted mice.', *The Journal of experimental medicine*, 178(6), pp. 2243–7. doi: 10.1084/jem.178.6.2243.

32. Cooper, A. M. (2009) 'Cell-mediated immune responses in tuberculosis.', *Annual review of immunology*, 27, pp. 393–422. doi: 10.1146/annurev.immunol.021908.132703.

33. Coulombe, F. *et al.* (2009) 'Increased NOD2-mediated recognition of N-glycolyl muramyl dipeptide', *Journal of Experimental Medicine*, 206(8), pp. 1709–1716. doi: 10.1084/jem.20081779.

34. Dalton, D. K. *et al.* (1993) 'Multiple defects of immune cell function in mice with disrupted interferon-gamma genes.', *Science (New York, N.Y.)*, 259(5102), pp. 1739–42. doi: 10.1126/science.8456300.

35. Divangahi, M. and Behr, M. A. (2018) 'Cracking the Vaccine Code in Tuberculosis.', *American journal of respiratory and critical care medicine*, 197(4), pp. 427–432. doi: 10.1164/rccm.201707-1489PP.

36. Donovan, M. L. *et al.* (2017) 'Type I interferons in the pathogenesis of tuberculosis: Molecular drivers and immunological consequences', *Frontiers in Immunology*. Frontiers Media S.A. doi: 10.3389/fimmu.2017.01633.

37. Esmail, H. *et al.* (2018) 'Complement pathway gene activation and rising circulating immune complexes characterize early disease in HIV-associated tuberculosis.', *Proceedings of the National Academy of Sciences of the United States of America*, 115(5), pp. E964–E973. doi: 10.1073/pnas.1711853115.

38. *FDA limits the use of Tecentriq and Keytruda for some urothelial cancer patients | FDA* (2018) at: https://www.fda.gov/drugs/resources-information-approved-drugs/fda-limits-use-tecentriq-and-keytruda-some-urothelial-cancer-patients.

39. Ferwerda, G. *et al.* (2005) 'NOD2 and toll-like receptors are nonredundant recognition systems of Mycobacterium tuberculosis.', *PLoS pathogens*, 1(3), pp. 279–85. doi: 10.1371/journal.ppat.0010034.

40. Fine, P. E. M. *et al.* (1999) *Department of vaccines and biologicals Issues relating to the use of BCG in immunization programmes A discussion document*, *World Health Organization Geneva*.

41. Flynn, J. L. *et al.* (1993) 'An essential role for interferon gamma in resistance to Mycobacterium tuberculosis infection.', *The Journal of experimental medicine*, 178(6), pp. 2249–54. doi: 10.1084/jem.178.6.2249.

42. Flynn, J. L. and Chan, J. (2001) 'Immunology of tuberculosis.', *Annual review of immunology*, 19, pp. 93–129. doi: 10.1146/annurev.immunol.19.1.93.

43. Fouts, D. E. *et al.* (2012) 'Integrated next-generation sequencing of 16S rDNA and metaproteomics differentiate the healthy urine microbiome from asymptomatic bacteriuria in neuropathic bladder associated with spinal cord injury.', *Journal of translational medicine*, 10, p. 174. doi: 10.1186/1479-5876-10-174.

44. Gan, C. *et al.* (2013) 'BCG immunotherapy for bladder cancer - The effects of substrain differences', *Nature Reviews Urology*. Nature Publishing Group, 10(10), pp. 580–588. doi: 10.1038/nrurol.2013.194.

45. Gautiar, E. L. *et al.* (2012) 'Gene-expression profiles and transcriptional regulatory pathways that underlie the identity and diversity of mouse tissue macrophages', *Nature Immunology*, 13(11), pp. 1118–1128. doi: 10.1038/ni.2419.

46. Ge, P. *et al.* (2018) 'Oncological Outcome of Primary and Secondary Muscle-Invasive Bladder Cancer: A Systematic Review and Meta-analysis', *Scientific Reports*, 8(1), pp. 4–11. doi: 10.1038/s41598-018-26002-6.

47. Gheorghiu, M. and Lagrange, P. H. (no date) 'Viability, heat stability and immunogenicity of four BCG vaccines prepared from four different BCG strains.', *Annales d'immunologie*, 134C(1), pp. 125–47.

48. Gordon, S. V *et al.* (1999) 'Identification of variable regions in the genomes of tubercle bacilli using bacterial artificial chromosome arrays.', *Molecular microbiology*, 32(3), pp. 643–55. doi: 10.1046/j.1365-2958.1999.01383.x.

49. Guinn, K. M. *et al.* (2004) 'Individual RD1-region genes are required for export of ESAT-6/CFP-10 and for virulence of Mycobacterium tuberculosis.', *Molecular microbiology*, 51(2), pp. 359–70. doi: 10.1046/j.1365-2958.2003.03844.x.

50. Harding, C. V. and Boom, W. H. (2010) 'Regulation of antigen presentation by Mycobacterium tuberculosis: A role for Toll-like receptors', *Nature Reviews Microbiology*. Nature Publishing Group, 8(4), pp. 296–307. doi: 10.1038/nrmicro2321.

51. Hong, Y. M. and Loughlin, K. R. (2008) 'Economic impact of tumor markers in bladder cancer surveillance.', *Urology*, 71(1), pp. 131–5. doi: 10.1016/j.urology.2007.08.014.

52. Hsu, T. *et al.* (2003) 'The primary mechanism of attenuation of bacillus Calmette-Guérin is a loss of secreted lytic function required for invasion of lung interstitial tissue', *Proceedings of the National Academy of Sciences of the United States of America*, 100(21), pp. 12420–12425. doi: 10.1073/pnas.1635213100.

53. Huang, K.-C. *et al.* (2019) 'Abstract 3269: Discovery and characterization of E7766, a novel macrocycle-bridged STING agonist with pan-genotypic and potent antitumor activity through intravesical and intratumoral administration', in *Immunology*. American Association for Cancer Research, pp. 3269–3269. doi: 10.1158/1538-7445.AM2019-3269.

54. Ingersoll, M. A. and Albert, M. L. (2013) 'From infection to immunotherapy: host immune responses to bacteria at the bladder mucosa.', *Mucosal immunology*, 6(6), pp. 1041–53. doi: 10.1038/mi.2013.72.

55. Jacquelot, N. *et al.* (2017) 'Predictors of responses to immune checkpoint blockade in advanced melanoma.', *Nature communications*, 8(1), p. 592. doi: 10.1038/s41467-017-00608-2.

56. Jacquelot, N. *et al.* (2019) 'Sustained Type I interferon signaling as a mechanism of resistance to PD-1 blockade.', *Cell research*. doi: 10.1038/s41422-019-0224-x.

57. Jiao, X. *et al.* (2002) 'Dendritic Cells Are Host Cells for Mycobacteria In Vivo That Trigger Innate and Acquired Immunity', *The Journal of Immunology*. The American Association of Immunologists, 168(3), pp. 1294–1301. doi: 10.4049/jimmunol.168.3.1294.

58. Kagina, B. M. N. *et al.* (2010) 'Specific T cell frequency and cytokine expression profile do not correlate with protection against tuberculosis after bacillus Calmette-Guérin vaccination of newborns.', *American journal of respiratory and critical care medicine*, 182(8), pp. 1073–9. doi: 10.1164/rccm.201003-0334OC.

59. Kamat, A M *et al.* (2016) 'Cytokine Panel for Response to Intravesical Therapy (CyPRIT): Nomogram of Changes in Urinary Cytokine Levels Predicts Patient Response to Bacillus Calmette-Guerin.[Erratum appears in Eur Urol. 2016 Jul;70(1):e26; PMID: 27302298]', *European Urology*, 69(2), pp. 197–200.

60. Kamat, Ashish M. *et al.* (2016) 'Definitions, end points, and clinical trial designs for non-muscle-invasive bladder cancer: Recommendations from the International Bladder Cancer Group', *Journal of Clinical Oncology*, 34(16), pp. 1935–1944. doi: 10.1200/JCO.2015.64.4070.

61. Kamat, A. M. *et al.* (2018) 'Predicting Response to Intravesical Bacillus Calmette-Guérin Immunotherapy: Are We There Yet? A Systematic Review', *European Urology*. European Association of Urology, 73(5), pp. 738–748. doi: 10.1016/j.eururo.2017.10.003.

62. Kauder, S. E. *et al.* (2018) 'ALX148 blocks CD47 and enhances innate and adaptive antitumor immunity with a favorable safety profile', *PLoS ONE*. Public Library of Science, 13(8). doi: 10.1371/journal.pone.0201832.

63. Kaufmann, E. *et al.* (2018) 'BCG Educates Hematopoietic Stem Cells to Generate Protective Innate Immunity against Tuberculosis.', *Cell*, 172(1–2), pp. 176-190.e19. doi: 10.1016/j.cell.2017.12.031.

64. Kaufmann, S. H. E. (2010) 'Future vaccination strategies against tuberculosis: thinking outside the box.', *Immunity*, 33(4), pp. 567–77. doi: 10.1016/j.immuni.2010.09.015.

65. Kaufmann, S. H. E., Evans, T. G. and Hanekom, W. A. (2015) 'Tuberculosis vaccines: Time for a global strategy', *Science Translational Medicine*. American Association for the Advancement of Science. doi: 10.1126/scitranslmed.aaa4730.

66. Kleinnijenhuis, J. *et al.* (2012) 'Bacille Calmette-Guérin induces NOD2-dependent nonspecific protection from reinfection via epigenetic reprogramming of monocytes',

Proceedings of the National Academy of Sciences of the United States of America, 109(43), pp. 17537–17542. doi: 10.1073/pnas.1202870109.

67. Knowles, M. A. and Hurst, C. D. (2015) 'Molecular biology of bladder cancer: New insights into pathogenesis and clinical diversity', *Nature Reviews Cancer*. Nature Publishing Group, 15(1), pp. 25–41. doi: 10.1038/nrc3817.

68. Kobayashi, T. *et al.* (2015) 'Modelling bladder cancer in mice: Opportunities and challenges', *Nature Reviews Cancer*. Nature Publishing Group, 15(1), pp. 42–54. doi: 10.1038/nrc3858.

69. Krutzik, S. R. and Modlin, R. L. (2004) 'The role of Toll-like receptors in combating mycobacteria.', *Seminars in immunology*, 16(1), pp. 35–41. doi: 10.1016/j.smim2003.10.005.

70. Kupz, A. *et al.* (2016) 'ESAT-6 – dependent cytosolic pattern recognition drives noncognate tuberculosis control in vivo Find the latest version : ESAT-6 – dependent cytosolic pattern recognition drives noncognate tuberculosis control in vivo', 126(6), pp. 2109–2122. doi: 10.1172/JCI84978.

71. Lamm, D. L. *et al.* (1991) 'A randomized trial of intravesical doxorubicin and immunotherapy with bacille calmette-guérin for transitional-cell carcinoma of the bladder', *New England Journal of Medicine*, 325(17), pp. 1205–1209. doi: 10.1056/NEJM199110243251703.

72. Leal, J. *et al.* (2016) 'Economic Burden of Bladder Cancer Across the European Union.', *European urology*, 69(3), pp. 438–47. doi: 10.1016/j.eururo.2015.10.024.

73. Lewis, K. N. *et al.* (2003) ' Deletion of RD1 from Mycobacterium tuberculosis Mimics Bacille Calmette-Guérin Attenuation ', *The Journal of Infectious Diseases*. Oxford University Press (OUP), 187(1), pp. 117–123. doi: 10.1086/345862.

74. Liu, X. *et al.* (2015) 'CD47 blockade triggers T cell-mediated destruction of immunogenic tumors.', *Nature medicine*, 21(10), pp. 1209–15. doi: 10.1038/nm.3931.

75. Mahairas, G. G. *et al.* (1996) 'Molecular analysis of genetic differences between Mycobacterium bovis BCG and virulent M. bovis.', *Journal of bacteriology*, 178(5), pp. 1274–82. doi: 10.1128/jb.178.5.1274-1282.1996.

76. Malmström, P.-U. *et al.* (2009) 'An individual patient data meta-analysis of the long-term outcome of randomised studies comparing intravesical mitomycin C versus bacillus Calmette-Guérin for non-muscle-invasive bladder cancer.', *European urology*, 56(2), pp. 247–56. doi: 10.1016/j.eururo.2009.04.038.

77. Mariathasan, S. *et al.* (2018) 'TGFβ attenuates tumour response to PD-L1 blockade by contributing to exclusion of T cells', *Nature*. Nature Publishing Group, 554(7693), pp. 544–548. doi: 10.1038/nature25501.

78. Mathé, G. *et al.* (1969) 'Active immunotherapy for acute lymphoblastic leukaemia.', *Lancet (London, England)*, 1(7597), pp. 697–9. doi: 10.1016/s0140-6736(69)92648-8.

79. Mayer-Barber, K. D. and Sher, A. (2015) 'Cytokine and lipid mediator networks in tuberculosis.', *Immunological reviews*, 264(1), pp. 264–75. doi: 10.1111/imr.12249.

80. McNab, F. *et al.* (2015) 'Type I interferons in infectious disease', *Nature Reviews Immunology*. Nature Publishing Group, 15(2), pp. 87–103. doi: 10.1038/nri3787.

81. Mellman, I., Coukos, G. and Dranoff, G. (2011) 'Cancer immunotherapy comes of age', *Nature*, 480(7378), pp. 480–489. doi: 10.1038/nature10673.

82. Miller, J. C. *et al.* (2012) 'Deciphering the transcriptional network of the dendritic cell lineage.', *Nature immunology*, 13(9), pp. 888–99. doi: 10.1038/ni.2370.

83. Mittrücker, H.-W. *et al.* (2007) 'Poor correlation between BCG vaccination-induced T cell responses and protection against tuberculosis.', *Proceedings of the National Academy of Sciences of the United States of America*, 104(30), pp. 12434–9. doi: 10.1073/pnas.0703510104.

84. Morales, A., Eidinger, D. and Bruce, A. W. (1976) 'Intracavitary Bacillus Calmette-Guerin in the treatment of superficial bladder tumors.', *The Journal of urology*, 116(2), pp. 180–3. doi: 10.1016/s0022-5347(17)58737-6.

85. Morton, D. L. *et al.* (1970) 'Immunological factors in human sarcomas and melanomas: a rational basis for immunotherapy.', *Annals of surgery*, 172(4), pp. 740–9. doi: 10.1097/00000658-197010000-00018.

86. Mostafid, A. H. *et al.* (2015) 'Therapeutic options in high-risk non-muscle-invasive bladder cancer during the current worldwide shortage of bacille Calmette-Guérin.', *European urology*, 67(3), pp. 359–60. doi: 10.1016/j.eururo.2014.11.031.

87. Mostowy, S. *et al.* (2003) 'The in vitro evolution of BCG vaccines', *Vaccine*. Elsevier BV, 21(27–30), pp. 4270–4274. doi: 10.1016/S0264-410X(03)00484-5.

88. Musella, M. *et al.* (2017) 'Type-I-interferons in infection and cancer: Unanticipated dynamics with therapeutic implications', *OncoImmunology*. Taylor & Francis, 6(5), pp. 1–12. doi: 10.1080/2162402X.2017.1314424.

89. Necchi, A. *et al.* (2018) 'Pembrolizumab as neoadjuvant therapy before radical cystectomy in patients with muscle-invasive urothelial bladder carcinoma (PURE-01): An open-label, single-arm, phase II study', *Journal of Clinical Oncology*. American Society of Clinical Oncology, 36(34), pp. 3353–3360. doi: 10.1200/JCO.18.01148.

90. Netea, M. G. *et al.* (2016) 'Trained immunity: A program of innate immune memory in health and disease', *Science*, 352(6284), p. 427. doi: 10.1126/science.aaf1098.

91. Nieto, M. A. *et al.* (2016) 'EMT: 2016', *Cell*. Cell Press, pp. 21–45. doi: 10.1016/j.cell.2016.06.028.

92. Norazmi Mohd Nor, Acosta, A. and Sarmiento, M. E. (2011) *The Art & Science of Tuberculosis Vaccine Development*.

93. North, R. J. and Jung, Y.-J. (2004) 'Immunity to tuberculosis.', *Annual review of immunology*, 22, pp. 599–623. doi: 10.1146/annurev.immunol.22.012703.104635.

94. O'Garra, A. *et al.* (2013) 'The immune response in tuberculosis.', *Annual review of immunology*, 31, pp. 475–527. doi: 10.1146/annurev-immunol-032712-095939.

95. O'Shea, J. J. and Paul, W. E. (2010) 'Mechanisms underlying lineage commitment and plasticity of helper CD4+ T cells.', *Science (New York, N.Y.)*, 327(5969), pp. 1098–102. doi: 10.1126/science.1178334.

96. OLD, L. J., CLARKE, D. A. and BENACERRAF, B. (1959) 'Effect of Bacillus Calmette-Guerin infection on transplanted tumours in the mouse.', *Nature*, 184(Suppl 5), pp. 291–2. doi: 10.1038/184291a0.

97. Orme, I. M. (1988) 'Characteristics and specificity of acquired immunologic memory to Mycobacterium tuberculosis infection.', *Journal of immunology (Baltimore, Md. : 1950)*, 140(10), pp. 3589–93.

98. Ottenhoff, T. H., Kumararatne, D. and Casanova, J. L. (1998) 'Novel human immunodeficiencies reveal the essential role of type-I cytokines in immunity to intracellular bacteria.', *Immunology today*, 19(11), pp. 491–4.

99. Pai, R. K. *et al.* (2004) 'Prolonged toll-like receptor signaling by Mycobacterium tuberculosis and its 19-kilodalton lipoprotein inhibits gamma interferon-induced regulation of selected genes in macrophages.', *Infection and immunity*, 72(11), pp. 6603–14. doi: 10.1128/IAI.72.11.6603-6614.2004.

100. Pearl, R. (1928) 'On the Pathological Relations Between Cancer and Tuberculosis', *Proceedings of the Society for Experimental Biology and Medicine*, 26(1), pp. 73–75. doi: 10.3181/00379727-26-4143.

101. Pennini, M. E. *et al.* (2007) 'CCAAT/enhancer-binding protein beta and delta binding to CIITA promoters is associated with the inhibition of CIITA expression in response to

Mycobacterium tuberculosis 19-kDa lipoprotein.', *Journal of immunology (Baltimore, Md. : 1950)*, 179(10), pp. 6910–8. doi: 10.4049/jimmunol.179.10.6910.

102. Pettenati, C. and Ingersoll, M. A. (2018) 'Mechanisms of BCG immunotherapy and its outlook for bladder cancer', *Nature Reviews Urology*. Springer US, 15(10), pp. 615–625. doi: 10.1038/s41585-018-0055-4.

103. Pichler, R. *et al.* (2017) 'Intratumoral Th2 predisposition combines with an increased Th1 functional phenotype in clinical response to intravesical BCG in bladder cancer', *Cancer Immunology, Immunotherapy*. Springer Berlin Heidelberg, 66(4), pp. 427–440. doi: 10.1007/s00262-016-1945-z.

104. Pietzak, E. J. *et al.* (2019) 'Genomic Differences Between "Primary" and "Secondary" Muscle-invasive Bladder Cancer as a Basis for Disparate Outcomes to Cisplatin-based Neoadjuvant Chemotherapy [Figure presented]', *European Urology*. European Association of Urology, 75(2), pp. 231–239. doi: 10.1016/j.eururo.2018.09.002.

105. Porcelli, S. *et al.* (1993) 'Analysis of T cell antigen receptor (TCR) expression by human peripheral blood CD4-8- alpha/beta T cells demonstrates preferential use of several V beta genes and an invariant TCR alpha chain.', *The Journal of experimental medicine*, 178(1), pp. 1–16. doi: 10.1084/jem.178.1.1.

106. Powles, T. *et al.* (2018) 'A phase II study investigating the safety and efficacy of neoadjuvant atezolizumab in muscle invasive bladder cancer (ABACUS).', *Journal of Clinical Oncology*. American Society of Clinical Oncology (ASCO), 36(15_suppl), pp. 4506–4506. doi: 10.1200/jco.2018.36.15_suppl.4506.

107. Pym, A. S. *et al.* (2002) 'Loss of RD1 contributed to the attenuation of the live tuberculosis vaccines Mycobacterium bovis BCG and Mycobacterium microti.', *Molecular microbiology*, 46(3), pp. 709–17. doi: 10.1046/j.1365-2958.2002.03237.x.

108. Redelman-Sidi, G. *et al.* (2013) 'Oncogenic activation of Pak1-dependent pathway of macropinocytosis determines BCG entry into bladder cancer cells', *Cancer Research*, 73(3), pp. 1156–1167. doi: 10.1158/0008-5472.CAN-12-1882.

109. Redelman-Sidi, G., Glickman, M. S. and Bochner, B. H. (2014) 'The mechanism of action of BCG therapy for bladder cancer-A current perspective', *Nature Reviews Urology*. Nature Publishing Group, 11(3), pp. 153–162. doi: 10.1038/nrurol.2014.15.

110. Rouanne, M. *et al.* (2018) 'Development of immunotherapy in bladder cancer: present and future on targeting PD(L)1 and CTLA-4 pathways', *World Journal of Urology*. doi: 10.1007/s00345-018-2332-5.

111. Rouanne, M. *et al.* (2019) 'Stromal lymphocyte infiltration is associated with tumour invasion depth but is not prognostic in high-grade T1 bladder cancer.', *European journal of cancer (Oxford, England : 1990)*, 108, pp. 111–119. doi: 10.1016/j.ejca.2018.12.010.

112. Sabir, N. *et al.* (2017) 'IFN-β: A contentious player in host–pathogen interaction in tuberculosis', *International Journal of Molecular Sciences*. MDPI AG. doi: 10.3390/ijms18122725.

113. Saeed, S. *et al.* (2014) 'Epigenetic programming of monocyte-to-macrophage differentiation and trained innate immunity', *Science*. American Association for the Advancement of Science, 345(6204). doi: 10.1126/science.1251086.

114. Scotet, E. *et al.* (2008) 'Bridging innate and adaptive immunity through γδ T - Dendritic cell crosstalk', *Frontiers in Bioscience*, 13(18), pp. 6872–6885. doi: 10.2741/3195.

115. Scriba, T. J. *et al.* (2017) 'Sequential inflammatory processes define human progression from M. tuberculosis infection to tuberculosis disease', *PLoS Pathogens*. Public Library of Science, 13(11). doi: 10.1371/journal.ppat.1006687.

116. Shekarian, T. *et al.* (2017) 'Pattern recognition receptors: Immune targets to enhance cancer immunotherapy', *Annals of Oncology*, 28(8), pp. 1756–1766. doi: 10.1093/annonc/mdx179.

117. Shin, K. *et al.* (2011) 'Hedgehog/Wnt feedback supports regenerative proliferation of epithelial stem cells in bladder.', *Nature*, 472(7341), pp. 110–4. doi: 10.1038/nature09851.

118. Shore, N. D. *et al.* (2017) 'Intravesical rAd–IFNa/Syn3 for patients with high-grade, bacillus calmette-guerin–refractory or relapsed non–muscle-invasive bladder cancer: A phase II randomized study', *Journal of Clinical Oncology*, 35(30), pp. 3410–3416. doi: 10.1200/JCO.2017.72.3064.

119. Siddiqui, H. *et al.* (2011) 'Assessing diversity of the female urine microbiota by high throughput sequencing of 16S rDNA amplicons.', *BMC microbiology*, 11, p. 244. doi: 10.1186/1471-2180-11-244.

120. Sikic, B. I. *et al.* (2019) 'First-in-human, first-in-class phase i trial of the anti-CD47 antibody Hu5F9-G4 in patients with advanced cancers', in *Journal of Clinical Oncology*. American Society of Clinical Oncology, pp. 946–953. doi: 10.1200/JCO.18.02018.

121. Singh, P. *et al.* (2017) 'S1605: Phase II trial of atezolizumab in BCG-unresponsive non-muscle invasive bladder cancer.', *Journal of Clinical Oncology*, 35(15_suppl), pp. TPS4591–TPS4591. doi: 10.1200/JCO.2017.35.15_suppl.TPS4591.

122. Singhania, A. *et al.* (2018) 'The value of transcriptomics in advancing knowledge of the immune response and diagnosis in tuberculosis', *Nature Immunology*. Springer US, 19(11), pp. 1159–1168. doi: 10.1038/s41590-018-0225-9.

123. Sockolosky, J. T. *et al.* (2016) 'Durable antitumor responses to CD47 blockade require adaptive immune stimulation', *Proceedings of the National Academy of Sciences of the United States of America*. National Academy of Sciences, 113(19), pp. E2646–E2654. doi: 10.1073/pnas.1604268113.

124. Spranger, S. and Gajewski, T. F. (2018) 'Mechanisms of Tumor Cell–Intrinsic Immune Evasion', *Annual Review of Cancer Biology*. Annual Reviews, 2(1), pp. 213–228. doi: 10.1146/annurev-cancerbio-030617-050606.

125. Stanley, S. A. *et al.* (2003) 'Acute infection and macrophage subversion by Mycobacterium tuberculosis require a specialized secretion system', *Proceedings of the National Academy of Sciences of the United States of America*, 100(22), pp. 13001–13006. doi: 10.1073/pnas.2235593100.

126. Tan, T. Z., Miow, Q. H., Miki, Y., Noda, T., Mori, S., Huang, R. Y.-J., *et al.* (2014) 'Epithelial-mesenchymal transition spectrum quantification and its efficacy in deciphering survival and drug responses of cancer patients.', *EMBO molecular medicine*, 6(10), pp. 1279–93. doi: 10.15252/emmm.201404208.

127. Tan, T. Z., Miow, Q. H., Miki, Y., Noda, T., Mori, S., Huang, R. Y., *et al.* (2014) 'Epithelial-mesenchymal transition spectrum quantification and its efficacy in deciphering survival and drug responses of cancer patients', *EMBO Molecular Medicine*, 6(10), pp. 1279–1293. doi: 10.15252/emmm.201404208.

128. Tan, T. Z. *et al.* (2019) 'Molecular Subtypes of Urothelial Bladder Cancer: Results from a Meta-cohort Analysis of 2411 Tumors', *European Urology*. European Association of Urology, 75(3), pp. 423–432. doi: 10.1016/j.eururo.2018.08.027.

129. Tilloy *et al.* (1999) 'An Invariant T Cell Receptor a Chain Defines a N ovel TAP-independent Major Histocompatibility Complex Class 1b restricted a/B T cell Subpopulationn Mammals', *Journal of Experimental Medicine*, 189(12). doi: 10.1084/jem.189.12.1907.

130. Treiner, E. *et al.* (2003) 'Selection of evolutionarily conserved mucosal-associated invariant T cells by MR1.', *Nature*, 422(6928), pp. 164–9. doi: 10.1038/nature01433.

131. Tribouley, J., Tribouley-Duret, J. and Appriou, M. (1978) '[Effect of Bacillus Callmette Guerin (BCG) on the receptivity of nude mice to Schistosoma mansoni].', *Comptes rendus des seances de la Societe de biologie et de ses filiales*, 172(5), pp. 902–4.

132. Tsung, K. and Norton, J. A. (2006) 'Lessons from Coley's Toxin.', *Surgical oncology*, 15(1), pp. 25–8. doi: 10.1016/j.suronc.2006.05.002.

133. Veillette, A. and Tang, Z. (2019) 'Signaling Regulatory Protein (SIRP)α-CD47 Blockade Joins the Ranks of Immune Checkpoint Inhibition.', *Journal of clinical oncology : official journal of the American Society of Clinical Oncology*, 37(12), pp. 1012–1014. doi: 10.1200/JCO.19.00121.

134. Zak, D. E. *et al.* (2016) 'A blood RNA signature for tuberculosis disease risk: a prospective cohort study', *The Lancet*. Lancet Publishing Group, 387(10035), pp. 2312–2322. doi: 10.1016/S0140-6736(15)01316-1.

135. Zasloff, M. (2007) 'Antimicrobial peptides, innate immunity, and the normally sterile urinary tract.', *Journal of the American Society of Nephrology : JASN*, 18(11), pp. 2810–6. doi: 10.1681/ASN.2007050611.

136. Zbar, B. *et al.* (1970) 'Tumor immunity produced by the intradermal inoculation of living tumor cells and living Mycobacterium bovis (strain BCG).', *Science (New York, N.Y.)*, 170(3963), pp. 1217–8. doi: 10.1126/science.170.3963.1217.

137. Zbar, B., Ribi, E. and Rapp, H. J. (1973) 'An experimental model for immunotherapy of cancer.', *National Cancer Institute monograph*, 39, pp. 3–9.

138. Zheng, Y. *et al.* (2008) 'Interleukin-22 mediates early host defense against attaching and effacing bacterial pathogens.', *Nature medicine*, 14(3), pp. 282–9. doi: 10.1038/nm1720.

139. Zlotta, A. R. *et al.* (1997) 'Evolution and clinical significance of the T cell proliferative and cytokine response directed against the fibronectin binding antigen 85 complex of

bacillus Calmette-Guerin during intravesical treatment of superficial bladder cancer', *Journal of Urology*. Elsevier Inc., 157(2), pp. 492–498. doi: 10.1016/S0022-5347(01)65185-1.

140. Zlotta, A. R. *et al.* (2000) 'What are the immunologically active components of bacille calmette-guerin in therapy of superficial bladder cancer?', *International Journal of Cancer*, 87(6), pp. 844–852. doi: 10.1002/1097-0215(20000915)87:6.

Aims of this PhD Project

Aim 1.

The first aim of this PhD research was to assess the immune impact of BCG on fresh human bladder tumors.

Aim 2.

The second aim of this work was to identify intrinsic cancer-cell resistance mechanisms to BCG.

Aim 3.

The third aim of this PhD has been to describe the evolving immune landscape *in situ* in a longitudinal cohort of BCG-resistant bladder tumors.

Chapter II. Results

HLA-I downregulation together with epithelial-mesenchymal transition is a mechanism of tumor escape to intravesical BCG immunotherapy in non-muscle invasive bladder cancers.

Patients with high-risk non muscle-invasive bladder cancers (NMIBC) frequently relapse after standard BCG immunotherapy and have a dismal outcome after progression to muscle-invasive bladder cancer (MIBC) (Ge *et al.*, 2018; Pietzak *et al.*, 2019). Although BCG induces potent inflammatory responses upon intravesical instillations, the mechanisms of tumor resistance to such immunotherapy remain elusive(Redelman-Sidi, Glickman and Bochner, 2014; Pettenati and Ingersoll, 2018). Here, we developed an *ex vivo* BCG therapy assay, using fresh human bladder tumors. We found that a subset of urothelial cancer cells downregulate HLA-I expression together with an epithelial to mesenchymal transition (EMT) upon co-incubation with BCG. This phenomenon was confirmed *in vitro* on several urothelial cancer cell lines and was associated to intracellular BCG infection. Pathological analyses from a cohort of NMIBC patients relapsing after BCG therapy confirmed that such phenotypic modifications of urothelial cancer cells identify the subset of patients with a fatal outcome. Interestingly, HLA-I loss on urothelial cancer cells at relapse post-BCG therapy was associated to a myeloid tumor microenvironment and an upregulation of immunosuppressive checkpoints. Taken together, our results demonstrate that live attenuated BCG may directly induce immune evasion by infecting a subset of cancer cells and offer a potential strategy for therapeutic stratification based on HLA-I expression in patients with BCG-refractory NMIBC**.**

Introduction

Bladder cancer is a heterogeneous disease that displays invasive and non-invasive histological features, and a wide spectrum of molecular alterations and subtypes (Knowles and Hurst, 2015; Tan *et al.*, 2019). Treatment of non-invasive tumors with high-risk features (carcinoma in situ, high-grade Ta, T1) includes trans-urethral resection of the tumor, followed by intravesical instillations of *bacillus* Calmette-Guérin (BCG) (Babjuk *et al.*, 2019).

The origin of the bacillus Calmette-Guérin (BCG), trace back to the determined and perseverant work of Albert Calmette and Camille Guérin, who developed an attenuated form of live Mycobacterium bovis after 13 years of culture and 231 passages (Calmette, 1927). BCG is still today the only available vaccine against tuberculosis and one of the most successful cancer immunotherapy as a standard treatment for high-risk non muscle-invasive bladder cancer (NMIBC). Despite a multitude of evidence for anti-tumor efficacy, half of high-risk NMIBC patients develop tumor recurrence and, up to 30% will progress to secondary MIBC. Ultimately, 10-15% of high-risk NMIBC patients die of metastatic disease (Van Den Bosch *et al.*, 2011; Chamie *et al.*, 2013).

New therapeutic strategies are currently in clinical development to treat BCG-unresponsive tumors including antagonistic antibodies directed against the T-cell immune checkpoints PD-1 and PD-L1, but also recombinant adenovirus interferon alfa (Ad-IFNα/Syn3), oncolytic virus and STING agonists (Shore *et al.*, 2017; Singh *et al.*, 2017; Annels *et al.*, 2019; Balar *et al.*, 2019; Huang *et al.*, 2019). Although recent studies have identified potential immune parameters that could impact clinical response (Biot, 2013; A M Kamat *et al.*, 2016; Chevalier, Trabanelli, *et al.*, 2017; Pichler *et al.*, 2017; Chevalier *et al.*, 2018), mechanisms of tumor resistance to BCG immunotherapy remain poorly understood. Indeed, modeling early stage bladder cancer in mice is particularly challenging, owing to the rapid tumor growth inside the bladder wall (Kobayashi *et al.*, 2015). Additionally, tumor heterogeneity and plasticity of

cancer cells undermine our attempts to precise dynamics of immune escape under selective pressure (Nieto *et al.*, 2016; Spranger *et al.*, 2018). How cancer cells evade to the anti-tumor immune response, and whether cancer cells acquire intrinsic undesirable characteristics upon BCG exposure remain unknown. Altogether, this highlights the crucial need to better understand the mechanisms of tumor resistance that occur during BCG immunotherapy in order to identify new targetable pathways and treatment strategies.

In this study, we investigated intrinsic cancer characteristics acquired by the cancer cells upon BCG exposure and found that this immunotherapy could induce an epithelial-mesenchymal transition with HLA-I downregulation. *O*ur results highlight a new mechanism of resistance to BCG immunotherapy and propose a biologically relevant and clinically feasible stratification strategy for the treatment of patients with relapsing NMIBC.

Results

BCG co-culture with fresh human bladder tumors induces cytokine inflammatory responses but do not activate tumor infiltrative lymphocytes

Dynamics of the immune responses following intravesical BCG remain poorly understood in humans. To assess the immunostimulatory effects of BCG in urothelial cancers, we co-incubated BCG for 72 hours with whole cell suspensions providing from freshly dissociated human bladder tumors (Fig. 1a). All the samples were obtained from patients with early-stage bladder tumors undergoing curative intent surgery. To explore the ability of BCG to induce early immune responses, we assessed the cytokines and chemokines released 3 days after a transient co-culture with tumor and immune cells. Strikingly, we observed that BCG led to a potent immune response dominated by IL-1β, TNFα, and GM-CSF production. Additionally, e*x vivo* BCG exposure significantly enhanced IL-2, IL-9 and CCL5 cytokines production. By contrast, we observed significant decreased levels of IFNγ, CCL2 and CCL4 (Fig.

1b, 1c). Overall, this data provides evidence that BCG induces a potent inflammatory response but fails to activate IFNγ-secreting cells in those early stages bladder tumors.

BCG co-culture with fresh human bladder tumors induces a downregulation of HLA-I of urothelial cancer cells

We also evaluated the impact of BCG on the phenotype of immune and tumor cells (Fig. 1d). We observed an unexpected diminution of CD45+ immune cells 3 days after BCG exposure. However, no variation among the immune cells subsets was observed. The relative proportion of lymphoïd (CD3+, CD20+, CD56+) and myeloïd (CD11b+) cell substets among live CD45+ cells remained stable in the BCG condition compared to medium and IFNγ (Fig. 1e). Additionally, the relative proportions of CD4+ and CD8+ among live CD3+ cells together with FoxP3+ among live CD4+ cells were also stable. To investigate the ability of BCG to activate T-cells and NK cells, we evaluated the relative proportion of HLA-DR+ in CD4+, CD8+, CD56+, and PD1+ in CD3+ immune cells. No difference was observed across conditions (Fig. 1 f). However, we noticed a significant HLA-I downregulation on tumor cells after BCG exposure both in terms of relative proportion among tumor cells and in terms of mean fluorescence intensity (Fig 2a, 2b). We further assessed the proliferative activity and apoptosis in HLA-I deficient tumor cells. Interestingly, the percentage of Ki67+ cells was not different according to HLA-I expression suggesting that HLA-I deficient tumor cells were actively proliferative. However, we observed a significant diminution of Annexin-V positive cells and EpCAM positive cells in HLA-I deficient cancer cells (Fig. 2c.).

BCG induces a durable HLA-I downregulation upon intracellular infection of some human urothelial cancer cells. To investigate the effect of BCG on HLA-I expression, we co-incubated BCG with low-grade (RT4), and high-grade (5637, HT1376, TCCSUP and UM-UC3)

human bladder cancer cell lines derived from human primary bladder tumors (Fig. 3a). We observed a concomitant and significant decrease of mean fluorescence intensity (MFI) for HLA-I (HLA-I subsets) and beta-2 microglobulin (B2m) in high-grade cancer cells 24h after BCG co-culture (Fig. 3b) By contrast, BCG enhanced HLA-I expression in low-grade RT4 cancer cells 24h after BCG exposure. Overall, these results indicate that BCG differently affects HLA-I expression in high-grade and low-grade cancer cells. Moreover, we observed that HLA-I deficiency affected only a subset of tumor cells across the cell lines tested (Fig. 3c). We next evaluated whether HLA-I downregulation was sustained over time. To test this approach, we cell-sorted cancer cells based on HLA-I expression 24 h after BCG exposure. Subsequently, we cultured HLA-I positive and negative cells independently in BCG-free medium for 7 days (Fig. 3d). We next analyzed HLA-I expression by flow cytometry at day 7. We still observed a significant reduction of MFI HLA-I in HLA-I negative cells (Fig. 3e). Then we wondered if that HLA-I downregulation was directly dependent from the live *bacilli* or from BCG elements, which could stimulate pattern recognition receptors. Indeed, BCG has been shown to contain molecular elements, which could directly activate toll-like receptors (TLR) 2, 4 and 9. Therefore, we compared the effects of live attenuated strains of BCG with agonists of TLR2, TLR4, and TLR9. Strikingly, neither TLR agonists alone nor combinations of TLR agonists including TLR2+TLR4 and TLR2+TLR4+TLR9 were able to induce HLA-I downregulation on cancer cells (Fig. 3f).

To assess whether therapeutic BCG was able to infect cancer cells, we co-incubated BCG labeled with calcein together with 3 cancer cell lines (RT4, 5637, and UM-UC3) and used ImageStream technology in order to visualize intracytoplasmic *bacilli* (Fig. 3g). Strikingly, we observed that BCG was able to infect cancer cells with variable frequency among cell-lines including at low BCG/cancer cells ratio (MOI as low as 1:10; Fig. 3h Fig. 3i). We demonstrated for the first time that therapeutically used lyophilized BCG for intravesical delivery directly

induced cytoplasmic infection of human cancer cells *in vitro*. Collectively, these data demonstrate that live attenuated mycobacteria provided from therapeutic BCG were able to directly infect bladder cancer cells, and induce a downregulating HLA-I in a subset of cancer cells.

BCG infected cancer cells acquire a senescent-like phenotype with EMT characteristics. We investigated whether HLA-I negative cells hold specific characteristics by comparison to HLA-I positive cells. First, we observed specific morphological differences between cancer cells after BCG exposure. HLA-I negative cells were characterized by lower forward scatter and side scatter, cell shrinkage, flattened bodies, and loss of adhesion to the neighbors cells in HLA-I negative cells (Fig. 4a,c). By contrast, HLA-I positive cells were morphologically similar to the parental cell-line. We next investigated the relative proportion of Ki67+ cells among live cells. Although the majority of HLA-I positive cells were proliferative, HLA-I negative cells partially or completely lost their ability to proliferate (Fig. 4b). Overall, these data suggest that HLA-I negative cells acquire a quiescent state with a senescent-like phenotype 24h after BCG exposure. These morphological changes were maintained over time after 7 days in culture with BCG-free medium.

However, some cancer cells reacquired the parental phenotype suggesting a transient and partially reversible state (Fig. 4c). Furthermore, we evaluated the membrane expression of EpCAM on a broad range of bladder cancer cells, ranging from epithelial to mesenchymal phenotype as previously described (Tan, *et al.*, 2014). Strikingly, we observed a correlation between HLA-I downregulation and EpCAM loss in epithelial cells (Fig. 4d, Fig. 4f.). Similarly to HLA-I downregulation, EpCAM loss was maintained over time (Fig. 4e). This data suggest that BCG may induce an epithelial-to-mesenchymal phenotype in epithelial cancer cells.

To further explore this hypothesis, we analyzed the EMT status of cancer cells after BCG

infection. In this experimental study, we used three cell-lines with the most extreme EMT status including the epithelial cell-line RT4, the mesenchymal cell-line UM-UC3 and the 5637 cancer cell-line with intermediate EMT status. In order to identify a shift toward a mesenchymal state, we cell-sorted the cells 24h after BCG exposure and extracted total RNA separately in HLA-I positive and negative cells. We next calculated the EMT score for each cancer cells. Although no difference was observed for RT4 and UM-UC3, we identified a significant shift to a mesenchymal score in HLA-I negative 5637 cancer cells (Fig. 4g). Overall, this data suggests that BCG exposure may induce a mesenchymal transition in epithelial cancer cells. To determinate whether BCG uptake by the cells induced this mesenchymal transition, we monitored these cancer cells using the ImageStream technology. Strikingly, we observed a significant correlation between EpCAM loss, and BCG uptake by cancer cells (Fig. 4h). Collectively, these data provide evidence that BCG infection may induce a senescent-like phenotype with EMT characteristics in a subset of cancer cells.

BCG induces specific cancer cells inflammatory responses.

To investigate whether BCG impacted gene expression, we identified the top 25 differentially expressed genes between EMT-high and EMT-low 5637 cell-line. Next, we applied unsupervised hierarchical analyses to RT4, 5637 and UM-UC3 based on the 25 selected genes quantified after BCG exposure. We confirmed that EMT-low 5637 cells clustered with the epithelial RT4 cell-line, and EMT-high 5637 with the mesenchymal UM-UC3 cell-line (Fig. 5a). Strikingly, cancer cells acquiring a mesenchymal status were associated with enhanced mRNA levels of IFN-stimulated genes IFI1, IFIT2, IFIT3, IFI6, IFI27, and CCL2. We also noticed increased expression of the EMT activator Zeb1, tumor-associated antigens MAGEA3/A6, MAGEC2, and metalloproteinase in EMT-high cancer cells (Fig. 5a). By contrast, EMT-low cancer cells were associated with enhanced IL1β and CXCL5

mRNA expression. We also noticed higher levels of EpCAM, E-Cadherin and integrin ITGB8 mRNA in this epithelial group. Overall, these results indicate that BCG infected cancer cells shifting to a mesenchymal state displayed a type I IFN pathway, by contrast with the pro-inflammatory IL1 cytokine pathway observed in epithelial cells.

Next, we investigated the levels of cytokines and chemokines release by cancer cells 24h after BCG exposure. Accordingly to prior experimental setting, cancer cells were cell-sorted based on HLA-I expression and cultured independently in BCG medium-free environment. At day 6, supernatants were analyzed by multiplex analysis. We observed different secretory profile in EMT-high and EMT-low cancer cells. Notably, cells acquiring a mesenchymal state after being infected by BCG displayed higher levels of G-CSF, VEGF, and IL15 (Fig. 5b). By contrast, sustained levels of IL8 and IL1-RA were observed in cancer cells that remained with an epithelial state. Overall, these results suggest that pro-tumoral cytokines release is enhanced in BCG infected cancer cells after acquiring a mesenchymal state.

To test whether the re-stimulation of cancer cells with BCG would enhance their cytokine production, we co-incubated cancer cells with BCG for 24h. Then, cells were cultivated in BCG-free medium for 6 days. At day 7, cancer cells were re-stimulated with BCG for 24h. We next analyzed the cytokine and chemokine release in the cancer cells supernatant. Strikingly, we observed increased levels of G-CSF, IL1-RA, IL6, PDGF-bb, VEGF, TNFα, and CCL5 (Fig. 5c). Overall, these data suggest that cancer cells acquire an immune memory after the first BCG stimulation that enables a stronger immune response to secondary BCG stimuli.

BCG generates *in situ* myeloid-suppressive immune responses in HLA-I deficient tumor cells. In order to investigate the immune response in BCG resistant tumors, we assessed the gene expression profile in a longitudinal cohort of patients with paired tumors before and after intravesical BCG immunotherapy (Fig. 6a). We observed a significant upregulation of

immune-related genes in BCG resistant tumors. Notably, we observed a significant increased IL8 and IL6 cytokine expression, as well as the activation of granulocyte and neutrophils pathways (Fig. 6b). We also identified higher levels of CD4 and CD8 mRNA, as well as immune-checkpoint inhibitory receptors CTLA-4, TIM3, Lag3, IDO1, PD1, TIGIT, BTLA and their respective ligands PD-L1, PD-L2 CD80/CD86 (Fig. 6b). Overall, these data provide evidence that both myeloid and adaptive immune responses significantly increased in BCG resistant tumors.

Next, we assessed HLA-I expression in tumor cells before and after acquiring BCG-resistance. Strikingly, we observed HLA-I downregulation in half of the tumors (Fig. 6c). Based on *in vitro* data, we hypothesized that the evolution of HLA-I expression in tumor cells could affect *in situ* cancer inflammatory responses and subsequently impact the immune microenvironment. To test this hypothesis, we evaluated the differential gene expression profile before and after intravesical BCG according to the evolution of HLA-I expression in tumor cells (Fig. 6d). First, we identified a myeloid-suppressive immune microenvironment with enhanced levels of IL10, CD163, CSF-1R, CSF-3R and IL8 mRNA transcripts in tumor cells with HLA-I downregulation (Fig. 6e). Subsequently, we also observed a macrophage signature in BCG-resistant tumors characterized by enhanced CD47, CD80/86, DDP4 mRNA expression (Fig. 6f). By contrast, HLA-I upregulation on tumor cells was significantly associated with a tumor-suppressive cytotoxic immune microenvironment characterized by increased levels of CD8, IFNg, GZMB, PFR, IL6, CXCL10, CXCL11 (Fig. 6d). Overall, these findings suggest that immunogenicity of tumor cells profoundly affect the establishment of effective anti-tumor immune response *in situ*.

To further validate our findings at the protein level, we investigated the evolution of tumor-infiltrating lymphocytes by immunohistochemistry before and at relpase after BCG immunotherapy (Fig. 6g). We confirmed that HLA-I upregulation on tumor cells after BCG

was significantly associated with an increased level of CD8+ among CD3+ T-cells, and PD-L1 upregulation on immune cells. By contrast, tumors with HLA-I downregulation were poorly infiltrated by CD8+ T-cells (Fig. 6h). Overall, these findings suggest that BCG generates distinct inflammatory responses in tumor microenvironment, owing to the cancer cells immunogenicity.

Next, we hypothesized that HLA-I deficiency was associated with poor prognosis. We observed significant increased risk of metastasis, reduced cancer-specific and overall survival in patients who acquired HLA-I downregulation on cancer cells after BCG exposure (Fig. 6i). Although HLA-I deficient tumor cells were associated with increased EMT score, this difference did not reach statistical significance. However, we compared the EMT score of each tumor sample before and at relapse after BCG immunotherapy. Strikingly, we observed a significant increased EMT level in patients who further developed bladder cancer metastases after BCG. Collectively, this data provide evidence that HLA-I deficiency following BCG exposure led to immune suppressive microenvironment, and increased metastatic potential of tumor cells.

Discussion

Although BCG intravesical therapy has been a NMIBC standard of care for decades, it is still unclear today how this immunotherapy actually works and can generate anti-tumor immune responses. Therefore, our work initially aimed at understanding the impact of BCG immunotherapy in bladder cancers and understand why some patients relapse post-BCG and eventually die from high-risk NMIBC. Our experiments on fresh bladder tumors first showed that while BCG generates potent cytokine inflammatory responses, including increases in IL1β, GM-CSF and TNFα, it had unexpectedly no effect on the activation phenotype of tumor infiltrative lymphocytes. More surprisingly, we observed that BCG exposure induced HLA-I

downregulation in a subset of cancer cells. Because lyophilized therapeutic BCG includes a lot of dead mycobacteria upon reconstitution, and that BCG molecular components have already been shown to directly stimulate TLR 2, 4 & 9 (Harding and Boom, 2010) we wondered if that HLA-I downregulation was not due to a consequence of such innate immune receptor stimulation. Therefore, we demonstrated that HLA-I deficient cancer cells are only observed after co-culture with live attenuated *Mycobacterium bovis* provided from therapeutic BCG and not from direct TLR signaling with agonists. Even combining TLR2, TLR4, and TLR9 agonists provided from heat-killed bacteria, did not induce HLA-I deficiency after co-culture with cancer cells. This question was also important because synthetic TLR agonists are currently actively developed in early phase clinical trials, in order to activate antigen presenting cells which are critical for antitumor T-cell mediated immune responses. They could therefore be envisioned as an alternative synthetic therapy to replace and address the shortage of BCG therapy (Mostafid *et al.*, 2015; Shekarian *et al.*, 2017; Aleynick *et al.*, 2019). Also, EpCAM loss in cancer cells observed upon BCG exposure, was not observed with TLR agonists, suggesting that live and intact bacteria might be necessary for the epithelial-mesenchymal transition. Other studies have shown that the therapeutic use of live and intact pathogens were more biologically active than pathogen extracts. This first observation would therefore suggest that the lack of efficacy of BCG therapy could be more in relationship with its direct effect on cancer cells and their ability to escape HLA-I recognition rather than on a direct activation of anti-tumor lymphocytes.

We also observed that such BCG exposure induced a senescence-like phenotype of urothelial cancer cells, with epithelial-to-mesenchymal transition and specific pro-inflammatory responses. In line with those *ex vivo* and *in vitro* functional assays, we found indeed that HLA-I downregulation could be found in a subset of BCG-refractory tumors. More surprisingly, this subset of patients with HLA-I low tumors after BCG therapy presented with

an immunosuppressive type of tumor microenvironment and a dismal survival outcome.

A prior study showed that intravesical BCG immunotherapy requires live attenuated *bacilli* to induce the priming of naïve CD4+ T-cells in draining lymph nodes by activated dendritic cells (Biot, 2013). Our data showed that therapeutic BCG is also able to directly infect cancer cells in vitro. Another study led to the same observation by co-incubating cancer cells with live BCG Pasteur strain (Redelman-Sidi *et al.*, 2013).

IFNγ is a critical mediator for cellular immune response against mycobacteria. More recently, non-restricted CD1+ T-cells have been also identified as a non-cognate source of IFNγ, providing notably from non-specific CD8+ T cells and NK cells (Kupz *et al.*, 2016). A prior study also showed evidence that pre-existing BCG immunity enhanced anti-tumor immune response, both in retrospective clinical data and experimental mouse models (Biot, 2013). One potential explanation for that observation was that intravesical BCG could trigger a rapid Th1 adaptive immune response leading to enhanced levels of IFNγ. The consequence would therefore be an increased activation of macrophages, a phagocytosis of infected tumor cells, and an activation and migration of dendritic cells (DCs) for tumor antigen-presentation to naïve CD4+ T-cells. In our experiments of BCG co-culture with fresh human bladder tumors could not show an IFNγ release in the supernatants of such functional assays. The fact that no IFNγ was found upon BCG exposure could be due to the fact that such variations are very small and would require more sensitive technique of titration. Another hypothesis would be that IFNγ peaks are short lived and not detected with our experimental settings. Last but not least, some biological effects could simply occur because of the differences in BCG strains that are used by research teams (Gan *et al.*, 2013). But it is also possible that IFNγ release is not a consequence of BCG exposure as it is suggested by our supernatant titration results and the fact that our positive control (pure IFNγ) did not lead to the same effect than BCG, notably regarding to the HLA-I downregulation by tumor cells.

Moreover, we demonstrated that infection of cancer cells by live attenuated Mycobacterium *bovis* was significantly associated with both HLA-I and EpCAM downregulation in a subset of cancer cells. These findings establish an unexpected association between BCG uptake by cancer cells, immune evasion and EMT induction. This data is reinforced by the activation of the type I IFN pathway observed in BCG infected cells. Recently, type I IFN signature has been established as a predictive factor for immune evasion leading to severe active tuberculosis infection (Singhania *et al.*, 2018). Several mechanisms underlying the pathogenic role of type I IFN in tuberculosis have been described, including induction of IL-10 and negative regulation of the IL-12/IFNγ and IL-1β/PGE2 host-protective responses (McNab *et al.*, 2015). Additionally, the type I IFN pathway has also been associated with apoptosis resistance, cancer-cell stemness and upregulation of immune inhibitory ligands such as PD-L1 (Benci *et al.*, 2016; Musella *et al.*, 2017; Jacquelot *et al.*, 2019). These findings may be one explanation for the observed association between BCG failure and worse clinical outcomes. Moreover, we observed that cancer cells acquired a quiescent state associated with immune evasion. This ability to downregulate HLA-I expression and stop proliferate has been recently highlighted as the main characteristic of stem cell to evade from immune surveillance (Agudo *et al.*, 2018). Because repeated BCG instillations are delivered every week for 6 weeks in routine practice, we tested the effect of a second BCG stimulation *in vitro* after a washout period of 6 days. Surprisingly, we found that after a 2nd BCG stimulation, the quantity of VEGF, G-CSF and IL15 cytokines released by cancer cells was increased compared to the first exposure. Trained innate immunity is a recent concept that elucidates the acquisition of immune memory by innate immune cells following first stimuli with pathogens (Netea *et al.*, 2016). Herein, we report for the first time that cancer cells may also acquire such immune memory following prior stimulation with a pathogen agent. In addition, these data indicate that cancer cells may attract myeloid cells by secreting G-CSF and

promote tumor neo-angiogenesis *in situ* following VEGF secretion.

Finally, i*n situ* analyses of paired bladder tumors before and after BCG immunotherapy supported our preclinical findings. Indeed, some patients displayed a dowregulation of HLA-I expression in their tumors after BCG exposure. This subset of patients showed an upregulation of myeloid genes and immunosuppressive pathways, together with a gene signature of EMT in their tumors. More importantly, those patients were strikingly more prone to have a cancer recurrence and to die from this cancer relapse. Alternatively, patients with a tumor keeping HLA-I expression after BCG exposure were more infiltrated by CD8+ T-cells and were more expressing IFNg and PD-L1. Therefore, our hypothesis is that HLA-I^{hi} bladder cancers would allow for the development of an anti-tumor cytotoxic CD8+ T-cell response and lead to an effective adaptive antitumor immunity with disease control over time. However, acquired HLA-I deficiency by tumor cells seem to induce a myeloid immunosuppressive microenvironment, which would then explain the absence of a meaningful antitumor immunity and a dismal cancer outcome.

Altogether, we demonstrate here for the first time that BCG induces HLA-I downregulation and senescent-like phenotype of cancer cells, leading to the cancer cell immune evasion, and dismal NMIBC prognosis. Our results have several clinical implications. First, our data have identified a subgroup of high-risk NMBIC patients with an easy-to-implement biomarker. Indeed, HLA-I expression by IHC staining is validated within all pathology departments and its downregulation could be easily assessed in routine practice by immunohistochemistry. Second, the identification of such HLA-I^{lo} patients having a bad outcome would offer an opportunity to stratify the clinical care of NMIBC. Indeed, dedicated clinical trials of treatment intensification should now be designed for this subgroup of HLA-I^{lo} patients in order to improve their survival. Third, our transcriptomic and IHC results have identified several molecules associated to the subgroup of HLA-I^{lo} patients, which are amenable to

therapeutic targeting such as the targeting of CSF1R, or CD47/SIRPα axis, which are currently in clinical development.

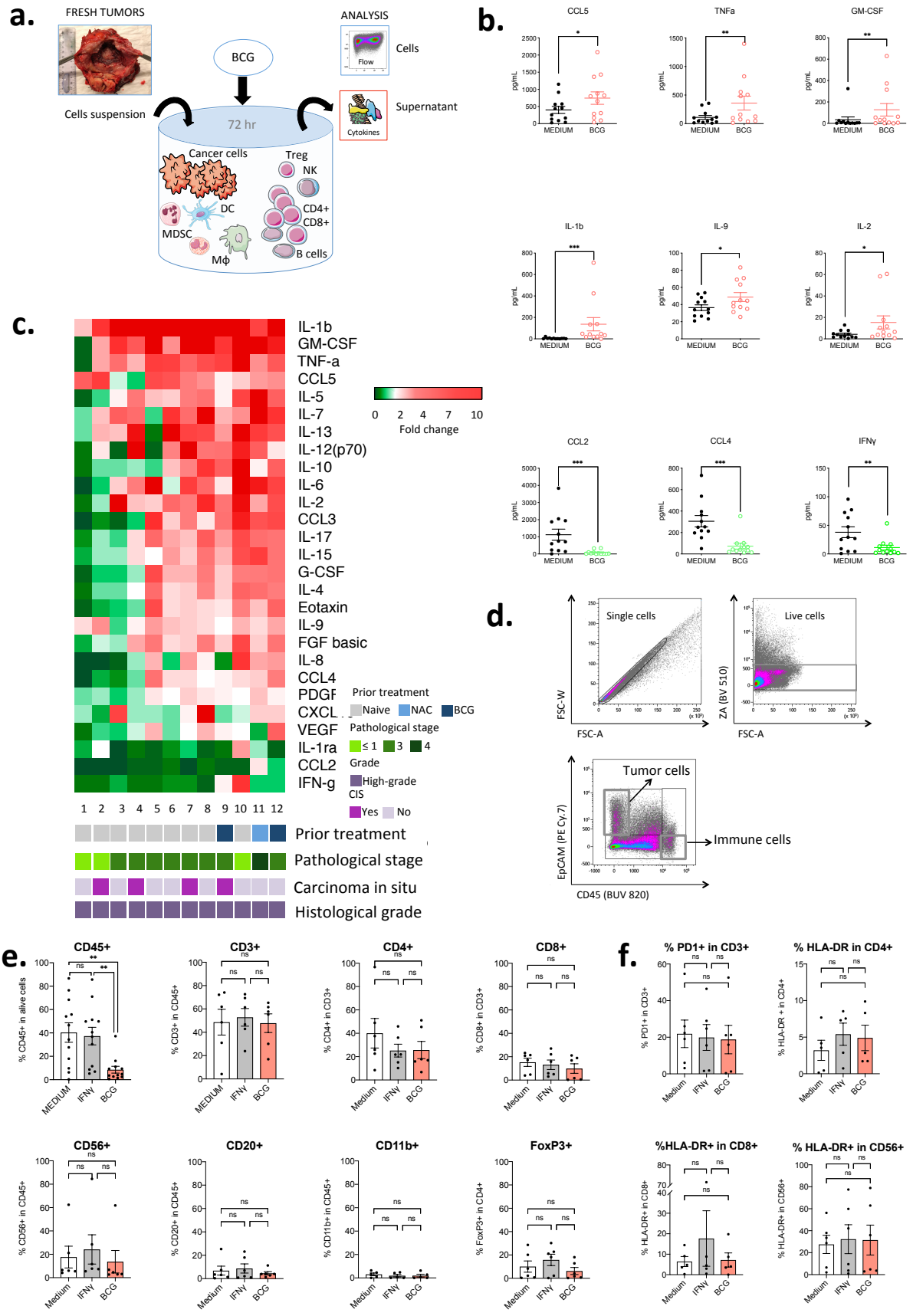
a.
FRESH TUMORS
Cells suspension
BCG
72 hr
Cancer cells
Treg
NK
DC
CD4+
CD8+
MDSC
Mφ
B cells
ANALYSIS
Flow
Cells
Cytokines
Supernatant
b.
CCL5
TNFa
GM-CSF
IL-1b
IL-9
IL-2
CCL2
CCL4
IFNγ
pg/mL
MEDIUM
BCG
c.
IL-1b
GM-CSF
TNF-a
CCL5
IL-5
IL-7
IL-13
IL-12(p70)
IL-10
IL-6
IL-2
CCL3
IL-17
IL-15
G-CSF
IL-4
Eotaxin
IL-9
FGF basic
IL-8
CCL4
PDGF
CXCL
VEGF
IL-1ra
CCL2
IFN-g
0 2 4 7 10
Fold change
Prior treatment
Naive NAC BCG
Pathological stage
≤ 1 3 4
Grade
High-grade
CIS
Yes No
1 2 3 4 5 6 7 8 9 10 11 12
Prior treatment
Pathological stage
Carcinoma in situ
Histological grade
d.
Single cells
FSC-W
FSC-A
Live cells
ZA (BV 510)
Tumor cells
Immune cells
EpCAM (PE Cy7)
CD45 (BUV 820)
e.
CD45+
% CD45+ in alive cells
CD3+
% CD3+ in CD45+
CD4+
% CD4+ in CD3+
CD8+
% CD8+ in CD3+
CD56+
% CD56+ in CD45+
CD20+
% CD20+ in CD45+
CD11b+
% CD11b+ in CD45+
FoxP3+
% FoxP3+ in CD4+
MEDIUM IFNγ BCG
Medium IFNγ BCG
f.
% PD1+ in CD3+
% HLA-DR in CD4+
%HLA-DR+ in CD8+
% HLA-DR+ in CD56+
ns

Figure 1.

Figure 1. *Ex vivo* BCG stimulation of fresh human bladder tumors induces inflammatory cytokine responses but no modifications of immune cell phenotype.

a. Primary bladder tumors were freshly mechanically and enzymatically dissociated after surgical resection. Whole cell suspensions were cultivated in complete medium, and stimulated with IFNγ or BCG for 72h. Cytokines and chemokine release (**b**, **c**), tumor-infiltrating immune cells (**d**, **e, f**) were analyzed after 72 hr.

b. Cytokine and chemokine levels in the supernatant were measured using a 27-plex Luminex assay (n=12, paired two-tailed Wilcoxon tests).

c. Cytokine and chemokine fold changes levels between the BCG condition and the medium control depicted in heatmap were determined per individual (rows) and cytokine (columns) (n=12).

d. Gating strategy adopted to detect CD45+ immune cells and CD45- EpCAM+ tumor cells for flow cytometry analysis.

e. Immunophenotyping of tumor-infiltrating lymphoid and myeloid cell subsets after BCG exposure (n=5 ; One-way ANOVA with Tukey's post test).

f. Immune activation of T-cells and NK-cells after BCG exposure (n=5; One-way ANOVA with Tukey's post test).

All data are presented as mean ± s.e.m.

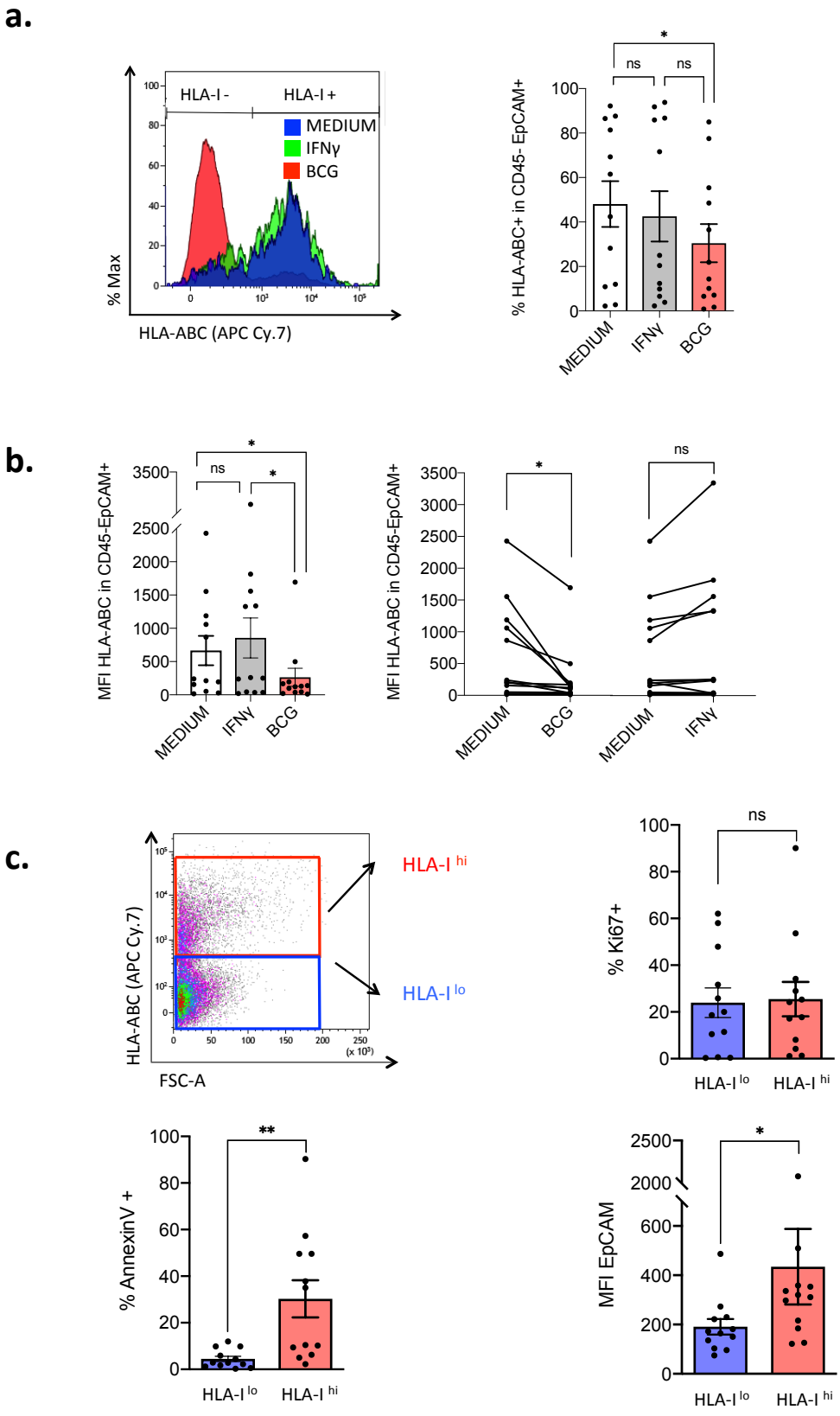
a.
HLA-I -
HLA-I +
MEDIUM
IFNγ
BCG
% Max
HLA-ABC (APC Cy.7)
% HLA-ABC+ in CD45- EpCAM+
ns
ns
*
MEDIUM
IFNγ
BCG
b.
MFI HLA-ABC in CD45-EpCAM+
ns
*
*
MEDIUM
IFNγ
BCG
MFI HLA-ABC in CD45-EpCAM+
*
ns
MEDIUM
BCG
MEDIUM
IFNγ
c.
HLA-ABC (APC Cy.7)
FSC-A
HLA-I hi
HLA-I lo
% Ki67+
ns
HLA-I lo
HLA-I hi
% AnnexinV +
**
HLA-I lo
HLA-I hi
MFI EpCAM
*
HLA-I lo
HLA-I hi

Figure 2.

Figure 2. *Ex vivo* BCG stimulation of fresh human bladder tumors induces a downregulation of HLA-I on urothelial cancer cells.

a) CD45- EpCAM+ cancer cells were analyzed after BCG co-incubation with freshly mechanically and enzymatically dissociated bladder tumors for 72 hr. Relative proportion of HLA-I + cells among living tumor cells population following ex vivo stimulation. (n=12; one-way ANOVA with Tukey's post test).

b) Mean fluorescence intensity (MFI) of HLA-I + cells within living tumor cells population following ex vivo stimulation. (n=12; one-way ANOVA with Tukey's post test).

c) Relative proportion of proliferative Ki67+ and apoptotic Annexin V+, and MFI of EpCAM among living tumor cells. (n=12; paired two-tailed t tests).

All data are presented as mean ± s.e.m.

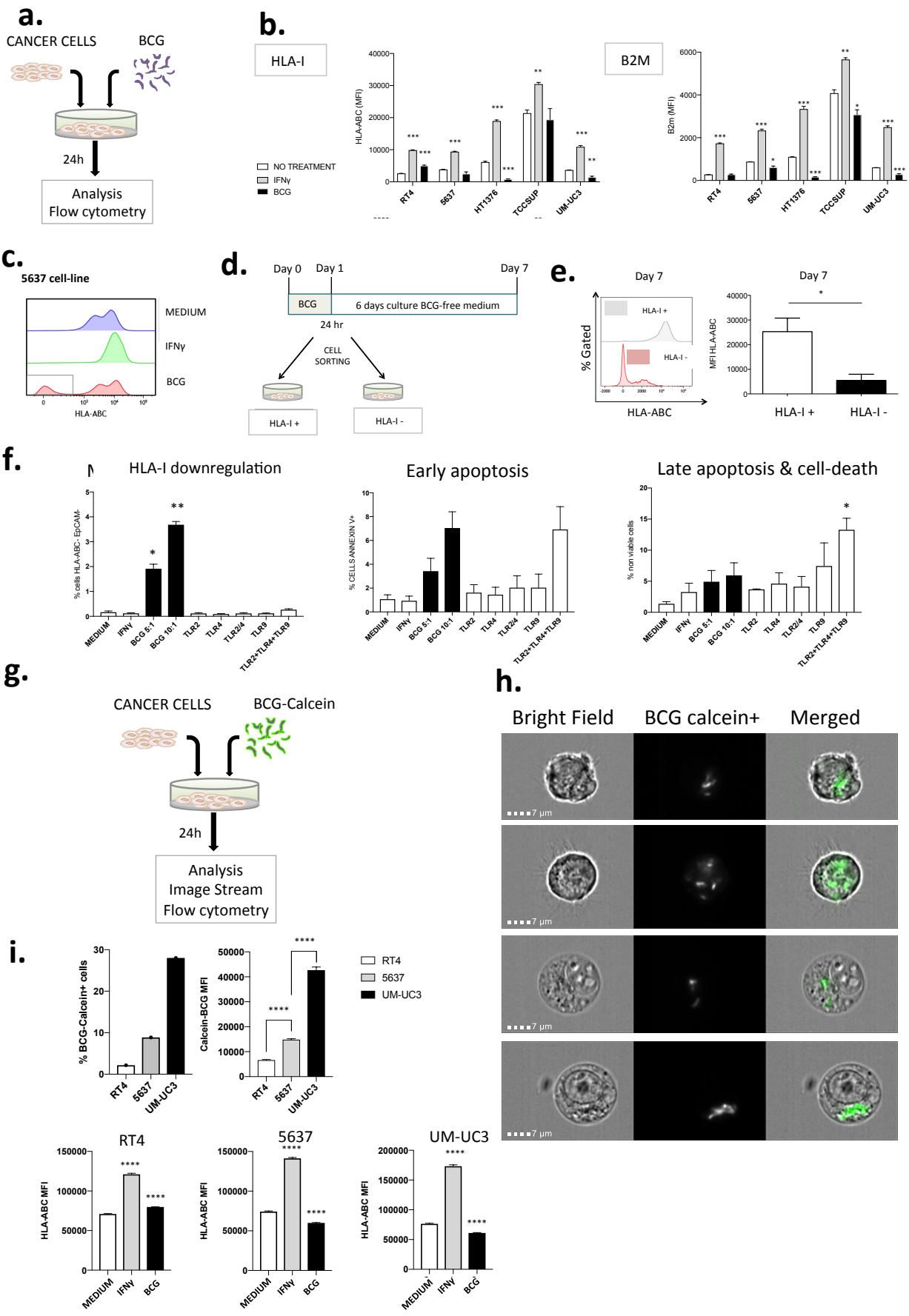
a.
CANCER CELLS
BCG
24h
Analysis
Flow cytometry
b.
HLA-I
B2M
NO TREATMENT
IFNγ
BCG
HLA-ABC (MFI)
B2m (MFI)
RT4
5637
HT1376
TCCSUP
UM-UC3
c.
5637 cell-line
MEDIUM
IFNγ
BCG
HLA-ABC
d.
Day 0
Day 1
Day 7
BCG
6 days culture BCG-free medium
24 hr
CELL SORTING
HLA-I +
HLA-I -
e.
Day 7
% Gated
HLA-ABC
MFI HLA-ABC
f.
HLA-I downregulation
Early apoptosis
Late apoptosis & cell-death
% cells HLA-ABC- EpCAM+
% CELLS ANNEXIN V+
% non viable cells
MEDIUM
IFNγ
BCG 5:1
BCG 10:1
TLR2
TLR4
TLR2/4
TLR9
TLR2+TLR4+TLR9
g.
CANCER CELLS
BCG-Calcein
24h
Analysis
Image Stream
Flow cytometry
h.
Bright Field
BCG calcein+
Merged
7 µm
i.
% BCG-Calcein+ cells
Calcein-BCG MFI
RT4
5637
UM-UC3
HLA-ABC MFI
MEDIUM
IFNγ
BCG

Figure 3.

Figure 3. Live attenuated BCG induces HLA-I downregulation in a subset of human bladder cancer cells.

a. High-grade (n=4) and low-grade (n=1) human bladder cancer cells were cultured in complete medium, and stimulated with IFNγ (10^3U/mL) or co-incubated with BCG (MOI 100:1) for 24h.

b. HLA-I and β2-microgobulin expression were analyzed by flow-cytometry after 24h stimulation. (n=3 conditions per cell-line; one-way ANOVA with Tukey's post test).

c. Representative histograms for 5637 cell-line highlighting HLA-I deficiency in a subset of cancer cells.

d. After 24h BCG co-culture, cell-sorting for HLA-I expression allowed independent culture for HLA-I+ and HLA-I- cancer cells in BCG-free medium for 6 additional days.

e. Immunophenotyping of cancer cells to assess HLA-I expression at day 7. (n=5 cell-lines; unpaired two-tailed t tests).

f. Stimulation assay of 5637 cell-line with TLR2, TLR4, TLR9, and combinations TLR2+TLR4, TLR2+TLR4+TLR9 agonists, compared to BCG. (unpaired two-tailed t test comparing each condition versus control_medium).

g. Experimental setting evaluating co-incubation of cancer cells (RT4, 5637, UM-UC3) with BCG-labeled calcein.

h. Representative images of BCG infected UM-UC3 cancer cells after 24h co-incubation (MOI10:1).

i. Percentage of cancer cells infected by BCG-labeled calcein and MFI BCG-labeled calcein among cell-lines (n=3 conditions per cell-line; one-way ANOVA with Tukey's post test).

j. MFI of HLA-I among cell-lines using ImageStream analysis (n=3 conditions per cell-line; one-way ANOVA with Tukey's post test). All data are presented as mean ± s.e.m.

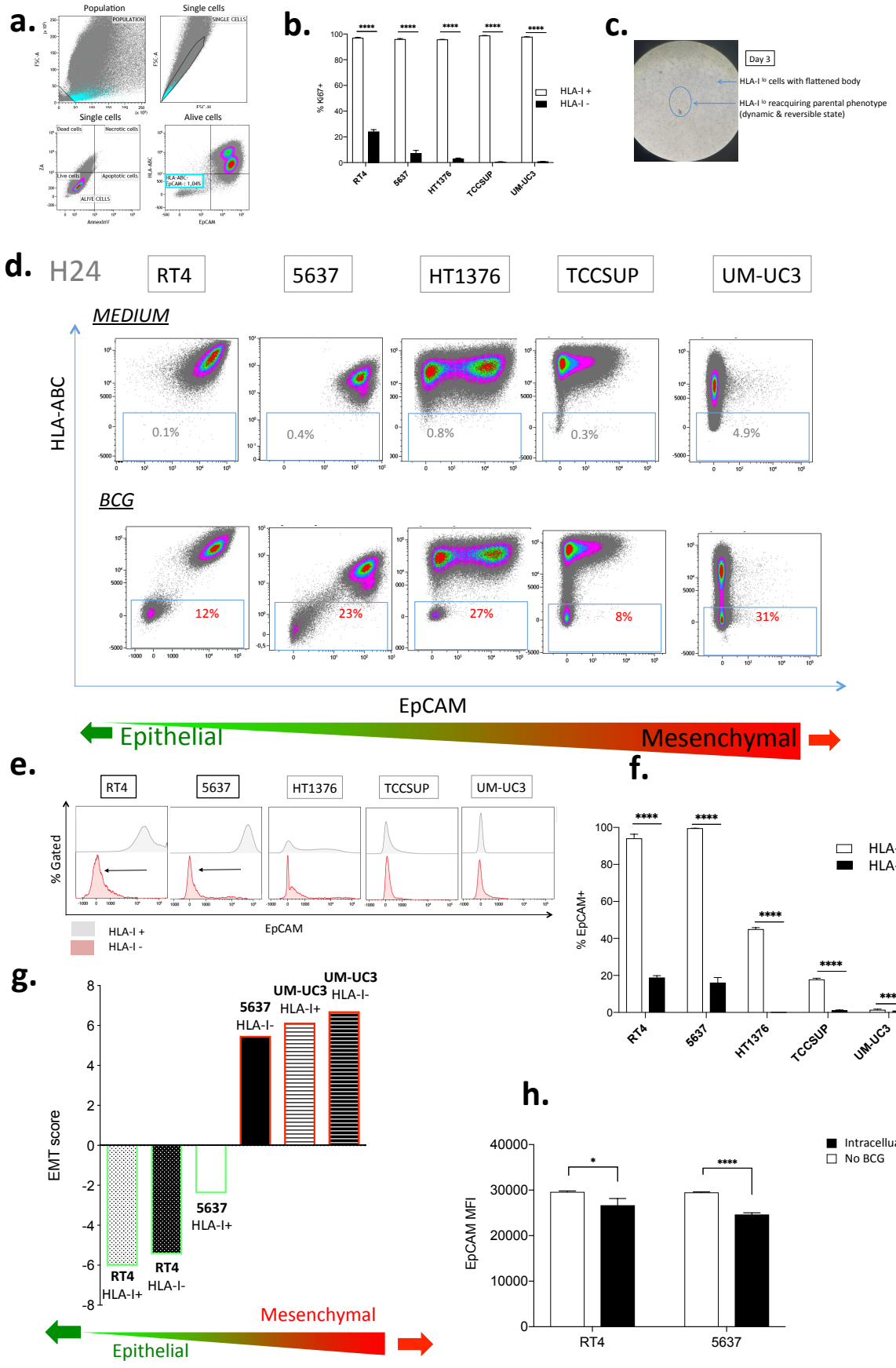
a.
Population
Single cells
Single cells
Alive cells
b.
% Ki67+
HLA-I +
HLA-I -
RT4
5637
HT1376
TCCSUP
UM-UC3
c.
Day 3
HLA-I lo cells with flattened body
HLA-I lo reacquiring parental phenotype
(dynamic & reversible state)
d.
H24
RT4
5637
HT1376
TCCSUP
UM-UC3
MEDIUM
HLA-ABC
0.1%
0.4%
0.8%
0.3%
4.9%
BCG
12%
23%
27%
8%
31%
EpCAM
Epithelial
Mesenchymal
e.
RT4
5637
HT1376
TCCSUP
UM-UC3
% Gated
EpCAM
HLA-I +
HLA-I -
f.
% EpCAM+
HLA-I +
HLA-I -
RT4
5637
HT1376
TCCSUP
UM-UC3
g.
EMT score
RT4
HLA-I+
RT4
HLA-I-
5637
HLA-I+
5637
HLA-I-
UM-UC3
HLA-I+
UM-UC3
HLA-I-
Mesenchymal
Epithelial
h.
EpCAM MFI
Intracelluar BCG
No BCG
RT4
5637

Figure 4.

Figure 4. BCG infected cells acquire a senescent-like phenotype with EMT characteristics.

a. Phenotypic characteristics of HLA-I negative cells (in blue) among cancer cells population (in grey). Representative dot-plots for 5637 cell-line.

b. Relative proportion of Ki67+ cells among different cancer cell-lines after 24h BCG co-culture (unpaired two-tailed t tests).

c. Morphology of HLA-I negative cells after cell-sorting. Representative imaging for 5637 cell-line 3 days after culture in BCG-free medium. Cells inside the circle reacquired parental cell-line morphology.

d. Dot-plots for HLA-I among EpCAM expression in live cancer-cells. Dot-plots illustrate control condition at the top, and BCG condition at the bottom. Cancer-cells are classified according to baseline expression of EpCAM (MFI) ranging from the left (epithelial cell RT4) to the right (mesenchymal UM-UC3).

e. Histograms depicting EpCAM expression for HLA-I positive and negative cells. Representative images for each cancer cell-line 6 days after culture in BCG-free medium.

f. Relative proportions of EpCAM+ cells among HLA-I positive and negative cells 24h after BCG exposure (unpaired two-tailed t tests).

g. EMT score of HLA-I negative and positive cells 24h after BCG exposure.

h. MFI for EpCAM in BCG infected (intracellular BCG-calcein) versus non-infected cancer cells (unpaired two-tailed t tests).

All data are presented as mean ± s.e.m.

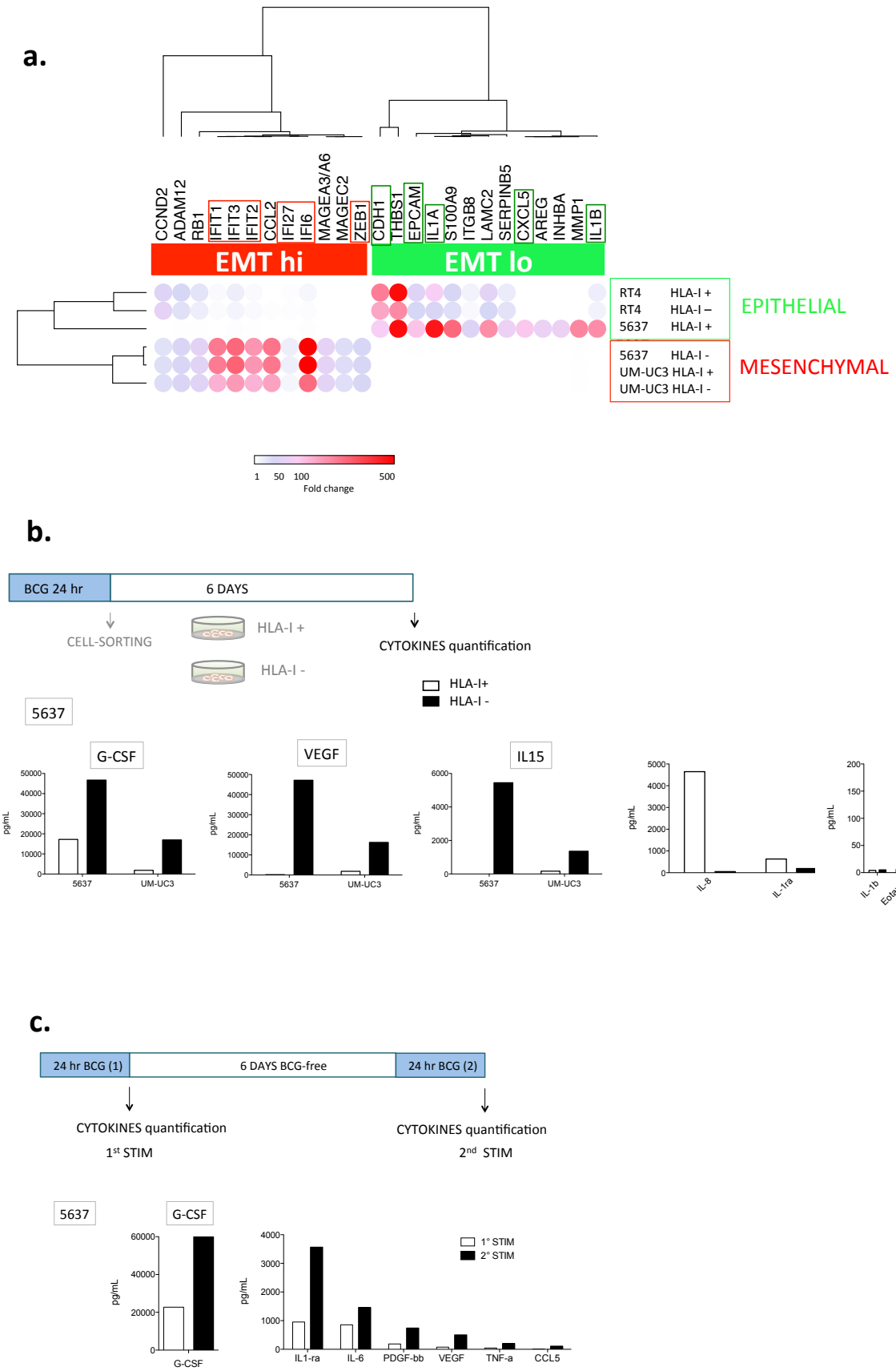
a.
CCND2
ADAM12
RB1
IFIT1
IFIT3
IFIT2
CCL2
IFI27
IFI6
MAGEA3/A6
MAGEC2
ZEB1
CDH1
THBS1
EPCAM
IL1A
S100A9
ITGB8
LAMC2
SERPINB5
CXCL5
AREG
INHBA
MMP1
IL1B
EMT hi
EMT lo
RT4 HLA-I +
RT4 HLA-I –
5637 HLA-I +
EPITHELIAL
5637 HLA-I -
UM-UC3 HLA-I +
UM-UC3 HLA-I -
MESENCHYMAL
1 50 100 500
Fold change
b.
BCG 24 hr
6 DAYS
CELL-SORTING
HLA-I +
HLA-I -
CYTOKINES quantification
HLA-I+
HLA-I -
5637
G-CSF
VEGF
IL15
pg/mL
5637
UM-UC3
IL-8
IL-1ra
IL-1b
Eotaxin
MIP-1b
IL-6
IP-10
GM-CSF
c.
24 hr BCG (1)
6 DAYS BCG-free
24 hr BCG (2)
CYTOKINES quantification
1st STIM
CYTOKINES quantification
2nd STIM
5637
G-CSF
pg/mL
1° STIM
2° STIM
IL1-ra
IL-6
PDGF-bb
VEGF
TNF-a
CCL5

Figure 5.

Figure 5. BCG induces different inflammatory responses in cancer cells depending on their EMT and HLA-I status and those responses are enhanced over time.

a. Hierarchical clustering analysis of cancer cells according to EMT status, depicted per cell-line (rows) and immune genes (columns).

b. Cytokine and chemokine levels in the supernatant were measured separately in HLA-I positive and negative cells (5637) 6 days after culture in BCG-free medium.

c. BCG restimulation assay evaluating immune memory of cancer cells (5637). First stimulation for 24hours, followed by 6 days culture in BCG-free medium and 2^{nd} BCG exposure for 24h. Cytokines measured after 1^{st} and 2^{nd} stimulation.

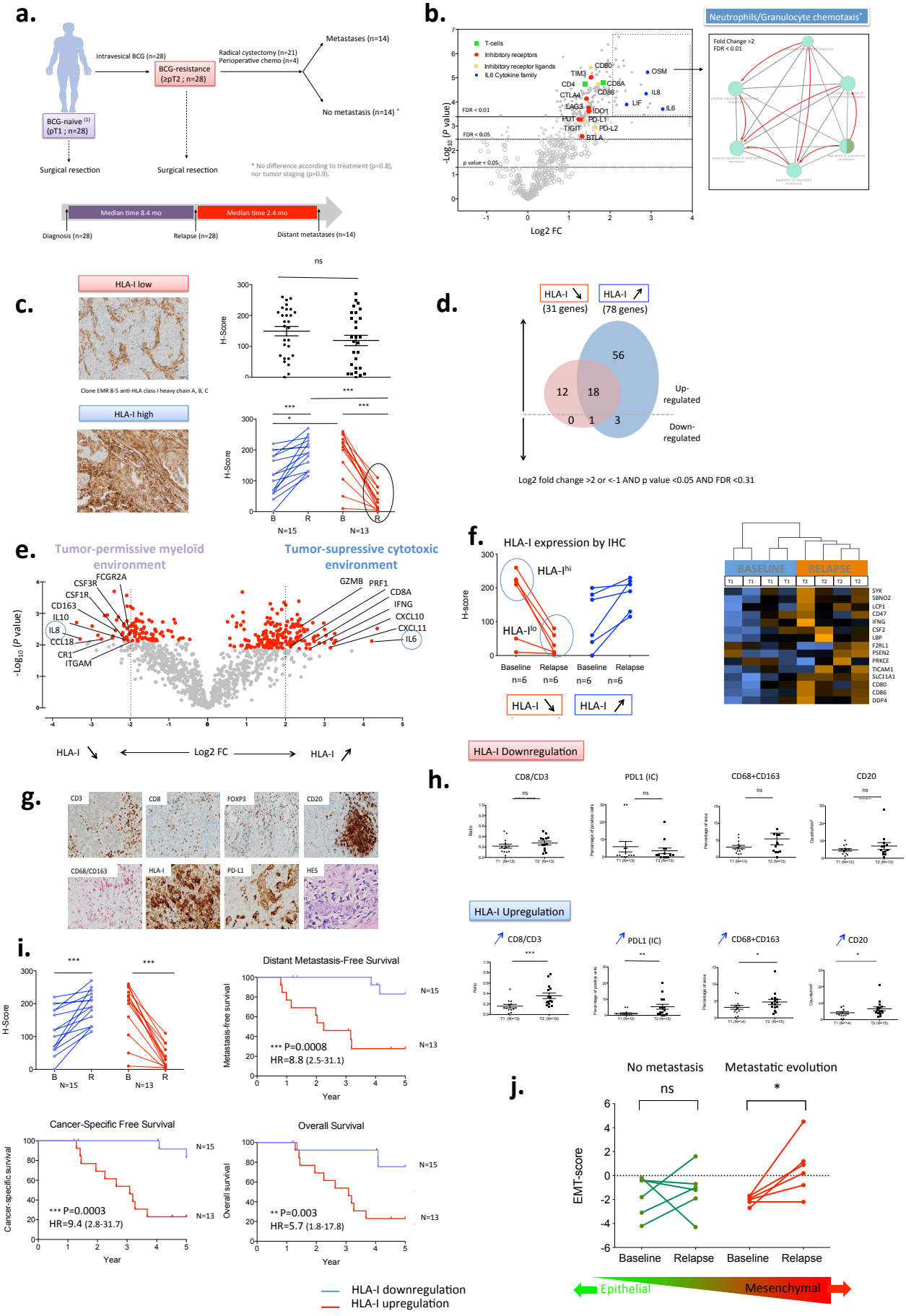
a.
Intravesical BCG (n=28)
BCG-naive (1) (pT1 ; n=28)
BCG-resistance (≥pT2 ; n=28)
Radical cystectomy (n=21)
Perioperative chemo (n=4)
Metastases (n=14)
No metastasis (n=14) *
Surgical resection
Surgical resection
* No difference according to treatment (p=0.8), nor tumor staging (p=0.9).
Median time 8.4 mo
Median time 2.4 mo
Diagnosis (n=28)
Relapse (n=28)
Distant metastases (n=14)
b.
T-cells
Inhibitory receptors
Inhibitory receptor ligands
IL6 Cytokine family
FDR < 0.01
FDR < 0.05
p value < 0.05
-Log10 (P value)
Log2 FC
Neutrophils/Granulocyte chemotaxis*
Fold Change >2
FDR < 0.01
c.
HLA-I low
HLA-I high
Clone EMR 8-5 anti-HLA class I heavy chain A, B, C
H-Score
ns
N=15
N=13
d.
HLA-I ↘ (31 genes)
HLA-I ↗ (78 genes)
56
12
18
0
1
3
Up-regulated
Down-regulated
Log2 fold change >2 or <-1 AND p value <0.05 AND FDR <0.31
e.
Tumor-permissive myeloïd environment
Tumor-supressive cytotoxic environment
-Log10 (P value)
Log2 FC
HLA-I ↘
HLA-I ↗
f.
HLA-I expression by IHC
H-score
HLA-Ihi
HLA-Ilo
Baseline
Relapse
n=6
HLA-I ↘
HLA-I ↗
BASELINE
RELAPSE
g.
CD3
CD8
FOXP3
CD20
CD68/CD163
HLA-I
PD-L1
HES
h.
HLA-I Downregulation
CD8/CD3
PDL1 (IC)
CD68+CD163
CD20
HLA-I Upregulation
i.
H-Score
Distant Metastasis-Free Survival
Metastasis-free survival
*** P=0.0008
HR=8.8 (2.5-31.1)
Year
Cancer-Specific Free Survival
Cancer-specific survival
*** P=0.0003
HR=9.4 (2.8-31.7)
Overall Survival
Overall survival
** P=0.003
HR=5.7 (1.8-17.8)
HLA-I downregulation
HLA-I upregulation
j.
No metastasis
Metastatic evolution
ns
*
EMT-score
Baseline
Relapse
Epithelial
Mesenchymal

Figure 6.

Figure 6. BCG generates a myeloid and immunosuppressive microenvironment in tumors with HLA-I downregulation.

a. Longitudinal study of paired bladder tumors before and after BCG immunotherapy (n=28).

b. Volcano plot showing differential gene expression between paired tumors (relapse vs. baseline). Paired FFPE samples with sufficient tumor area at baseline and relapse have been selected (n=12).

c. Representative images of HLA-I staining by immunohistochemistry. Evolution of HLA-I expression is depicted at the individual level. Unpaired two-tailed t tests.

d. Volcano plot showing upregulated genes according to HLA-I expression (relapse (n=6) vs. baseline (n=6)). Specifically upregulated genes among each group HLA-I ^{hi} *vs* HLA-I ^{lo} are highlighted. Red dot indicate genes with p value<0.05 and FDR<0.31.

e. Venn diagram showing the number of shared and specific genes according to HLA-I ^{hi} *vs* HLA-I ^{lo} (n=12).

f. Heat-map depicting gene expression profile between baseline and relapse for tumors with HLA-I downregulation (n=4). A circle at the left indicates selected cases for this analysis.

g. Representative images of antibodies selected for IHC study.

h. *In situ* immune microenvironment before and after BCG immunotherapy (two-tailed paired t tests).

i. Prognostic value according to HLA-I expression before and after BCG immunotherapy. (Log rank tests, Hazard Ratio, p value).

j. EMT-score before and after BCG immunotherapy according to the development of metastasis (n=6, two-tailed paired t tests).

Methods

Patient cohort. Tumor samples and medical records were obtained from a cohort of 147 patients with bladder cancer treated at the Hôpital Foch and previously reported (Rouanne *et al.*, 2019). BCG resistant tumors provided from 28 patients. Formalin-fixed paraffin-embedded tumor specimens with sufficient bladder tumor content were selected for RNA extraction and IHC profiling. Paired bladder samples before and after BCG immunotherapy were used for this study. All the patients gave their written informed consent for use of clinical data and scientific purposes. This cohort has been declared to the CNIL (DC-2017-2942) and approved by the Ethical and Scientific Committee.

***Ex vivo* bladder tumor stimulation assay.** Fresh tumor samples were prospectively obtained from Hôpital Foch. All the tumors were collected within 1 hour from surgery and stored at 4°C in complete medium until use. Experimental settings were conducted as previously described (Jacquelot *et al.*, 2017). Primary bladder tumors were freshly mechanically and enzymatically dissociated using the Miltenyi Gentle MACS equipment for 1 hour at 37°C under rotation (2 incubation steps of 30 minutes). We performed an *ex vivo* tumor stimulation assay from 12 primary bladder tumors. Dissociated cells were seeded in 96-wells plate and incubated in complete medium, or stimulated with IFNγ (1.10^3 UI/mL) or with reconstituted ImmuCyst (BCG substrain Connaught 2.10^7 CFU/mL). The *ex vivo* stimulation lasted 72h before flow cytometric analyses of live $CD45^+$ cells and CD45- cells.

Cell-lines. All cell lines were purchased from the American Type Culture Collection (ATCC No.TCP-1020). Cell-lines with known genomic characteristics included RT4, SW780, HT1376, 5637, TCCSUP, and UM-UC3. All cell-lines were maintained in culture with antibiotic-free media RPMI 1640 following the addition of 10% heat-inactivated fetal bovine serum (GE Healthcare) at 37 °C in a humid atmosphere containing 5% CO2. Cell-lines were tested and found negative for Mycoplasma contamination.

Flow cytometry and cell-sorting. Cells from 12 primary BC were stained with fluorochrome coupled mAbs, incubated for 20 min at 4°C and washed with PBS1X. Cells were then permeabilized with Foxp3/Transcription factor Fixation/Permeabilization kit (eBiosciences) and intranuclearly stained anti-Foxp3 APC (eBiosciences) and anti-Ki67 (BD Biosciences) mAbs for 30 min, at 4°C, protected from light. Cell culture supernatants were collected at 72h and stored at -20°C until use. Cancer cell-lines were detached with trypsin and stained with mAbs as described below. Panel of antibodies are listed below. Cell samples were acquired on a BD FACS LSR Fortessa X-20-cytometer with single-stained antibody capturing beads used for compensation (Compbeads, BD Biosciences). Data were analyzed with Kaluza 1.3 (Beckman). For cell sorting, ZA negative cells, HLA-I^{hi} and HLA-I^{lo} cancer cells were FACS sorted after BCG co-culture for 24h.

BCG reconstitution. ImmuCyst BCG is a freeze-dried preparation made from the Connaught substrain of Bacillus Calmette-Guerin, which is an attenuated strain of living bovine tubercle bacillus Mycobacterium bovis. The bacilli are lyophilized (freeze-dried) and are viable upon reconstitution. It is produced from a suspension containing viable bacteria of the Connaught strain of Bacillus Calmette-Guerin (BCG) and formulated to contain 81 mg (dry weight) of BCG and 150 mg monosodium glutamate. Each vial of ImmuCyst is reconstituted with 3 mL of sterile, preservative-free saline solution. The reconstituted dose contains approximately 10.5 ± 8.7 x 10^8 colony-forming units (CFU). For clinical use, the reconstituted material from the vial is further diluted in an additional 50 mL of sterile, preservative-free saline solution to a final volume of 53 mL for instillation into the bladder. Therefore, the final concentration in the bladder is approximately 2 x 10^7 CFU/mL.

BCG co-culture. Cancer cells were plated a day prior to infection in antibiotic-free media to reach 80-90% confluence on the day of infection. Lyophilized ImmuCyst Bacillus Calmette-Guérin (BCG) (Connaught substrain, 81 mg at 10.5 ± 8.7 10^8 CFU/mL) was reconstituted

within PBS 1X as recommended for clinical use. BCG was co-incubated in antibiotic-free media to achieve a multiplicity of infection of 10:1 or 100:1 as reported. Plates were incubated at 37°C for the indicated time period and then washed with 1XPBS, detached using trypsin, resuspended in complete medium. After passage on 70µm filter and centrifugation, cells were resuspended in 1XPBS for analysis by flow-cytometry.

In vitro BCG restimulation assay. This protocol has been originally described to study trained innate immunity in human monocytes. Cancer cells (250,000 cells/ well) were added to flat-bottom 6-well plates. After incubation for 24 h at 37°C and washing with warm PBS, cancer cells were incubated with culture medium only as a negative control or BCG MOI 100:1, for 24 h (in 2000 µl /well RPMI plus 10% heat-inactivated fetal bovine serum). After 24h, the cells were washed twice with 500 µl warm 1XPBS and incubated for 6 days in culture medium with 10% serum, and the medium was changed once at day 3. Cells were harvested at day 5 using trypsin protocol, washed twice with 1XPBS, and seeded (250,000 cells/ well) in flat-bottom 6-well plates for 24h. Cells were restimulated with BCG MOI 100:1. After 24 h, supernatants were collected and stored at-20°C until cytokine measurement.

NanoString gene expression profiling. For FFPE tumor samples analysis, macrodissection of selected tumor areas following by RNA extraction using High Pure FFPET RNA Isolation Kit – Roche Life Science (ref:06483852001) was performed. The samples were stored at –80°C. Isolated RNA was hybridized with the NanoString nCounter PanCancer Immune Profiling Human Panel CodeSet. For cancer cells analysis, cell-sorting was performed 24h after BCG co-culture. Next, RNA was extracted using the Direct-zol RNA MiniPrep Kit (Zymo Research). The samples were stored at –80°C. Isolated RNA was hybridized with the NanoString nCounter IO360 Panel Human Panel CodeSet and quantified using the nCounter Digital Analyzer. Data were processed with nSolver Analysis Software (NanoString) using the Advanced Analysis module.

Immunohistochemistry. One representative formalin-fixed, paraffin-embedded (FFPE) tumor block of the primary tumor and relapse was selected. Consecutive 3µm thickness sections of FFPE tumor tissues were cut on a microtome and float on a 40°C water bath containing distilled water. Sections were transferred onto positively charged glass slides (Superfrost Plus). Slides were dried overnight and stored at 4°C until use. Consecutive FFPE slides were stained using validated and standardized protocols on Ventana Discovery Ultra or Benchmark Ultra automated platforms (Roche Diagnostics, Ventana Medical Systems, Tucson, AZ). The main steps for chromogenic IHC are decribed below. Sections were deparaffinized in xylene. Antigen retrieval was performed using ultra cell conditioning 1 (CC1) buffer for 36 minutes at 95°C. Sections were incubated with a primary antibody (see table below) during 1 hour at room temperature. Amplification was achieved using an UltraView universal DAB detection kit. Revelation using 3,3'diaminobenzidine as chromogen was applied to sections. Nuclear counterstaining was performed with Hematoxylin II and bluing reagent. Coverslip was applied with a permanent mounting medium.

Immunohistochemical analysis for PD-L1 and HLA-I expression. For HLA-1 (clone EMR 8-5 anti-HLA class I heavy chain A, B, C), intensity of tumor cells membrane staining was scored using a semi-quantitative scale: 0 (negative), 1 (weak), 2 (moderate) and 3 (strong). Then, the percentage of positive tumor cells was multiplied by the staining intensity of tumor cell to obtain a final semi quantitative H score (0-300). For PD-L1 staining (E1L3N clone, Cell Signaling Technology, Danvers, MA), primary antibody was incubated at 1 µg/mL dilution for 1 hour at room temperature. Detection was performed using a HQ amplification kit and 3,3'-diaminobenzidine as a chromogen. For each tumor sample, PD-L1 expression was scored by a trained pathologist in tumor cells (percentage of cells with membranous staining) and immune cells (percentage of tumor areas covered by PD-L1 expressing tumor cells).

Image analysis. Image acquisition was performed with a Virtual Slide microscope VS120-SL (Olympus, Tokyo, Japan), 20X air objective (0.75 NA, 345 nm/pixel). CD3+, CD4+ and CD8+ lymphocytes were detected using an algorithm created in Definiens Developer software (Definiens Munchen Germany). Image analysis was done on manually selected (exclusion of areas of necrosis, preparation artifacts) regions of interest (ROI). As these regions were large, they were divided into blocks of pixels processed individually and stitched at the end. The method combined watershed segmentation on DAB staining and color and morphological characteristics to retrieve automatically CD3+, CD4+ or CD8+ cells. The program exports the number of CD3+, CD4+ or CD8+ cells and the tissue areas in µm² for each analyzed ROI. FoxP3+ lymphocytes were detected using ManualROI_Nuclei (Positive vs. Negative) routine in Definiens Tissue Studio (Definiens Munchen Germany). DAB stained nucleus are automatically detected using their IHC spectral properties in manually selected regions of interest. The routine scores (low, medium and high) each nucleus on its intensity. In our cases, low classification corresponded to false positive staining and was discarded. The program exports the number of FoxP3+nucleus and the tissue area in µm² for each analyzed case. Macrophages were analyzed using an algorithm created in ImageJ (NIH, Bethesda, Maryland, USA) applied on manually selected ROI. Macrophages results are expressed as an area of CD163+ and CD68+ CD163- stained cells divided by the ROI area.

Multiplex Luminex assay. The cytokine release was quantified by commercial 27-plex Luminex assay for monitoring the immune activity of BCG on fresh bladder tumors and cell-lines. Cytokine titration was performed using the Bio-Rad Bio-Plex 200 Luminex® multiplex ELISA (Bio-Rad 27-Plex Human Chemokine Panel, kit #M500KCAF0Y). This kit detects IL-1β, IL-1ra, IL-4, IL-5, IL-6, IL-7, IL-8, IL-10, IL-12 (p70), IL-13, IL-15, IL-17, TNFα, IFNγ, CXCL10, G-CSF, GM-CSF, Eotaxin, CCL2, CCL3, CCL4, CCL5, VEGF, FGF basic, PDFG-bb. Titrations were performed following the Bio-Plex Pro Assays Chemokine Quick Guide protocol.

ImageStream analysis. For in vitro infection, BCG was labelled with calcein-AM after co-incubation in complete medium for 30 min at 37°C 5%CO2 protected from light. Cancer cells were co-incubated with BCG-calcein AM (MOI 100:1) for 24 hours, or incubated with IFNγ (1000U/mL) or RMPI 10% heat-inactivated FBS. Cells were harvested using trypsin, washed twice with 1xPBS and stained with surface antibodies. Hoeschst was added 15 minutes before image acquisition. Images were captured on an Amnis ImageStream Mark II Imaging Flow Cytometer with 40x magnification (EMD Millipore). Data were acquired and analyzed using Amnis INSPIRE software and Amnis IDEAS software, respectively.

Statistical analysis. Statistical tests were calculated in GraphPad Prism v.8.0. Paired two-tailed Student's t-test were used to compare two groups, unless indicated otherwise; one-way ANOVA was used to compare multiple (>2) groups with one independent variable followed by Tukey's correction for multiple comparisons. For Kaplan–Meier survival experiments, we performed a log-rank (Mantel–Cox) test. P values depicted as * <0.05, ** <0.005, *** <0.001, **** <0.0001, were considered statistically significant.

References

1. Pietzak, E. J. *et al.* Genomic Differences Between “Primary” and “Secondary” Muscle-invasive Bladder Cancer as a Basis for Disparate Outcomes to Cisplatin-based Neoadjuvant Chemotherapy [Figure presented]. *Eur. Urol.* **75**, 231–239 (2019).

2. Ge, P. *et al.* Oncological Outcome of Primary and Secondary Muscle-Invasive Bladder Cancer: A Systematic Review and Meta-analysis. *Sci. Rep.* **8**, 4–11 (2018).

3. Redelman-Sidi, G., Glickman, M. S. & Bochner, B. H. The mechanism of action of BCG therapy for bladder cancer-A current perspective. *Nat. Rev. Urol.* **11**, 153–162 (2014).

4. Pettenati, C. & Ingersoll, M. A. Mechanisms of BCG immunotherapy and its outlook for bladder cancer. *Nat. Rev. Urol.* **15**, 615–625 (2018).

5. Tan, T. Z., Rouanne, M., Tan, K. T., Huang, R. Y. J. & Thiery, J. P. Molecular Subtypes of Urothelial Bladder Cancer: Results from a Meta-cohort Analysis of 2411 Tumors. *Eur. Urol.* **75**, 423–432 (2019).

6. Knowles, M. A. & Hurst, C. D. Molecular biology of bladder cancer: New insights into pathogenesis and clinical diversity. *Nat. Rev. Cancer* **15**, 25–41 (2015).

7. Babjuk, M. *et al.* European Association of Urology Guidelines on Non-muscle-invasive Bladder Cancer (TaT1 and Carcinoma In Situ) - 2019 Update. *Eur. Urol.* (2019). doi:10.1016/j.eururo.2019.08.016

8. Calmette, A. (1927) *La Vaccination préventive contre la tuberculose par le "BCG"*. Paris : Masson et cie.

9. Chamie, K. *et al.* Recurrence of high-risk bladder cancer: A population-based analysis. *Cancer* **119**, 3219–3227 (2013).

10. Van Den Bosch, S. & Witjes, J. A. Long-term cancer-specific survival in patients with high-risk, non-muscle-invasive bladder cancer and tumour progression: A systematic review. *European Urology* **60**, 493–500 (2011).

11. Balar, A. V. *et al.* Keynote 057: Phase II trial of Pembrolizumab (pembro) for patients (pts) with high-risk (HR) nonmuscle invasive bladder cancer (NMIBC) unresponsive to bacillus calmette-guérin (BCG). *J. Clin. Oncol.* **37**, 350–350 (2019).

12. Singh, P. *et al.* S1605: Phase II trial of atezolizumab in BCG-unresponsive non-muscle invasive bladder cancer. *J. Clin. Oncol.* **35**, TPS4591–TPS4591 (2017).

13. Shore, N. D. *et al.* Intravesical rAd–IFNa/Syn3 for patients with high-grade, bacillus calmette-guerin–refractory or relapsed non–muscle-invasive bladder cancer: A phase II randomized study. *J. Clin. Oncol.* **35**, 3410–3416 (2017).

14. Huang, K.-C. *et al.* Abstract 3269: Discovery and characterization of E7766, a novel macrocycle-bridged STING agonist with pan-genotypic and potent antitumor activity through intravesical and intratumoral administration. in *Immunology* 3269–3269 (American Association for Cancer Research, 2019). doi:10.1158/1538-7445.AM2019-3269

15. Annels, N. E. *et al.* Viral Targeting of Non-Muscle-Invasive Bladder Cancer and Priming of Antitumor Immunity Following Intravesical Coxsackievirus A21. *Clin. Cancer Res.* (2019). doi:10.1158/1078-0432.CCR-18-4022

16. Kamat, A. M. *et al.* Cytokine Panel for Response to Intravesical Therapy (CyPRIT): Nomogram of Changes in Urinary Cytokine Levels Predicts Patient Response to Bacillus Calmette-Guerin.[Erratum appears in Eur Urol. 2016 Jul;70(1):e26; PMID: 27302298]. *Eur. Urol.* **69**, 197–200 (2016).

17. Chevalier, M. F. *et al.* ILC2-modulated T cell-to-MDSC balance is associated with bladder cancer recurrence. *J. Clin. Invest.* **127**, 2916–2929 (2017).

18. Chevalier, M. F. *et al.* Conventional and PD-L1-expressing Regulatory T Cells are Enriched During BCG Therapy and may Limit its Efficacy. *Eur. Urol.* **74**, 540–544 (2018).

19. Pichler, R. *et al.* Intratumoral Th2 predisposition combines with an increased Th1 functional phenotype in clinical response to intravesical BCG in bladder cancer. *Cancer*

Immunol. Immunother. **66**, 427–440 (2017).

20. Biot, C. BCG immunotherapy for bladder cancer : characterization and modeling of the bladder immune response to BCG identify strategies for improving anti-tumor activity. (2013).

21. Kobayashi, T., Owczarek, T. B., McKiernan, J. M. & Abate-Shen, C. Modelling bladder cancer in mice: Opportunities and challenges. *Nat. Rev. Cancer* **15**, 42–54 (2015).

22. Spranger, S. & Gajewski, T. F. Mechanisms of Tumor Cell–Intrinsic Immune Evasion. *Annu. Rev. Cancer Biol.* **2**, 213–228 (2018).

23. Nieto, M. A. *et al*. EMT: 2016. *Cell* **166**, 21–45 (2016).

24. Tan, T. Z. *et al.* Epithelial-mesenchymal transition spectrum quantification and its efficacy in deciphering survival and drug responses of cancer patients. *EMBO Mol. Med.* **6**, 1279–93 (2014).

26. Harding, C. V. & Boom, W. H. Regulation of antigen presentation by Mycobacterium tuberculosis: A role for Toll-like receptors. *Nat. Rev. Microbiol.* **8**, 296–307 (2010).

27. Shekarian, T. *et al.* Pattern recognition receptors: Immune targets to enhance cancer immunotherapy. *Ann. Oncol.* **28**, 1756–1766 (2017).

28. Aleynick, M., Svensson-Arvelund, J., Flowers, C. R., Marabelle, A. & Brody, J. D. Pathogen Molecular Pattern Receptor Agonists: Treating Cancer by Mimicking Infection. *Clin. Cancer Res.* (2019). doi:10.1158/1078-0432.ccr-18-1800

29. Mostafid, A. H., Palou Redorta, J., Sylvester, R. & Witjes, J. A. Therapeutic options in high-risk non-muscle-invasive bladder cancer during the current worldwide shortage of bacille Calmette-Guérin. *Eur. Urol.* **67**, 359–60 (2015).

30. Redelman-Sidi, G., Iyer, G., Solit, D. B. & Glickman, M. S. Oncogenic activation of Pak1-dependent pathway of macropinocytosis determines BCG entry into bladder cancer cells. *Cancer Res.* **73**, 1156–1167 (2013).

31. Kupz, A. *et al.* ESAT-6 – dependent cytosolic pattern recognition drives noncognate tuberculosis control in vivo Find the latest version : ESAT-6 – dependent cytosolic pattern recognition drives noncognate tuberculosis control in vivo. **126**, 2109–2122 (2016).

32. Gan, C., Mostafid, H., Khan, M. S. & Lewis, D. J. M. BCG immunotherapy for bladder cancer - The effects of substrain differences. *Nat. Rev. Urol.* **10**, 580–588 (2013).

33. Singhania, A., Wilkinson, R. J., Rodrigue, M., Haldar, P. & O'Garra, A. The value of transcriptomics in advancing knowledge of the immune response and diagnosis in tuberculosis. *Nat. Immunol.* **19**, 1159–1168 (2018).

34. McNab, F., Mayer-Barber, K., Sher, A., Wack, A. & O'Garra, A. Type I interferons in infectious disease. *Nat. Rev. Immunol.* **15**, 87–103 (2015).

35. Jacquelot, N. *et al.* Sustained Type I interferon signaling as a mechanism of resistance to PD-1 blockade. *Cell Res.* (2019). doi:10.1038/s41422-019-0224-x

36. Benci, J. L. *et al.* Tumor Interferon Signaling Regulates a Multigenic Resistance Program to Immune Checkpoint Blockade. *Cell* **167**, 1540-1554.e12 (2016).

37. Musella, M., *et al.*. Type-I-interferons in infection and cancer: Unanticipated dynamics with therapeutic implications. *Oncoimmunology* **6**, 1–12 (2017).

38. Agudo, J. *et al.* Quiescent Tissue Stem Cells Evade Immune Surveillance. *Immunity* **48**, 271-285.e5 (2018).

39. Netea, M. G. *et al.* Trained immunity: A program of innate immune memory in health and disease. *Science (80-.).* **352**, 427 (2016).

40. Rouanne, M. *et al.* Stromal lymphocyte infiltration is associated with tumour invasion depth but is not prognostic in high-grade T1 bladder cancer. *Eur. J. Cancer* **108**, 111–119 (2019).

41. Jacquelot, N. *et al.* Predictors of responses to immune checkpoint blockade in advanced melanoma. *Nat. Commun.* **8**, 592 (2017).

Chapter III. General discussion and perspectives

High-risk non muscle-invasive bladder cancers (NMIBC) frequently relapse after standard BCG immunotherapy, and up to 30% of patients experience progression to muscle-invasive disease(Van Den Bosch and Witjes, 2011; Chamie *et al.*, 2013); such patients are referred to as having secondary muscle-invasive bladder cancer (MIBC), which are highly lethal disease(Ge *et al.*, 2018; Pietzak *et al.*, 2019). Although it is broadly accepted that intravesical BCG therapy efficacy relies on its ability to generate an anti-tumor immune response, the mechanisms of tumor resistance to BCG therapy remain elusive. Worse clinical outcomes have been observed in patients developing secondary MIBC or metastasis after BCG immunotherapy compared to those with primary MIBC or de novo metastatic disease(Ge *et al.*, 2018; Pietzak *et al.*, 2019). These clinical observations suggest that BCG-resistant cancer cells could acquire intrinsic characteristics upon BCG exposure, which lead to immune escape, tumor invasion and metastasis. Overall, our data strengthen this hypothesis, and provide new insights into the mechanisms of resistance to BCG.

In this study, using *ex-vivo* BCG co-culture assay with fresh human bladder tumors, we demonstrated that BCG induces HLA-I downregulation in a subset of urothelial cancer cells. We further validate that live bacilli providing from lyophilized therapeutic BCG can infect a subset of urothelial cancer cells, which subsequently downregulate HLA-I expression. We did not have the opportunity to study the precise mechanism by which intracellular BCG infection leads to HLA-I downregulation but this question would be an important cellular biology question to be solved. We cannot say with our data if the low HLA-I membrane expression is a consequence of an internalization of the molecules or a diminution of its

expression. Indeed, the BCG detrimental effects could be either at the transcriptomic level by direct modification of the expression of HLA-I genes (secondary to epigenetic mechanisms for example), but could also be at the post-translational level where BCG metabolism could interfere with the HLA-I membrane expression. Strikingly, loss of heterozygosity (LOH) at chromosome 6 & 15 has been described as a mechanism of acquired resistance to BCG immunotherapy (Carretero *et al.*, 2011). In this retrospective series, the authors suggest that BCG induced selection of HLA-class I deficient tumors at relapse after BCG immunotherapy. Comparative analysis of HLA-I expression in recurrent bladder tumors in patients treated with mitomycin or BCG was analyzed by RTq-PCR and immunohistochemical techniques. Loss of heterozygosity was determined by microsatellite amplification of markers in chromosome 6 and 15. In this seminal study, more profound alterations in HLA class I expression were found in post-BCG recurrent tumors rather than in pre-BCG lesions, whereas mitomycin treatment did not change the HLA class I expression pattern. The authors suggest that cancer cells with high HLA-I expression at baseline are eliminated after BCG exposure, while tumor cells with structural HLA alterations before BCG led to the outgrowth of cancer cells.

Most interestingly, cancer cells becoming HLA-I deficient upon BCG exposure also displayed a senescent-like phenotype, with specific cancer inflammatory responses including sustained activation of type I IFN pathway. Among the cytokines secreted, we identified higher levels of G-CSF and VEGF released by class-I deficient cancer cells. This data suggest that cancer cells not only acquire immune evasion features, but also the ability to recruit *in situ* potentially immunosuppressive myeloid cells, and stimulate tumor angiogenesis. Taken together, these data emphasize that live attenuated BCG may induce immune evasion and mesenchymal transition after intracellular infection in a subset of cancer cells.

Our results have broad clinical implications. Indeed, HLA-I downregulation could be easily

assessed in routine practice by pathologists. Therefore, patients with HLA-I^{lo} BCG-unresponsive tumors could be identified and benefit from treatment intensification. Thanks to the advent of immune checkpoint targeted immunotherapies in oncology, an unprecedented number of new therapeutic strategies are currently in clinical development for BCG-unresponsive tumors. Beyond anti-PD(L)1 monotherapies, those include intravesical oncolytic viruses (NCT02316171) and combinations of intravenous anti-PD1 with intravesical BCG (NCT03711032) or oral IDO1 inhibitors (NCT03519256). Preliminary results showed potential benefit of pembrolizumab in this clinical setting with 40% of patients without relapse after 3-months treatment(Balar *et al.*, 2019). These results have to be confirmed with a longer patient follow-up in an ongoing randomized phase III clinical trial. Intravesical administration of immunostimulatory components are also evaluated in this clinical setting in early phase trials. The US FDA has recently granted fast track and breakthrough therapy designations to rAd-IFN/Syn3, a non-replicating adenovirus vector harboring the human IFN alpha2b gene, delivered intravesically to treat high-grade NMIBC patients, who are unresponsive to BCG therapy(Shore *et al.*, 2017). A phase III trial is currently ongoing (NCT02773849).

Our study shed light on the immune microenvironment in BCG-resistant tumors. Taken together, our data collectively suggests that acquired HLA-class I deficiency by tumor cells after BCG immunotherapy induced myeloid-suppressive immune microenvironment, thus preventing efficient antitumor immunity, leading to local invasion and metastatic disease. By contrast, immunogenic HLA-I high tumor cells led to increased cytotoxic CD8+ T-cells, and long-term disease control. Additionally, we identified a macrophage signature with high expression of CD47 in HLA-I deficient tumors after BCG immunotherapy. Recent studies have demonstrated that CD47 blockade not only increases phagocytosis of cancer cells but also promotes cross-presentation of tumor antigens to enhance priming of anti-tumor effector T

cells in syngeneic mouse tumor models(Liu *et al.*, 2015; Sockolosky *et al.*, 2016; Kauder *et al.*, 2018). The CD47 targeted macrophage checkpoint inhibitor 5F9 showed monotherapy activity in ovarian cancers and B-cell lymphomas(Sikic *et al.*, 2019). When combined with rituximab it showed promising activity in patients with rituximab refractory aggressive and indolent lymphomas(Advani *et al.*, 2018). To improve its therapeutic profile, engineered non-pathogenic bacteria expressing a nanobody against CD47 has recently been developed(Chowdhury *et al.*, 2019). Local delivery of CD47nb by tumor-colonizing bacteria increases activation of tumor-infiltrating T-cells, stimulated rapid tumor regression, prevented metastasis and led to long-term survival in a syngeneic tumor model in mice. Therefore, we believe that treatment targeting the CD47-SIRPα axis in BCG-unresponsive tumors could also be explored in a follow-up trial. Here we demonstrate for the first time that BCG induces HLA-class I downregulation, senescent-like and mesenchymal transition in a subset of cancer cells, leading to immune evasion, and cancer cell intrinsic capacity of local invasion at the tumor site. Thus, we propose to stratify the risk of disease progression according to HLA-I expression in BCG-unresponsive tumors.

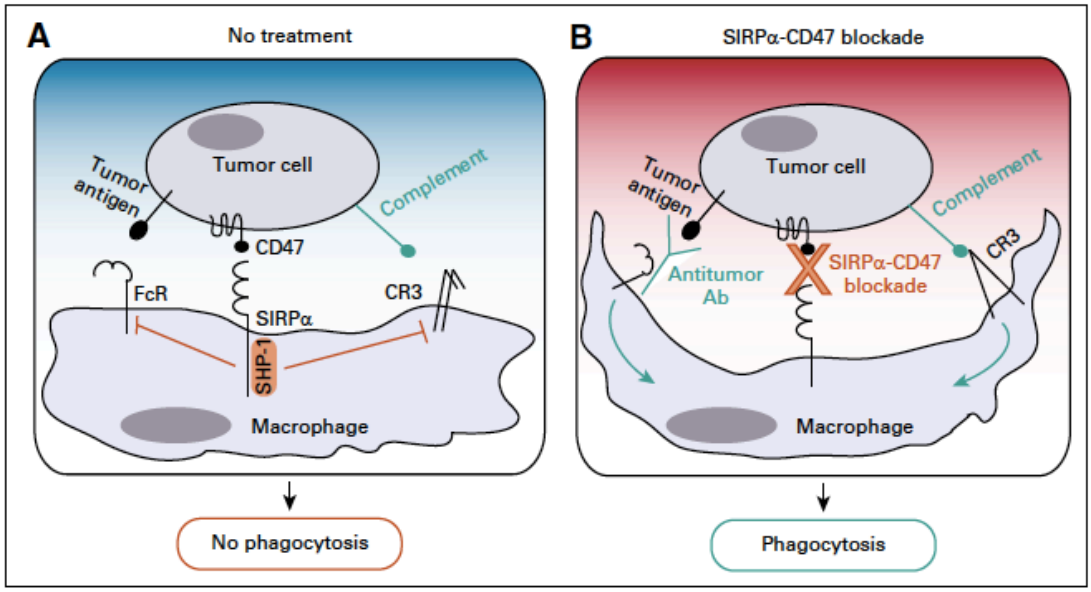

Fig. 1. Regulation of phagocytosis by the SIRPα-CD47 immune checkpoint (from Veillette at al. J Clin Oncol 2019(Veillette and Tang, 2019))

References

1. Chamie, K. *et al.* Recurrence of high-risk bladder cancer: A population-based analysis. *Cancer* **119**, 3219–3227 (2013).
2. Van Den Bosch, S. & Witjes, J. A. Long-term cancer-specific survival in patients with high-risk, non-muscle-invasive bladder cancer and tumour progression: A systematic review. *European Urology* **60**, 493–500 (2011).
3. Ge, P. *et al.* Oncological Outcome of Primary and Secondary Muscle-Invasive Bladder Cancer: A Systematic Review and Meta-analysis. *Sci. Rep.* **8**, 4–11 (2018).
4. Pietzak, E. J. *et al.* Genomic Differences Between "Primary" and "Secondary" Muscle-invasive Bladder Cancer as a Basis for Disparate Outcomes to Cisplatin-based Neoadjuvant Chemotherapy [Figure presented]. *Eur. Urol.* **75**, 231–239 (2019).
5. Carretero, R. *et al.* Bacillus Calmette-Guerin immunotherapy of bladder cancer induces selection of human leukocyte antigen class I-deficient tumor cells. *Int. J. Cancer* **129**, 839–846 (2011).
6. Balar, A. V. *et al.* Keynote 057: Phase II trial of Pembrolizumab (pembro) for patients (pts) with high-risk (HR) nonmuscle invasive bladder cancer (NMIBC) unresponsive to bacillus calmette-guérin (BCG). *J. Clin. Oncol.* **37**, 350–350 (2019).
7. Shore, N. D. *et al.* Intravesical rAd–IFNa/Syn3 for patients with high-grade, bacillus calmette-guerin–refractory or relapsed non–muscle-invasive bladder cancer: A phase II randomized study. *J. Clin. Oncol.* **35**, 3410–3416 (2017).
8. Sockolosky, J. T. *et al.* Durable antitumor responses to CD47 blockade require adaptive immune stimulation. *Proc. Natl. Acad. Sci. U. S. A.* **113**, E2646–E2654 (2016).
9. Liu, X. *et al.* CD47 blockade triggers T cell-mediated destruction of immunogenic tumors. *Nat. Med.* **21**, 1209–15 (2015).
10. Kauder, S. E. *et al.* ALX148 blocks CD47 and enhances innate and adaptive antitumor

immunity with a favorable safety profile. *PLoS One* **13**, (2018).

11. Sikic, B. I. *et al.* First-in-human, first-in-class phase i trial of the anti-CD47 antibody Hu5F9-G4 in patients with advanced cancers. in *Journal of Clinical Oncology* **37**, 946–953 (American Society of Clinical Oncology, 2019).
12. Advani, R. *et al.* CD47 Blockade by Hu5F9-G4 and Rituximab in Non-Hodgkin's Lymphoma. *N. Engl. J. Med.* **379**, 1711–1721 (2018).
13. Chowdhury, S. *et al.* Programmable bacteria induce durable tumor regression and systemic antitumor immunity. *Nat. Med.* **25**, 1057–1063 (2019).
14. Veillette, A. & Tang, Z. Signaling Regulatory Protein (SIRP)α-CD47 Blockade Joins the Ranks of Immune Checkpoint Inhibition. *J. Clin. Oncol.* **37**, 1012–1014 (2019).

Original articles

European Journal of Cancer 108 (2019) 111–119

Available online at www.sciencedirect.com

ScienceDirect

journal homepage: www.ejcancer.com

Original Research

Stromal lymphocyte infiltration is associated with tumour invasion depth but is not prognostic in high-grade T1 bladder cancer

Mathieu Rouanne [a,b,*], Reem Betari [b], Camélia Radulescu [c], Aïcha Goubar [d], Nicolas Signolle [e], Yann Neuzillet [b], Yves Allory [c,f], Aurélien Marabelle [a,g], Julien Adam [d,h,1], Thierry Lebret [b,1]

[a] INSERM Unit U1015, Laboratoire de Recherche Translationnelle en Immunothérapie, Gustave Roussy, Villejuif, France
[b] Department of Urology, Hôpital Foch, Université Versailles-Saint-Quentin-en-Yvelines, Université Paris-Saclay, Suresnes, France
[c] Department of Pathology, Hôpital Foch, Université Versailles-Saint-Quentin-en-Yvelines, Université Paris-Saclay, Suresnes, France
[d] Department of Biostatistics, INSERM Unit U981, Gustave Roussy, Université Paris-Sud, Université Paris-Saclay, Villejuif, France
[e] Department of Experimental Pathology, INSERM Unit U981, Gustave Roussy, Université Paris-Sud, Université Paris-Saclay, Villejuif, France
[f] Institut Curie, CNRS, UMR144, Paris, France
[g] Drug Development Department (DITEP), Gustave Roussy, Université Paris-Sud, Université Paris-Saclay, Villejuif, France
[h] Department of Pathology, Gustave Roussy, Université Paris-Sud, Université Paris-Saclay, Villejuif, France

Received 3 October 2018; received in revised form 23 November 2018; accepted 5 December 2018

KEYWORDS
T1G3;
Bladder cancer;
Tumour lymphocyte infiltration;
Prognosis

Abstract ***Introduction:*** Assessment of tumour-infiltrating lymphocytes (TILs) can provide important prognostic information in various cancers and may be of value in predicting response to immunotherapy. The objective of the present study was to investigate the association of stromal lymphocytic infiltration with clinicopathological parameters and their correlation with outcomes in patients with high-grade pT1 non–muscle-invasive bladder cancer (NMIBC).

Abbreviations: NMIBC, non–muscle-invasive bladder cancer; MIBC, muscle-invasive bladder cancer; HGT1, high-grade T1; TILs, tumour-infiltrating lymphocytes; H&E, haematoxylin and eosin; BCG, Bacillus Calmette–Guérin; CD3, cluster of differentiation 3; PD-L1, programmed death ligand 1; EORTC, European Organization for Research and Treatment of Cancer; WHO, World Health Organization; CSS, cancer-specific survival; OS, overall survival; PFS, progression-free survival; RFS, recurrence-free survival; TUR, transurethral resection.

* *Corresponding author:* INSERM U1015, Laboratoire de Recherche Translationnelle en Immunothérapie, Université Paris-Saclay, Gustave Roussy, Villejuif, France.
E-mail address: mathieu.rouanne@gustaveroussy.fr (M. Rouanne).
[1] Co-senior authors.

https://doi.org/10.1016/j.ejca.2018.12.010

Materials and methods: We retrospectively analysed clinical data and formalin-fixed paraffin-embedded (FFPE) tissues of 147 patients with primary high-grade pT1 NMIBC who underwent transurethral resection of the bladder. The stromal TIL density was scored as percentage of the stromal area infiltrated by mononuclear inflammatory cells over the total intratumoural stromal area. The main end-point was correlation with cancer-specific survival (CSS).
Results: Median follow-up was 8.2 years (6.1–9.5). Induction Bacillus Calmette–Guérin therapy was undergone by 126 patients (86%). Stromal TILs were high (≥10%) in 82 tumours (56%) and were positively associated with the tumour invasion depth ($p = 0.01$) and cancers with variant histology ($p = 0.01$). For the CSS analysis, high (≥10%) versus. low (<10%) stromal TIL hazard ratio (95% confidence interval) was 1.70 (0.7–3.9, $p = 0.2$).
Conclusions: A higher density of stromal TILs was associated with the tumour invasion depth in pT1 NMIBC. The level of TILs was not associated with survival outcomes. These data suggest that tumour aggressiveness is associated with an increased adaptive immune response in pT1 NMIBC. Characterisation of T-cell subtypes along with B-cells may be critical to enhance our knowledge of the host immune response in patients with high-risk NMIBC.

1. Introduction

High-grade T1 (HGT1) bladder cancer is the highest risk subgroup of non–muscle-invasive bladder cancer (NMIBC). It represents approximately 25% of bladder cancer at diagnosis [1]. These tumours have a variable but potentially lethal prognosis as they can exhibit biological behaviour of muscle-invasive bladder cancer (MIBC) [2]. Despite adjuvant Bacillus Calmette–Guérin (BCG) therapy, half of the patients will experience tumour recurrence within 5 years, and 20%–30% of the patients will progress to MIBC [3]. Ultimately, 10%–15% of patients will die of bladder cancer. Although the European Organization for Research and Treatment of Cancer (EORTC) risk score represents a major improvement for scoring the prognosis of NMIBC, it does not fully capture tumour heterogeneity [4]. Currently, one of the most important unmet needs is to identify potentially lethal HGT1 bladder cancer so that they can be managed aggressively before they become life threatening for the patient [5].

Assessment of tumour-infiltrating lymphocytes (TILs) can provide important prognostic information in various cancers and may also be of value in predicting response to treatments. High lymphocytic infiltration, detected using standard haematoxylin and eosin (H&E) staining, has been associated with a favourable prognosis in many different tumours types [6]. Recent efforts have been taken to standardise the assessment of TILs by morphology in routine pathology practice, resulting in guidelines for scoring TILs in solid tumours [7,8]. To our knowledge, large studies investigating the prognostic value of TILs in a homogeneous cohort of HGT1 bladder cancer have not been reported [9].

In the present study, we analysed the density of stromal TILs before BCG therapy, in a homogeneous cohort of patients with primary HGT1 bladder cancer. The primary objective of this study was to evaluate the association between the density of stromal TILs and the cancer-specific survival.

2. Methods

2.1. Patients

We analysed a cohort of 147 primary high-grade cT1N0M0 patients (CNIL declaration number 2059719) treated at the Hôpital Foch between January 2000 and May 2015. We solely included newly diagnosed, treatment-naive, non-metastatic HGT1 bladder tumours, excluding muscle-invasive (≥T2), recurrent, intradiverticular and upper tract urothelial carcinoma (Supplementary data Fig. S1). All patients underwent clinical examination, radiographic tests and transurethral resection (TUR) by an urologist at our institution. BCG therapy, radical cystectomy and management of metastatic disease were performed according to the national guidelines. Clinical follow-up included cystoscopy and urine cytology every 3 months for the first 2 years, then every 6 months. The study was approved by our institutional review board and was conducted according to ethical rules regarding research on tissue specimens and patients. Updated follow-up data were obtained from the patient records (up until a close out date of August 31, 2017, patient death or the last follow-up visit, whichever came last).

2.2. Tumour samples and pathology review

All surgical specimens were initially reviewed by a pathologist specialised in uropathology (C.R.). Tumours were graded according to the World Health Organization (WHO) 2016 system [10] and staged

according to the 2017 TNM classification, 8th edition [11]. Only initial high-grade tumours with a visible, clearly identifiable and disease-free muscularis propria were included in this study. The characteristics of lamina propria invasion were assessed to distinguish superficial invasion, defined as invasion of the lamina propria to the level of the muscularis mucosa (T1a); all other types of invasions into or beyond the muscularis mucosa were categorised as non-superficial (T1b). Progression and recurrence risk scores were calculated using the EORTC risk model (high score $\geq$ 14 and low score <14 for progression; high score $\geq$ 10 and low score <10 for recurrence).

2.3. Scoring of TILs

Representative slides from the initial TUR were reviewed for the purpose of the study and were evaluated independently for the presence of TILs, defined as mononuclear cells with lymphocytes and plasma cell's morphology, excluding granulocytes, following the recommendations of the international TILs Working Group [12]. TILs were reviewed by two pathologists (C.R. and J.A.) blinded to outcome data, using whole slides H&E-stained sections. TILs were evaluated in the stroma of the areas with infiltration of the lamina propria, excepted in areas with necrosis and artefacts secondary to coagulation in TUR samples. The percentage of the stromal area occupied by TILs was reported as a semicontinuous variable (1% increment between 1 and 10% and 5% increments above 10%). A binary scoring system was used to describe non-intense (stromal TILs $\geq$10%) versus intense lymphocytic infiltration (stromal TILs <10%). The overall agreement was good between the two readers (κ = 0.75). (see Fig. 1)

2.4. Study end-points

Recurrence was defined as reappearance on TUR of histologically proven high-risk disease after the start of therapy (any high grade and/or T1 and/or CIS). Progression was defined as development of muscle-invasive tumour, nodal or distant metastasis. Time to recurrence was defined as time from the first TUR to the first local recurrence or distant recurrence or death due to bladder cancer whatever occurs first. In the absence of recurrence event or death due to other cause, patients were censored at the date when last seen or dead. Time to progression was defined as the time from the first TUR to progression or death due to any cause. Time to bladder cancer–related death was defined as the time between the first TUR and death attributable to bladder cancer. Patients alive or died from other cause than bladder cancer were censored at the date of the last follow-up or date of death. Overall survival (OS) was defined as the time from the first TUR to the date of the last follow-up or death. Patients for whom none of these events were recorded were censored at the date of their last known follow-up.

2.5. Statistical analyses

As no formal recommendation for a clinically relevant TIL threshold has been identified for urothelial carcinoma of the bladder, we focussed on stromal TILs as a continuous parameter. We first investigated the prognostic performance of percentage of TILs as a continuous variable regarding the association with recurrence, progression, cancer-specific and non-specific related deaths. Then, we performed the same analyses using 10% as the cut-off to define a high level of stromal lymphocyte infiltration. The association of clinicopathological factors with the percentage of TILs as a continuous or a categorical variable was respectively performed using the Mann–Whitney test and the Chi-square or Fisher's exact test when it was appropriate. For each time to event endpoint, time to event will be presented graphically using Kaplan–Meier methods, and comparisons between groups will be made using the log-rank test. Association of each known clinical prognostic factor was investigated and analysed, and an unadjusted Cox proportional hazards model was used to calculate hazard ratios (HRs) to estimate the variable effect. The assumption of proportionality used by the Cox model was tested using log–log plots and Schoenfeld residuals. If the assumptions were found not to hold, methods for non-proportional hazards were considered. If the hazard is proportional between groups, but not other covariates, this was resolved by fitting non-proportional covariates as strata. Factors with a p-value $\leq$0.20 in univariate analysis were included in a multivariate analysis in addition to TILs. Forward selection was used to establish the final multivariate model. The significance threshold was 5%. Analyses were performed with R software, version 3.4.3.

3. Results

3.1. Patient characteristics

The median follow-up was 8.2 years (range 6.1–9.5 years). The median age was 71.1 years, and 130/147 (88%) were male. Associated CIS was found in 65 patients (44%). Primary treatment strategies included primary BCG therapy in 121 patients, up-front radical cystectomy in five patients and only TUR in 21 patients. Seventy-one patients were BCG non-responders (Fig. 2). Radical cystectomy was performed in 45 patients (31%) due to BCG resistance (n = 16) or muscle-invasive disease (n = 29). At the time of analysis, deaths and distant metastasis occurred in 41 (28%) and 25 (14%) patients, respectively. Clinicopathological characteristics of the cohort are reported in Table 1.

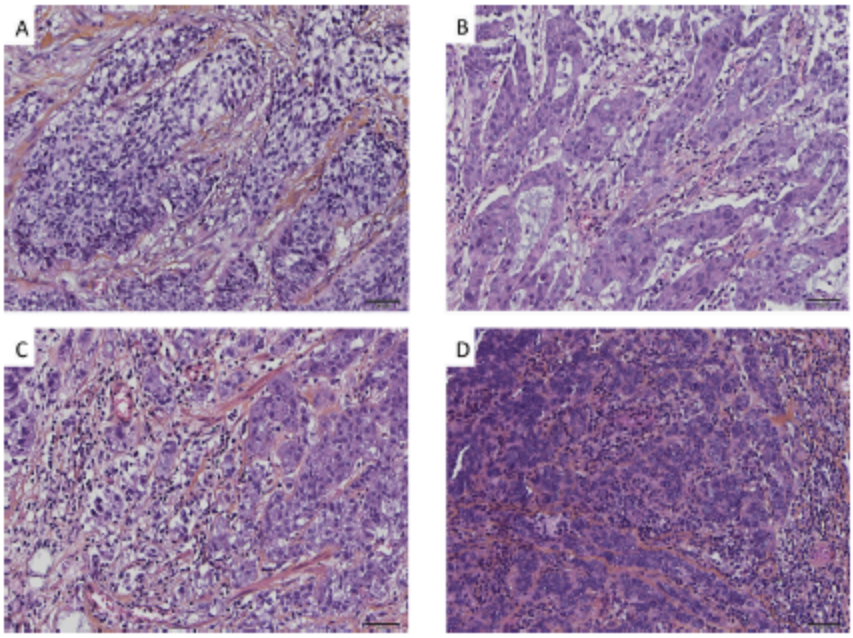

Fig. 1. Histopathologic examples of stromal lymphocytic infiltration in high-grade T1 urothelial carcinoma. (A) Non-intense lymphocytic infiltration (TIL density 0%) B. Non-intense lymphocytic infiltration (TIL density 5%) C. Intense lymphocytic infiltration (TIL density 20%) D. Intense lymphocytic infiltration (TIL density 60%).

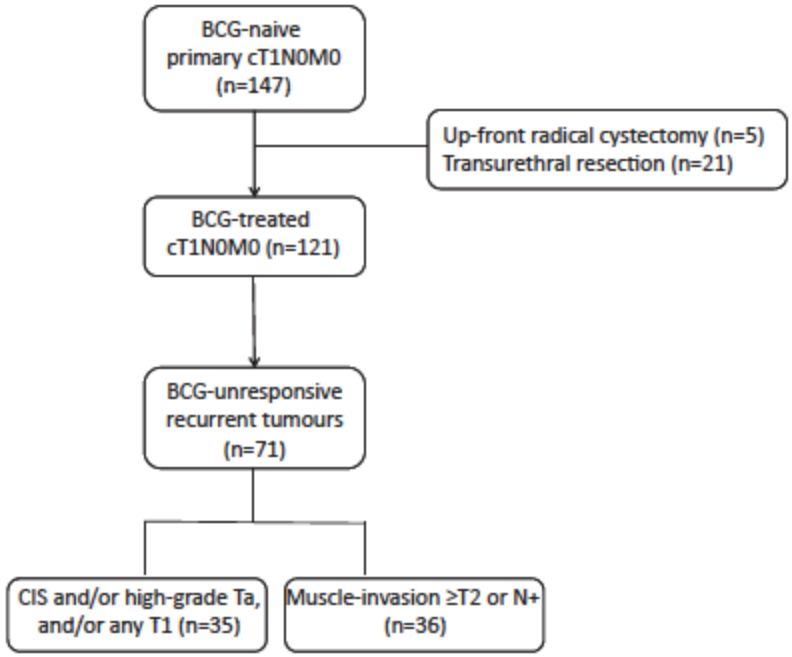

Fig. 2. Flowchart of the primary treatment strategies. BCG, Bacillus Calmette–Guérin.

Table 1
Patient characteristics.

Characteristics		All patients	Stromal TILs		p value
			<10%	≥10%	
		n (%)	n (%)	n (%)	
		147 (100)	65 (44)	82 (56)	
Age	<70 yr.	69 (47)	30 (46)	39 (47)	0.99
	≥70 yr.	78 (53)	35 (54)	43 (53)	
Sex	Female	17 (12)	6 (9)	11 (13)	0.59
	Male	130 (88)	59 (91)	71 (87)	
Smoking	Never	24 (16)	6 (9)	18 (22)	0.18
	Former	62 (42)	29 (45)	33 (40)	
	Current	29 (20)	12 (18)	17 (21)	
	Unknown	32 (22)	18 (28)	14 (17)	
Tumour size	<3 cm	31 (21)	14 (22)	17 (21)	1
	≥3 cm	54 (37)	25 (38)	29 (35)	
	Unknown	62 (42)	26 (40)	36 (44)	
Multifocality	Single	52 (36)	23 (35)	29 (35)	0.87
	Multiple	73 (50)	35 (54)	39 (48)	
	Unknown	21 (14)	7 (11)	14 (17)	
Growth pattern	Papillary	67 (45)	30 (46)	37 (45)	0.92
	Solid	36 (25)	15 (23)	21 (26)	
	Unknown	44 (30)	20 (31)	24 (29)	
Concomitant CIS	Yes	65 (44)	29 (45)	36 (44)	0.99
	No	82 (56)	36 (65)	46 (56)	
Lymphovascular invasion	Yes	15 (10)	06 (9)	9 (11)	0.94
	No	132 (90)	59 (91)	73 (89)	
Invasion depth	T1a	102 (70)	51 (79)	51 (62)	0.05
	T1b	45 (30)	14 (21)	31 (38)	
Histological variants	Yes	40 (27)	11 (17)	29 (35)	0.02
	No	107 (73)	54 (83)	53 (65)	
EORTC risk score	Low	16 (10)	6 (9)	10 (12)	0.67
	High	85 (58)	40 (62)	45 (55)	
	Unknown	46 (32)	19 (29)	27 (33)	
Second look performed	Yes	67 (46)	30 (46)	37 (45)	1
	No	80 (54)	35 (54)	45 (55)	
Primary BCG treatment	Yes	126 (86)	56 (91)	70 (85)	0.99
	No	21 (14)	9 (9)	12 (15)	

TILs, tumour-infiltrating lymphocytes; EORTC, European Organization for Research and Treatment of Cancer; BCG, Bacillus Calmette–Guérin.

3.2. TILs positively associated with the tumour invasion depth and variant histologies

At baseline, the median level of TILs was 20% (range 5%–60%). Stromal lymphocytic infiltration was ≥10% (intense) in 82 tumours (56%) and <10% (non-intense) in 65 tumours (44%). Heterogeneity was observed between the intense (≥10% TILs) versus the non-intense (<10% TILs) subgroups, for tumour invasion depth ($p = 0.05$) and variant histologies ($p = 0.03$) (Table 1). The distribution of lymphocytic infiltration among tumours with variant histologies is reported in Supplementary data Table S1. None of the other clinicopathological characteristics of the patients were associated with the baseline TILs levels. Particularly, no association was found between the density of TILs and concomitant CIS ($p = 0.78$) or lymphovascular invasion ($p = 0.53$). The baseline TIL level was significantly higher ($p = 0.009$) in patients with T1b substage (median, interquartile range [IQR]; 22.8, 10–30) compared with T1a substage (median, IQR; 17.7, 10–28.8) (Fig. 3A). Similarly, the density of TILs significantly increased ($p = 0.01$) in patients with variant histologies (median, IQR; 20, 10–30 compared with patients with pure urothelial carcinoma (median, IQR; 10, 10–27.5) (Fig. 3B).

3.3. Survival analysis

Tumour multiplicity and a high EORTC score were significantly associated with high-risk recurrence in the univariate analysis. Similarly, the tumour size (≥3 cm) was significantly associated with progression-free survival in the univariate analysis (Supplementary data Table S2). Age ≥70 years and lymphovascular invasion remained independent prognostic factors, respectively, for OS and bladder cancer-specific survival in the multivariate models (Table 2). Kaplan–Meier analysis of cancer-specific survival according to the TIL density showed an HR of 1.70 with 95% CI (0.7–3.9; $p = 0.2$). No statistical difference was found when adjusting on other prognostic factors (adjusted HR = 1.8; 95% CI 0.8–4.2; $p = 0.18$). Similar results were observed for OS (unadjusted and adjusted HR = 1.2; 95% CI 0.6–2.2, $p = 0.6$); PFS (unadjusted HR = 1.91; 0.6–6.1, $p = 0.3$; adjusted HR = 2.10; 0.7–6.7, $p = 0.22$) and recurrence-free survival (RFS) analyses (unadjusted HR = 0.8; 95% CI 0.4–1.5, $p = 0.5$; adjusted HR = 0.7; 95% CI 0.4–1.4), $p = 0.33$) (Fig. 4).

4. Discussion

Our study encompasses a homogenous population of 147 treatment-naive, primary cT1N0M0 bladder cancer with a long-term median follow-up of 8.2 years. We demonstrate a correlation between stromal TILs and clinical outcomes. The major finding is that the density of stromal TILs was not associated with a better clinical outcome including cancer-specific survival and OS as opposed to numerous neoplasms for other organs. Second, we found that the level of TILs significantly increased with the tumour invasion depth. Third, we also identified a statistically significant difference between the density of stromal TILs in tumours with variant histologies, listed on the WHO 2016 classification of bladder tumours, compared with pure urothelial carcinoma [11]. Altogether, these data further suggest that tumour aggressiveness may be associated with an increased adaptive immune response to the invasion depth and variant histologies in T1 bladder cancer.

Morphological assessment of TILs has been shown to provide prognostic and potentially predictive significance in many different tumour types [6]. A dense T-cell infiltrate is a common characteristic of tumours that have a favourable prognosis [13,14]. However, an

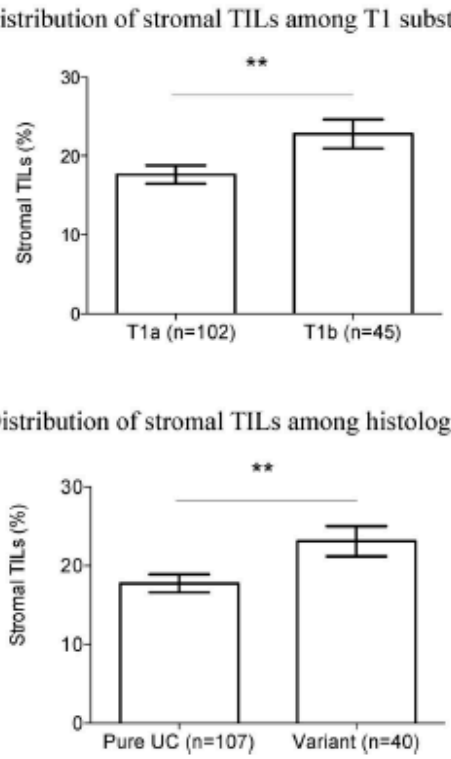

Fig. 3. Association among the density of stromal TILs, tumour invasion depth (A) and variant histologies (B). TILs, tumour-infiltrating lymphocytes; SEM, standard error of the mean.

association between high densities of CD8+ cytotoxic T-cells and short PFS and OS durations has also been reported in several solid tumours, including clear cell renal cell carcinoma and prostate cancer [15–17]. Large studies investigating the pattern of T-cell infiltrate and its potential prognostic value among various stages of urothelial carcinoma are lacking [9].

Sharma *et al.* [18] reported one of the first analyses evaluating the prognostic value of T-cell infiltration in urothelial carcinoma of the bladder (n = 38 pTa or pT1; n = 31 pT2-T4). Indeed, the authors reported that the presence of CD8+ TILs did not influence disease-free survival time among patients with NMIBC ($p = 0.693$) but had a substantial influence among patients with muscle-invasive disease ($p < 0.001$). This finding also suggests that TIL density may be a marker of disease aggressiveness rather than a sign of an ongoing effective antitumour immune response. To enhance the statistical power of our study, we focussed only our analysis on pT1 bladder tumours rather than a mixed population of high-risk NMIBC tumours.

In a previous study, Patschan *et al.* [19] assessed CD3+ T-cells infiltration in a cohort of primary T1 bladder cancer (n = 156) using a tissue microarray technique. The authors showed that high levels of CD3+ T-cells were significantly associated with poor prognosis and progressive disease. In agreement with our findings, they also reported a strong association between high levels of CD3+ T-cells and invasive ≥ pT1b tumours. The authors hypothesised that pT1b disease with high CD3 scores represented tumours that have reached an epithelial depth, which could allow a better immune recognition and therefore trigger an antitumour immune response. Whether the intense lymphocytic infiltration is directly linked to the tumour invasion depth remains difficult to demonstrate. Also, the use of tissue microarray (TMA) calls for great caution regarding the heterogeneity of the *in situ* antitumour immune response. In our study, the pathological assessment of stromal TILs was independently performed by two pathologists using a standardised, reference methodology on whole tissue sections using H&E staining [8,12]. This analysis allowed a specific characterisation of the immune response in the stromal infiltration (pT1) as the immune infiltrate in pTa and CIS is limited to the urothelial layer.

Recently, Wang *et al.* [20] investigated the clinical significance of CD103+ T-cells, a marker of tissue

Table 2
Multivariate analysis of clinicopathological factors for recurrence, progression, cancer-specific and overall survival.

Clinicopathological factors		No. events/ No. Patients	Univariate		Multivariate	
			HR (95% CI)	p	HR (95% CI)	p
Overall survival						
TILs	<10%	17/65	1		1	
	≥10%	24/82	1.2 (0.6–2.2)	0.6	1.2 (0.6–2.2)	0.6
Age (years)	<70	16/69	1		1	
	≥70	25/78	2.4 (1.3–4.5)	0.01	2.2 (1.2–4.2)	**0.02**
Variant	No	36/107	1		1	
	Yes	5/40	0.4 (0.2–1.1)	0.06	0.4 (0.2–1.1)	0.09
Cancer-specific free survival						
TILs	<10%	8/65	1		1	
	≥10%	17/82	1.7 (0.7–3.9)	0.2	1.8 (0.8–4.2)	0.18
Age (years)	<70	10/69	1		1	
	≥70	15/78	2.1 (0.9–4.8)	0.07	2.1 (0.9–4.7)	0.08
Lymphovascular invasion	No	20/132	1		1	
	Yes	5/15	2.7 (1.0–7.3)	0.04	3.1 (1.2–8.4)	**0.03**
Variant	No	22/107	1		1	
	Yes	3/40	0.4 (0.1–1.3)	0.1	0.40 (0.1–1.3)	0.14
Progression-free survival[b]						
TILs	<10%	4/26	1		1	
	≥10%	10/33	1.9 (0.6–6.1)	0.3	2.10 (0.7–6.7)	0.22
Growth pattern	Papillary	4/34	1		1	
	Solid	10/25	3.9 (1.2–12.5)	0.02	2.50 (0.7–9.8)	0.18
EORTC score	Low	1/15	1		1	
	High	13/44	5.2 (0.7–40.0)	0.1	3.19 (0.3–31.4)	0.32
Tumour size	<3 cm	4/29	1		1	
	≥3 cm	10/30	3.19 (1–10.2)	0.05	1.27 (0.3–5.3)	0.75
Recurrence-free survival [a]						
TILs	<10	18/33	1		1	
	≥10	21/41	0.8 (0.4–1.5)	0.5	0.7 (0.37–1.39)	0.33
No. tumours	Unique	19/44	1		1	
	Multiple	20/30	1.9 (1–3.5)	0.05	1.8 (0.9–3.6)	0.12
Growth pattern	Papillary	5/15	1		1	
	Solid	34/59	2.3 (0.9–5.9)	0.08	1.8 (0.7–5.1)	0.25
EORTC score	Low	11/25	1		1	
	High	28/49	1.5 (0.8–3.1)	0.2	1.0 (0.5–2.3)	0.95

TILs, tumour-infiltrating lymphocytes; EORTC, European Organization for Research and Treatment of Cancer; HR, hazard ratio; CI, confidence interval; Bold values $p<0.05$.
[a] Seventy-four.
[b] Fifty-nine patients with all the risk factors available were included in the multivariable analyses.

resident memory CD8+ T-cells, in a cohort of Ta-T4 urothelial carcinoma of the bladder (n = 302). Interestingly, the authors reported that the density of intratumour CD103 + TILs could represent a favourable prognostic of overall and RFS. As the dual role of the host's immunity in promoting or suppressing tumour growth has been well established [21], in depth analysis of inhibitory mechanisms negatively regulating T-cell activation is required.

Several studies analysed the impact of the tumour immune microenvironment on BCG therapy, without reaching formal and definitive conclusions [22–24]. Anti-PD1/PD-L1 immune checkpoint inhibitors have become the gold standard treatment in the second-line setting of metastatic urothelial carcinoma [25,26]. Interestingly, data from a large retrospective study (n = 296) showed that high mRNA expression of PD-L1 was associated with better outcomes in pT1 NMIBC [27]. These antibodies are now evaluated in monotherapies or combination therapies in the HGT1 setting [28]. From a research standpoint, extensive characterisation of the immune infiltrate using longitudinal samples during immunotherapy may further improve our understanding of immune escape.

Limitations of this study include the retrospective nature of the analysis and the absence of validated scoring system to assess stromal TILs. Therefore, external validation of the results is required. Furthermore, not all patients had a second-look TUR performed. Thus, understaging may not be formally excluded even if only HGT1 tumours with a visible, clearly identifiable and disease-free muscularis propria were included. Unquestionably, constitution of NMIBC cohorts with sufficient amount of tumour tissue available and high-quality clinical annotations is a critical step to further allow in-depth molecular and immune profiling of such tumours.

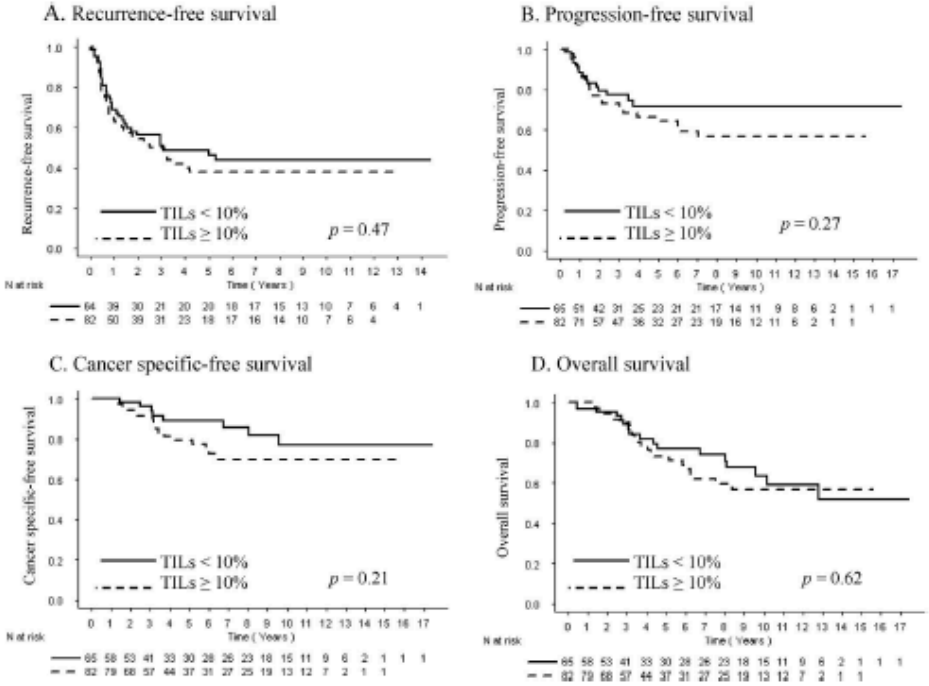

Fig. 4. Kaplan–Meier survival curves according to stromal TILs percentage for recurrence-free survival (A), progression-free survival (B) cancer-specific survival (C) and overall survival (D). The P value of the log-rank test is reported. TILs, tumour-infiltrating lymphocytes.

5. Conclusions

In summary, the present study showed that the density of stromal TILs is associated with tumour invasion depth and aggressive variant histologies in patients with completely resected primary high-grade T1 bladder cancer. A lack of correlation with clinical outcomes suggests a different prognostic value of TILs between NMIBC and MIBC. These data suggest that tumour progression is associated with an increased adaptive immune response in HGT1 bladder cancer. The role of other parameters including myeloid cells, B-cells and tumour stroma cells may be critical to enhance our knowledge of the host immune response in HG T1 bladder cancer. Therefore, the assessment of the immune infiltrate in longitudinal samples may be a cornerstone to unravel the mechanisms of BCG refractory tumours.

Conflict of interest statement

All the authors have no conflict of interest to declare.

Acknowledgements

The authors would like to thank Alice Perchenet for technical support.

Appendix A. Supplementary data

Supplementary data to this article can be found online at https://doi.org/10.1016/j.ejca.2018.12.010.

Funding

This work was supported by a grant for research into cancer immunotherapy from the French Association of Urology (AFU).

References

[1] Hurst C, Rosenberg J, Knowles M. SnapShot: bladder cancer. Cancer Cell 2018 13;34(2). https://doi.org/10.1016/j.ccell.2018.07.013. 350-350.
[2] Hedegaard J, Lamy P, Nordentoft I, et al. Comprehensive transcriptional analysis of early-stage urothelial carcinoma. Cancer Cell 2016;30(1):27–42. https://doi.org/10.1016/j.ccell.2016.05.004.
[3] Gontero P, Sylvester R, Pisano F, et al. Prognostic factors and risk groups in T1G3 non-muscle-invasive bladder cancer patients initially treated with Bacillus Calmette-Guérin: results of a retrospective multicenter study of 2451 patients. Eur Urol 2015;67(1):74–82. https://doi.org/10.1016/j.eururo.2014.06.040.
[4] Kakiashvili DM, van Rhijn BW, Trottier G, et al. Long-term follow-up of T1 high-grade bladder cancer after intravesical bacille Calmette-Guérin treatment. BJU Int 2011;107(4):540–6. https://doi.org/10.1111/j.1464-410X.2010.09572.x.

[5] Tan TZ, Rouanne M, Tan KT, Huang RY, Thiery TP. Molecular subtypes of urothelial bladder cancer: results from a meta-cohort analysis of 2411 tumors. Eur Urol 2018 Sep 10. https://doi.org/10.1016/j.eururo.2018.08.027. pii: S0302-2838(18)30619-5, [Epub ahead of print] PMID: 30213523.

[6] Fridman WH, Zitvogel L, Sautès-Fridman C, et al. The immune contexture in cancer prognosis and treatment. Nat Rev Clin Oncol 2017;14(12):717–34. https://doi.org/10.1038/nrclinonc.2017.101.

[7] Pruneri G, Lazzeroni M, Bagnardi V, et al. The prevalence and clinical relevance of tumor-infiltrating lymphocytes (TILs) in ductal carcinoma in situ of the breast. Ann Oncol 2017;28(2):321–8. https://doi.org/10.1093/annonc/mdw623.

[8] Hendry S, Salgado R, Gevaert T, et al. Assessing tumor-infiltrating lymphocytes in solid tumors: a practical review for pathologists and proposal for a standardized method from the international immuno-oncology biomarkers working group: Part 2: TILs in melanoma, gastrointestinal tract carcinomas, non-small cell lung carcinoma and mesothelioma, endometrial and ovarian carcinomas, squamous cell carcinoma of the head and neck, genitourinary carcinomas, and primary brain tumors. Adv Anat Pathol 2017;24(6):311–35. https://doi.org/10.1097/PAP.0000000000000161.

[9] Solinas C, Chanzá NM, Awada A, et al. The immune infiltrate in prostate, bladder and testicular tumors: an old friend for new challenges. Cancer Treat Rev 2017;53:138–45. https://doi.org/10.1016/j.ctrv.2016.12.004.

[10] Humphrey PA, Moch H, Cubilla AL, et al. The 2016 WHO classification of tumours of the urinary system and male genital organs-Part B: prostate and bladder tumours. Eur Urol 2016;70(1):106–19. https://doi.org/10.1016/j.eururo.2016.02.028.

[11] Paner GP, Stadler WM, Hansel DE, et al. Updates in the eighth edition of the tumor-node-metastasis staging classification for urologic cancers. Eur Urol 2018;73(4):560–9. https://doi.org/10.1016/j.eururo.2017.12.018.

[12] Salgado R, Denkert C, Demaria S, et al. The evaluation of tumor-infiltrating lymphocytes (TILs) in breast cancer: recommendations by an International TILs Working Group 2014. Ann Oncol 2015;26(2):259–71. https://doi.org/10.1093/annonc/mdu450.

[13] Fridman WH, Pagès F, Sautès-Fridman C, et al. The immune contexture in human tumours: impact on clinical outcome. Nat Rev Canc 2012;12(4):298–306. https://doi.org/10.1038/nrc3245.

[14] Fridman WH, Galon J, Pagès F, et al. Prognostic and predictive impact of intra- and peritumoral immune infiltrates. Cancer Res 2011;71(17):5601–5. https://doi.org/10.1158/0008-5472.CAN-11-1316.

[15] Giraldo NA, Becht E, Pagès F, et al. Orchestration and prognostic significance of immune checkpoints in the microenvironment of primary and metastatic renal cell cancer. Clin Canc Res 2015;21(13):3031–40. https://doi.org/10.1158/1078-0432.CCR-14-2926.

[16] Becht E, Giraldo NA, Beuselinck B, et al. Prognostic and theranostic impact of molecular subtypes and immune classifications in renal cell cancer (RCC) and colorectal cancer (CRC). Oncolmmunology 2015;4(12). e1049804.

[17] Petitprez F, Fossati N, Vano Y, et al. PD-L1 expression and CD8+ T-cell infiltrate are associated with clinical progression in patients with node-positive prostate cancer. Eur Urol Focus 2017;(17):30151–7. https://doi.org/10.1016/j.euf.2017.05.013. pii: S2405-4569.

[18] Sharma P, Shen Y, Wen S, et al. CD8 tumor-infiltrating lymphocytes are predictive of survival in muscle-invasive urothelial carcinoma. Proc Natl Acad Sci U S A 2007;104(10):3967–72.

[19] Patschan O, Sjödahl G, Chebil G, et al. A molecular pathologic framework for risk stratification of stage T1 urothelial carcinoma. Eur Urol 2015;68(5):824–32. https://doi.org/10.1016/j.eururo.2015.02.021. discussion 835-6.

[20] Wang B, Wu S, Zeng H, et al. CD103+ tumor infiltrating lymphocytes predict a favorable prognosis in urothelial cell carcinoma of the bladder. J Urol 2015;194(2):556–62. https://doi.org/10.1016/j.juro.2015.02.2941.

[21] Schreiber RD, Old LJ, Smyth MJ. Cancer immunoediting: integrating immunity's roles in cancer suppression and promotion. Science 2011;331(6024):1565–70. https://doi.org/10.1126/science.1203486.

[22] Ayari C, LaRue H, Hovington H, et al. Bladder tumor infiltrating mature dendritic cells and macrophages as predictors of response to bacillus Calmette-Guérin immunotherapy. Eur Urol 2009;55(6):1386–95. https://doi.org/10.1016/j.eururo.2009.01.040.

[23] Pichler R, Fritz J, Zavadil C, et al. Tumor-infiltrating immune cell subpopulations influence the oncologic outcome after intravesical Bacillus Calmette-Guérin therapy in bladder cancer. Oncotarget 2016;7(26):39916–30. https://doi.org/10.18632/oncotarget.9537.

[24] Pichler R, Gruenbacher G, Culig Z, et al. Intratumoral Th2 predisposition combines with an increased Th1 functional phenotype in clinical response to intravesical BCG in bladder cancer. Cancer Immunol Immunother 2017;66(4):427–40. https://doi.org/10.1007/s00262-016-1945-z.

[25] Siefker-Radtke AO, Apolo AB, Bivalacqua TJ, et al. Immunotherapy with checkpoint blockade in the treatment of urothelial carcinoma. J Urol 2018;199(5):1129–42. https://doi.org/10.1016/j.juro.2017.10.041.

[26] Rouanne M, Roumiguié M, Houédé N, et al. Development of immunotherapy in bladder cancer: present and future on targeting PD(L)1 and CTLA-4 pathways. World J Urol 2018. https://doi.org/10.1007/s00345-018-2332-5.

[27] Breyer J, Wirtz RM, Otto W, et al. High PDL1 mRNA expression predicts better survival of stage pT1 non-muscle-invasive bladder cancer (NMIBC) patients. Cancer Immunol Immunother 2018;67(3):403–12. https://doi.org/10.1007/s00262-017-2093-9.

[28] Wankowicz SAM, Werner L, Orsola A, et al. Differential expression of PD-L1 in high grade T1 vs muscle invasive bladder carcinoma and its prognostic implications. J Urol 2017;198(4):817–23. https://doi.org/10.1016/j.juro.2017.04.102.

EUROPEAN UROLOGY 75 (2019) 423–432

available at www.sciencedirect.com
journal homepage: www.europeanurology.com

European Association of Urology

Platinum Priority – Urothelial Cancer

Editorial by Lars Dyrskjøt on pp. 433–434 of this issue

Molecular Subtypes of Urothelial Bladder Cancer: Results from a Meta-cohort Analysis of 2411 Tumors

Tuan Zea Tan [a,*], *Mathieu Rouanne* [b,c], *Kien Thiam Tan* [d], *Ruby Yun-Ju Huang* [a,e,f,*], *Jean-Paul Thiery* [g,h,i,j]

[a] *Cancer Science Institute of Singapore, National University of Singapore, Center for Translational Medicine, Singapore;* [b] *Department of Urology, Hôpital Foch, Université Versailles-Saint-Quentin-en-Yvelines, Université Paris-Saclay, Suresnes, France;* [c] *INSERM Unit 1015, Laboratoire de Recherche Translationnelle en Immunologie (LRTI), Gustave Roussy, Université Paris-Saclay, Villejuif, France;* [d] *ACT Genomics Co., Ltd., Taipei city, Taiwan;* [e] *Department of Obstetrics and Gynecology, National University Health System, Singapore;* [f] *Department of Anatomy, Yong Loo Lin School of Medicine, National University of Singapore, Singapore;* [g] *Biochemistry Yong Loo Lin School of Medicine, National University of Singapore, Singapore;* [h] *Guangzhou Institute of Biomedicine and Health, Chinese Academy of Science, Guangzhou, People's Republic of China;* [i] *CNRS Emeritus CNRS UMR 7057 Matter and Complex Systems, University Paris Denis Diderot, Paris, France;* [j] *INSERM UMR 1186, Integrative Tumor Immunology and Genetic Oncology, Gustave Roussy, EPHE, PSL, Fac. de Médecine - University Paris-Sud, Université Paris-Saclay, Villejuif, France*

Article info

Article history:
Accepted August 16, 2018

Associate Editor:
James Catto

Keywords:
Bladder carcinoma
Microarray gene expression
Molecular subtypes

Abstract

Background: Previous molecular subtyping for bladder carcinoma (BLCA) involved <450 samples, with diverse classifications.
Objective: To identify molecular subtypes by curating a large BLCA dataset.
Design, setting, and participants: Gene expression publicly available were combined and reanalyzed. The dataset contained 2411 unique tumors encompassing non-muscle-invasive (NMIBC) and muscle-invasive BLCA (MIBC). Subtypes were reproduced on The Cancer Genome Atlas, UROMOL, and IMvigor210.
Intervention: Subtypes were assigned by gene expression.
Outcome measurements and statistical analysis: Kaplan-Meier analyses were performed for subtype-clinical outcome correlations; Chi-square/Fisher exact tests were used for subtype-clinicopathological parameters associations.
Results and limitations: We identified six molecular subtypes with different overall survival (OS) and molecular features. Subtype Neural-like (median OS, 87 mo) is prevalent in MIBC and characterized by high WNT/β-catenin signaling. HER2-like (107.7 mo) is distributed evenly across NMIBC and MIBC, with higher *ERBB2* amplification and signaling. Papillary-like (>135 mo), an NMIBC subtype enriched in urothelial differentiation genes, shows a high frequency of actionable *FGFR3* mutations, amplifications, and *FGFR3-TACC3* fusion. Luminal-like (91.7 mo), predominantly NMIBC, has higher MAPK signaling and more *KRAS* and *KMT2 C/D* mutations than other subtypes. Mesenchymal-like (MES; 86.6 mo) and Squamous-cell carcinoma-like (SCC; 20.6 mo) are predominant in MIBC. MES is high in AXL signaling, whereas SCC has elevated PD1, CTLA4 signaling, and macrophage M2 infiltration. About 20% of NMIBCs show MIBC subtype traits and a lower 5-yr OS rate than Papillary-like NMIBC (81% vs 96%). The main limitations of our study are the incomplete clinical annotation, and the analyses were

* Corresponding authors. Cancer Science Institute (T.Z. Tan and R.Y.-J. Huang) and Department of Biochemistry (J.-P. Thiery) Yong Loo Lin School of Medicine, National University of Singapore, 8 Medical Drive, Blk MD7, #02-03, Singapore 117597. Tel. +65 6516 1148 (T.Z. Tan and R.Y.-J. Huang) and +65 6516 3242 (J.-P. Thiery); Fax: +65 6516 1453.
E-mail addresses: csittz@nus.edu.sg (T.Z. Tan), bchtjp@nus.edu.sg (J.-P. Thiery).

https://doi.org/10.1016/j.eururo.2018.08.027

based on transcriptome subset due to comparisons across gene expression quantification technologies.
Conclusions: BLCA can be stratified into six molecular subtypes. NMIBC, with a high risk of progression, displays the molecular features of MIBC.
Patient summary: Biomarkers are urgently needed to guide patient treatment selection and avoid unnecessary toxicities in those who fail to respond. We believe molecular subtyping is a promising way to tailor disease management for those who will benefit most.

1. Introduction

Bladder carcinoma (BLCA) is one of the most common and lethal diseases worldwide, with approximately 430 000 new cases and more than 165 000 related deaths per year [1], a figure anticipated to double in the near future [2]. Urothelial carcinoma (UC) is the predominant histological type, with less-frequent histological variants including squamous (Squa), glandular differentiation (GD), neuroendocrine (NE), micro-papillary (MP), sarcomatoid, (Sarco) and plasmocytoid tumors. At diagnosis, 75% of patients have non–muscle-invasive BLCA (NMIBC), whereas the remaining 25% have muscle-invasive BLCA (MIBC) [2]. NMIBC is characterized by common activating *FGFR3* mutations, diploid or near-diploid karyotypes, frequent recurrence (50–70%) but a low propensity to progress (10–15%), and a 5-yr survival of ~90% [2,3]. MIBC, however, is characterized by frequent *TP53* mutations, aneuploidy, with many chromosomal alterations, high rates of metastasis, and a 5-yr survival of <50% despite radical surgery [4].

On the therapeutic front, the management is distinct for NMIBC and MIBC. The treatment has remained essentially unchanged over the past few decades [3] until the launch of clinical trials using fibroblast growth factor receptor (FGFR)-targeting agents [5] and the US Food and Drug Administration approval of immune checkpoint inhibitors [6,7] in first-line or metastatic settings. However, most patients do not benefit from these cancer therapies. The IMvigor210 phase II trial in platinum-treated locally advanced UC reported that the molecular subtype proposed by The Cancer Genome Atlas (TCGA) was associated with atezolizumab clinical response [8,9]. This suggests that stratification of BLCA based on molecular subtype could be an effective strategy for therapeutic regimen allocation.

Apart from TCGA [10,11], several studies have shown that NMIBC and MIBC could be assigned across 2–7 molecular subtypes based on transcriptomic [12–16] or genomic [17] data and with distinct clinicopathological characteristics. To facilitate clinical adoption, a consensus classification unifying these different subtypes is needed. Attempts have been made to unravel the complexity and refine these molecular subtypes [16,18–20] based on biomarkers and pathways, mutations and copy number aberrations, or protein abundance [21]. Motivated by the need for a unifying subtype scheme, in this original study, we collated and analyzed a collection of 2411 BLCA gene expression profiles. Such a large sample size allows for greater statistical power in subtype identification and characterization, and minimizes sampling bias [22]. This study is also motivated by one of the most important unmet clinical needs of identifying potentially lethal NMIBCs. These NMIBCs, with a very high risk of disease progression, can be subjected to more aggressive disease management [23]. As high-risk NMIBC may display MIBC traits [14,17], NMIBC and MIBC tumors were analyzed together in this meta-cohort to allow for comparisons between the two progression pathways at the molecular level.

2. Materials and methods

2.1. Inclusion criteria

We adopted broad inclusion criteria because the aim of the study was to compile a database for broader generalization (covering different stages, grades, and histologies) and for a larger sample size [24]. All publicly available data annotated as BLCA were included (last accessed May 4, 2018). Clinical data of GSE38264 [25] was kindly provided by the authors.

2.2. Gene expression analysis

We downloaded the publicly available BLCA gene expression datasets (Supplementary Fig. 1; Supplementary data). A total of 36 cohorts were collected. Cohorts with <20 tumors and cohorts hybridized on older (Affymetrix U133A) or two-color microarray platforms were removed from meta-cohort compilation (Supplementary Tables 1 and 2; Supplementary data). We performed a quality check, platform-specific normalization, and combined them by ComBat [26] (Supplementary Fig. 2; Supplementary data). Duplicate samples were removed from the meta-cohort (Supplementary Table 3). Principal component analysis, clinicopathological parameter correlations, and batch effect metrics [27] assessment were performed to ensure minimization of batch effect (Supplementary Fig. 2; Supplementary data). Validation RNA-seq datasets—TCGA BLCA version 2016_01_28 [28], UROMOL E-MTAB-4321, and IMvigor210—were downloaded from GDAC, ArrayExpress, and the Supplementary data of Mariathasan et al. [9], respectively. Significantly mutated genes and focal copy number aberrations were extracted from Robertson et al. [11], and the distribution of these mutations and aberrations was analyzed.

We employed the R ConsensusClusterPlus v1.36.0 [29] to identify clusters in the meta-cohort using the most varying 5328 genes out of the 10596 genes common across the expression microarray platforms (Supplementary data). Core samples were defined by silhouette width of >0.01. Previously reported subtypes were inferred by the published predictor [30] or consensus clustering using subtype signatures [15,20,21]. We employed an epithelial-mesenchymal transition projection [31] and R GSVA 1.20.0 to estimate pathway enrichment scores for each sample. Immune cell infiltration was estimated using CIBERSORT [32].

2.3. Statistical analysis

Statistical tests were computed using Matlab R2016b (MathWorks; Natick, MA, USA). Kaplan-Meier analyses were computed using

GraphPad Prism v5.04 (GraphPad Software; La Jolla, CA, USA). Differences in the mean expression or pathway enrichment scores between subtypes were computed using Significant Analysis of Microarray (SAM, software website, https://github.com/MikeJSeo/SAM) or analysis of variance test. Subtype association analyses of clinical parameters were computed using chi-square/Fisher exact tests. Correlation analyses were computed using the Spearman's rank correlation coefficient test.

3. Results

3.1. UC meta-cohort shows six molecular subtypes, displaying good overlap with published subtypes

To identify molecular subtype based on gene expression, we compiled a BLCA meta-cohort of 2411 samples from 19 UC cohorts and applied a consensus clustering algorithm [29] (Table 1; Supplementary Table 1; Supplementary Figs. 1–4; Supplementary data). Based on similarity matrix, change in the area under the curve value, and sample cluster consensus metrics, we selected a stable classification of six major molecular subtypes (MC1–6; $n > 100$ in each cluster; Fig. 1A; Supplementary Fig. 3), hereafter denoted as "BOLD" for BLCA subtypes Of Large meta-cohort Database. To ensure that BOLD did not result from potential confounding factors (eg. batch effect, tissue source), we checked the distribution of BOLD across different clinical parameters, tissue sources, cohorts, and microarray platforms (Supplementary Fig. 3D; Supplementary Table 4). All six subtypes were distributed evenly across clinicopathological parameters, cohorts, and gene expression microarray platforms. We labeled several genes implicated in BLCA subtyping, such as basal, luminal, immune, proliferation, differentiation, and other subtype markers previously reported [16,20,21] (Fig. 1; Supplementary Table 9).

To investigate if BOLD subtypes overlapped with published subtypes, we adopted a three-pronged strategy to compare BOLD against published subtypes (Supplementary data). First, we checked the markers expressed in each subtype (Fig. 1A; Supplementary Tables 8 and 9). Second, we extracted the existing subtype annotation (Supplementary Fig. 5A). Third, we re-performed consensus clustering on a subset of the BLCA meta-cohort (selected by microarray platform) using most varying genes and published subtype signatures [10,13–15,30], and then annotated the samples with published subtypes based on biomarkers or predictor outputs (Fig. 1B and 1C; Supplementary Fig. 5B; Supplementary data). The three-pronged strategy yielded accordant results that BOLD has good agreement with published subtypes (Supplementary Fig. 5C; Supplementary data). We annotated the BOLD MC1-6 with selected biological features (Fig. 1D): MC1/Neural-like (NEURAL) is similar to LUND_SC/NE and TCGA_Neuronal subtypes; MC2/Luminal-like (LUM) is most similar to UROMOL2016_C3; MC3/Papillary-like (PAP) to LUND_Urobasal (Uro)/TCGA_Luminal-papillary; MC4/HER2-like (HER2L) to LUND_Genomic Unstable (GU)/TCGA_Luminal; MC5/Squamous-cell carcinoma-like (SCC) to LUND_ SCC-like)/MDA_basal/TCGA_Basal-Squamous; and MC6/Mesenchymal-like (MES) to LUND_Infiltrated (Inf)/MDA_TP53/TCGA_Luminal-infiltrated. UNC_Luminal encapsulated HER2L, LUM, and PAP, whereas basal captured NEURAL, MES, and SCC (Fig. 1D). Compared with published NMIBC subtypes (Fig. 1C and 1D), the HER2L, MES, and SCC subtypes were similar to the aggressive genomic subtype LICAP_HG2 [17], and paradoxically, PAP was akin to LICAP_HG1 ($p = 5.3E-27$; Fig. 1C). Similarly, we observed the poor prognosis of HER2L and SCC subtypes enriched in the aggressive, MIBC-like UROMOL2016_C2 [33]. However, LUM was enriched in another aggressive UROMOL2016_C3 [33] ($p = 3.2E-155$; Fig. 1C).

Table 1 – Clinical information of urothelial carcinoma meta-cohort

	n	%
No. of cohorts	19	100
No. of samples	2533	100
Normal	122	4.82
Primary	2388	94.58
Recurrent	23	0.91
Histology		
Urothelial carcinoma (with CIS)	1973 (37)	81.8 (1.5)
Micropapillary	53	2.2
Squamous/epidermoid	46	1.91
Sarcomatoid	6	0.25
Glandular/adenocarcinoma/lymphoepithelioma	6	0.25
Neuroendocrine/small cell	6	0.25
Mixed/other	5/9	0.21/0.37
Not available	307	12.73
Gender		
Male	797	33.07
Female	225	9.33
Not available	1,389	57.61
Age		
Median (yr)	67	–
Min–max	20–96	–
Muscle-invasive		
Yes	1386	57.49
No	653	27.08
Not available	372	15.43
Stage[a]		
pTa/pT1	678	26.77
pT2	579	22.86
pT3/pT4	440	17.37
Not available	580	24.06
Lymph node invasion		
No	596	24.72
Yes	143	5.93
Not available/not applicable	1226/446	50.9/18.5
Metastasis		
Loco-regional	622	25.79
Distant	88	3.65
Not available/not applicable	1235/466	51.2/19.3
Overall survival		
Median (mo)	35.35	–
No. of events	347	14.39
Disease-free survival		
Median (mo)	18.99	–
No. of events	49	2.03
Grade		
Low[b]	331	13.73
High	828	34.34
Not available	1252	51.93
Surgery		
Cystectomy	414	17.17
Transurethral resection	992	41.15
Not available	1005	41.68

CIS = carcinoma in situ.
[a] pT0, Tx excluded.
[b] Combined with 130 (5.4%) originally labeled punlump samples.

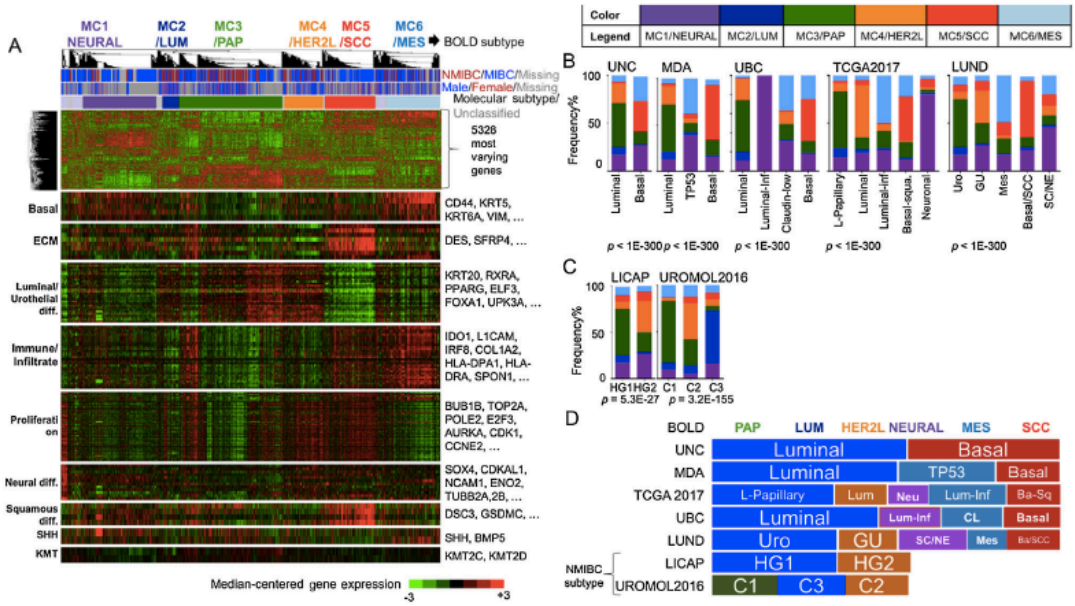

Fig. 1 – Unsupervised hierarchical clustering of urothelial carcinoma (UC) meta-cohort revealed six molecular subtypes. (A) Gene expression heatmap (red = high expression; green = low expression) of UC (*n* = 2411) aligned by identified molecular subtypes using 5328 most varying genes. Color bars show stage (NMIBC = red, MIBC = blue, grey = no annotation), and gender (female = red, male = blue, grey = no annotation). The subtypes are labeled as NEURAL (neural-like), LUM (luminal-like), PAP (papillary-like), HER2L (HER2-like), MES (mesenchymal-like), SCC (squamous-cell carcinoma-like), and denoted as BOLD (bladder carcinoma subtype of large meta-cohort database). Selected biomarkers for differentiation, proliferation are labeled. (B) Bar plots showing the frequency% (*y*-axis) association of BOLD with published molecular subtype: UNC, MDA, UBC, TCGA, and LUND. (C) Bar plots showing the frequency% (*y*-axis) of BOLD in the published NMIBC molecular subtypes of LICAP (left) [17], and UROMOL2016 [33] (right), using only the NMIBC found in BLCA meta-cohort. (D) A scheme depicting the inter-relationship between the BOLD and published molecular subtypes. The *p* values were computed by chi-square tests.
Color code: Purple = NEURAL; dark blue = LUM; green = PAP; orange = HER2L; red = SCC; light blue = MES.
Ba/SCC = basal/squamous-cell carcinoma-like; Ba-Sq = basal-squamous; BOLD = bladder carcinoma subtypes of large meta-cohort database; CL,= claudin-low; diff. = differentiation; ECM = extracellular matrix; GU = genomic unstable; HER2L, HER2-like; LICAP = Leeds Institute of Cancer and Pathology; L-papillary = luminal-papillary; Lum = luminal; LUM = luminal-like; Lum-inf = luminal infiltrated; LUND = Lund University; MDA = MD Anderson Cancer Center; Mes, mesenchymal; MES = mesenchymal-like; MIBC = muscle-invasive bladder carcinoma; Neu = neuronal; NEURAL = neural-like; NMIBC = non-muscle-invasive bladder cancer; PAP = papillary-like; SC/NE = small cell/neuroendocrine; TCGA = The Cancer Genome Atlas Network; UBC = University of British Columbia, UNC = University of North Carolina; Uro = urobasal.

Together, BOLD represents an umbrella subtype scheme capturing the various subtype schemes previously published.

3.2. *Both NMIBC and MIBC harbor BOLD subtypes, with distinct clinicopathological associations and pathways*

We next compared the characteristics of BOLD with those of the published subtypes it resembles. We applied silhouette analysis (Supplementary Fig. 6A; Supplementary data) to identify core samples for analyses of clinicopathological associations (Fig. 2; Table 2) and pathways. Unclassified samples or samples not associated with one of the BOLD subtypes were excluded from the analyses. In the entire BLCA meta-cohort, BOLD had different median overall survival (OS) outcomes ($p < 0.0001$; Fig. 2A): PAP (>135 mo), HER2L (107.7 mo), NEURAL, LUM, MES (~90 mo), and SCC (20.6 mo). The survival difference between PAP and LUM is most profound in NMIBC (Fig. 2A; middle panel). Intriguingly, the PAP subtype had a similar prognosis in MIBC (Fig. 2A; right panel), which may be due to the lower number of samples. Insufficient data did not allow an assessment of correlation with disease-free survival (Supplementary Fig. 6B). NEURAL, PAP, and SCC were significantly correlated to OS, and NEURAL, LUM, and MES were an independent prognostic factor (univariate and multivariate Cox regression analyses; Supplementary Table 10). The age at diagnosis was marginally different across BOLD, with the youngest age associated with the PAP subtype ($p = 0.0011$; Supplementary Fig. 6C). Interestingly, there were more females than males in the SCC subtype (Fig. 2B). LUM and PAP had more NMIBC, whereas NEURAL, MES, and SCC had more MIBC. HER2L had a comparable prevalence of NMIBC and MIBC. Interestingly, most Ta BLCAs were PAP, and T1 BLCAs were LUM and HER2L (Supplementary Fig. 6D; Table 2). Notably, ~20% of NMIBCs were NEURAL, MES, and SCC—subtypes predominantly comprising MIBC (Fig. 2B). Poor prognosis HER2L, MES, and SCC were characterized by late-stage ($p < 1E-300$), high-grade ($p = 3.3E-116$) cancers and were prone to lymph node invasion ($p = 6.2E-57$; Fig. 2B).

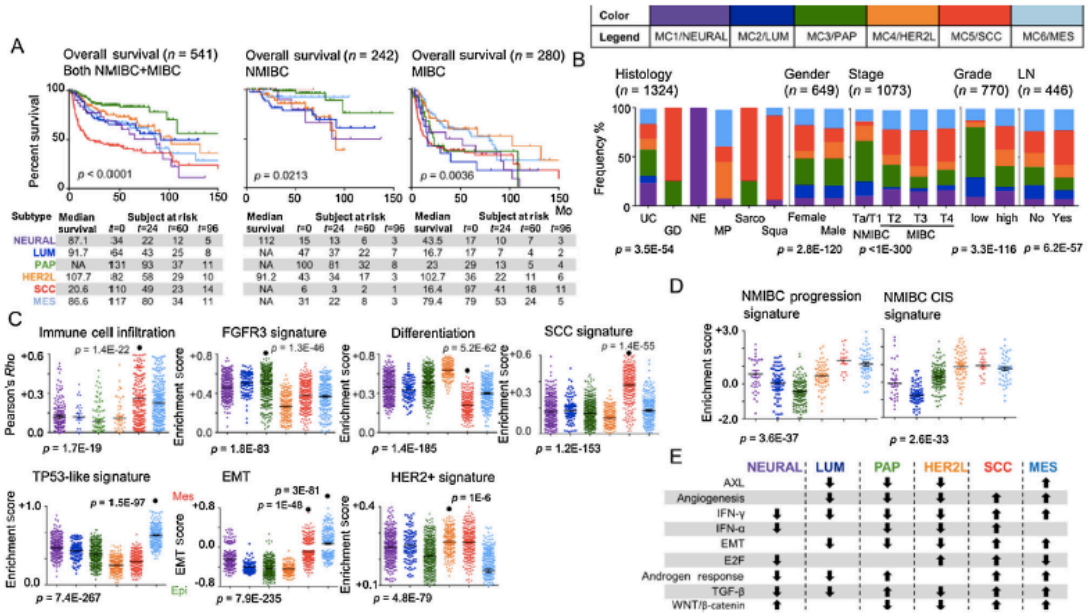

Fig. 2 – Characterization of BOLD. (A) Kaplan-Meier analysis of overall survival and BOLD in both NMIBC + MIBC (left), NMIBC only (middle), and MIBC (right). Median survival and subject at risks in months are given for each subtype. *T* denotes the time in months. Note that the summation of patients is not equal due to missing information of stage in certain patients. (B) Frequency% bar plot showing percentage of molecular subtype (*y*-axis) in different histology, gender, stage, grade, and lymph node/lymphovascular invasion) (*x*-axes). (C) Dot plot of immune cell infiltration, FGFR3 signature, Differentiation signature, Blaveri's SCC-like signatures, MDA TP53-like signature, EMT and breast cancer HER2+ subtype signature (*y*-axis) in BOLD (*x*-axis). Only core samples defined by silhouette width >0.01 were used for analysis. (D) Enrichment score (*y*-axis) of progression (left) and carcinoma in situ (right) in BOLD. The computation was performed only on NMIBC samples in BLCA meta-cohort. (E) Chart showing the elevated (up arrow) or depleted (down arrow) of selected pathways in BOLD. The *p* values were computed by log-rank (A), chi-square test (B), ANOVA (C, D; bottom) or Mann-Whitney (C; upper) tests. Data are presented as the mean ± SEM.
Color code: Purple = NEURAL; dark blue = LUM; green = PAP; orange = HER2L; red = SCC; light blue = MES.
ANOVA = analysis of variance; BOLD = bladder carcinoma subtypes of large meta-cohort database; CIS = carcinoma in situ; EMT = epithelial-mesenchymal transition; FGFR = fibroblast growth factor receptor; GD = glandular; HER2L, HER2-like; LN = lymph node; LUM = luminal-like; MES = mesenchymal-like; MIBC = muscle-invasive bladder cancer; MP = micro-papillary; NE = neuroendocrine; NEURAL = neural-like; NMIBC = non-muscle-invasive bladder cancer; PAP = papillary-like; Sarco = sarcomatoid; SCC = squamous-cell carcinoma-like; SEM = standard error of the mean; Squa = squamous; UC = urothelial cancer.

BLCAs of non-UC histologies are rare, aggressive, and have worse prognosis than UC (Supplementary Fig. 4A). Not surprisingly, the majority of non-UC histologies were distributed in the poor prognosis SCC and MES subtypes (Fig. 2B). The GD histology was mainly SCC; NE displayed similarity to NEURAL; MP was evenly distributed between HER2L and MES; and expectedly, BLCAs with Sarco and Squa differentiation were assigned primarily to SCC (Fig. 2B; Supplementary Table 5). Of note, LUM only had UC. This indicates that the rare variant histologies resembled transcriptomically the aggressive and poor prognosis subtypes of BOLD.

To ensure that the results presented were not biased by samples without complete clinical annotations (Table 1), we checked the distribution of clinicopathological parameters as well as the subtype in samples with annotation of histology, age, gender, stage, and grade available ($n = 802$), and samples without one or more of the annotation ($n = 1609$). Although there are differences in terms of distribution, all subtypes and clinicopathological parameters were represented in samples with or without complete clinical annotation (Supplementary Table 6). To affirm that the association results reported (Fig. 2; Supplementary Fig. 6C and 6D) were not an artefact arising from samples with missing data, we repeated the clinical association analyses using only core samples with complete annotation of histology, age, gender, stage, and grade ($n = 544$; Supplementary Fig. 6E–G; Supplementary Table 7). We observed that the subtype-clinicopathological parameters associations were highly concordant (Fig. 2B; Supplementary Fig. 6), demonstrating that the results were not distorted by the samples with incomplete clinical annotation.

From transcriptomic data, we observed higher infiltration of immune cells in MES and SCC subtypes. PAP is enriched for FGFR3 signature ($p = 1.3E-46$; Fig. 2C). The differentiation signature [34] showed that SCC was the most dedifferentiated ($p = 5.2E-62$). In concordance with the observation that MES is similar to the MDA_TP53 subtype, MES had the highest TP53-like signature ($p = 1.5E-97$; Fig. 2C). Likewise, SCC had the highest enrichment score for an SCC signature ($p = 1.4E-55$; Fig. 2C), and HER2L had the highest enrichment score of ERBB2+ signature [35]

Table 2 – Distribution of BOLD subtypes in selected clinicopathological parameters[a]

Parameter/subtype	*n*	NEU, *n* (%)	LUM, *n* (%)	PAP, *n* (%)	HER2L, *n* (%)	SCC, *n* (%)	MES, *n* (%)
Subtype prevalence	1543	350 (22.7)	89 (5.8)	422 (27.4)	170 (11)	268 (17.4)	244 (15.8)
Invasiveness							
NMIBC	424	38 (9)	64 (15.1)	175 (41.3)	70 (16.5)	17 (4)	60 (14.2)
MIBC	779	205 (26.3)	18 (2.3)	162 (20.8)	69 (8.9)	191 (24.5)	134 (17.2)
Stage							
Ta	209	17 (8.5)	24 (11.5)	122 (57.5)	14 (7)	9 (4)	23 (11.5)
T1 low-grade	75	11 (14.7)	24 (32)	24 (32)	5 (6.7)	0 (0)	11 (14.7)
T1 high-grade	113	10 (8.9)	9 (8.0)	25 (22.1)	44 (38.9)	6 (5.3)	19 (16.8)
T2	385	66 (17.1)	9 (2.3)	90 (23.4)	43 (11.2)	99 (25.7)	78 (20.3)
T3	173	26 (15)	5 (2.9)	21 (12.1)	19 (11)	64 (37)	38 (22)
T4	77	12 (15.6)	4 (5.2)	12 (15.6)	7 (9.1)	26 (33.8)	16 (20.8)
Lymph node invasion	72	6 (8.3)	6 (8.3)	9 (12.5)	9 (12.5)	26 (36.1)	16 (22.2)
Distant metastasis	47	3 (6.4%)	3 (6.4%)	11 (23.4%)	6 (12.8%)	15 (31.9%)	9 (19.1%)
Gender							
Female	150	12 (8.0%)	20 (13.3%)	41 (27.3%)	12 (8.0)	39 (26.0)	26 (17.3)
Male	499	42 (8.4)	60 (12.0)	139 (27.9)	87 (17.4)	71 (14.2)	100 (20.0)

HER2L = HER2-like; LUM = luminal-like; MES = mesenchymal-like; MIBC = muscle-invasive bladder carcinoma; NEU = neural-like; NMIBC = non–muscle-invasive bladder carcinoma; PAP = papillary-like; SCC = squamous-cell carcinoma-like.

[a] Percentage computation is based on a subset of core samples displaying the BOLD subtype only ($n \leq 1543$; silhouette width > 0.01), limited by the availability of clinical information (see column *n*). Please note that the number of samples with available clinical information is different from that of Table 1 due to our finer categorization of the clinical parameters. Only parameters related to invasiveness/staging were selected here.

($p = 1E\text{-}6$; Fig. 2C). The EMT score is a value representing the position of a cell or a tumor in a spectrum ranging from the most epithelial (−1.0) to the most mesenchymal phenotype (+1.0) [31]; this score indicates that MES and SCC are more EMT than other subtypes ($p = 3E\text{-}81$ and $1E\text{-}48$, respectively; Fig. 2C). Interestingly, MES and SCC showed enrichment of claudin-low breast cancer and basal signatures (Supplementary Fig. 7A; Supplementary data). MES was prone to co-occur with carcinoma in situ (CIS; $p = 5.3E\text{-}37$; Supplementary Fig. 6D; albeit, this was not conclusive [$n < 50$]). In addition, SCC, consistent with its high EMT characteristics (Fig. 2C), had greater propensity than the other subtypes to invade lymph node and to form distant metastasis ($p = 4.9Ee\text{-}37$; Table 2; Supplementary Fig. 6D). For BLCA treated by methotrexate, vinblastine, adriamycin, and cisplatin combination regimen, MES subtype samples were less likely to respond ($p = 0.0109$; Supplementary Fig. 6D). Looking at only NMIBC samples, consistently, MIBC-like subtypes NEURAL, SCC, and MES had higher enrichment of the progression signature [36] (Fig. 2D). Of note, LUM and HER2L—the more aggressive subtypes found in NMIBC—were significantly enriched for the progression signature (Fig. 2D). CIS signature [37] suggests that HER2L, SCC, and MES would be more likely to occur with CIS (Fig. 2D); the finding that HER2L and MES were likely to co-occur with CIS was concordant with clinical association (Supplementary Fig. 6D); however, SCC was not associated with CIS. Briefly, BOLD had different clinical outcomes and clinicopathological characteristics. Importantly, the distributions of good and poor prognosis subtypes were not exclusive to NMIBC or MIBC despite the prevalent differences.

Pathway analyses (Molecular Signature database version 6.1 [38]) revealed differential (increased) pathway enrichment across subtypes (Fig. 2D; Supplementary Table 11): WNT/β-catenin, neural-related pathways (GO axon, cranial-nerve, glial-cell) in NEURAL; MYC signaling in LUM; AXL signaling in MES; microtubule-related, ERBB signaling, DNA mismatch repair pathways in HER2L; androgen receptor (AR) signaling in PAP, MES, and SCC; wound healing pathway in more EMT subtypes NEURAL, MES, and SCC. TGF-β signaling in PAP, MES, and SCC; and EGF signaling in SCC. When comparing PAP and LUM—the two transcriptomically akin subtypes (Supplementary Table 12)—LUM had significantly higher MAPK activity, indicating LUM is a more proliferative form of PAP. Notably, PD1 and CTLA4 pathways were enriched in MES and SCC (Supplementary Table 11). Interferon-γ, angiogenesis, and inflammatory pathways were up-regulated in NEURAL, MES, and SCC. As several subtypes showed high immune cell infiltration and immune signature enrichment, we investigated if the BOLD classification results in differential immune cell infiltration allocation (Supplementary Table 13; Supplementary Fig. 7B). LUM has higher T-cell CD8+ infiltration, whereas MES and SCC have higher infiltration of tumor-associated macrophage M2 (Supplementary Fig. 7B). Because CD8+ cells are associated with anti-PD1 response [9], we projected a CD8 effector and a PD1 responder signature [39] (Supplementary Fig. 7C) and observed no significant correlation. Overall, BOLD recapitulated the existing published subtypes [10,11,13–15,21,30,40] and provided an elaborated classification of differential clinical outcomes.

3.3. *BOLD subtype stratification is reproducible in independent NMIBC, MIBC, and metastatic BLCA cohorts*

To examine the reproducibility of BOLD, we projected the subtype signatures derived using core samples (Supplementary Table 14; Supplementary data) on an NMIBC cohort (UROMOL), MIBC cohort (TCGA), and metastatic BLCA cohort (IMvigor210; Fig. 3A; Materials and methods). Of note, few samples in UROMOL were allocated to the NEURAL subtype. Subtype-clinicopathological associations were similar to those observed in the meta-cohort (Supplementary Fig. 8): PAP was associated with early-

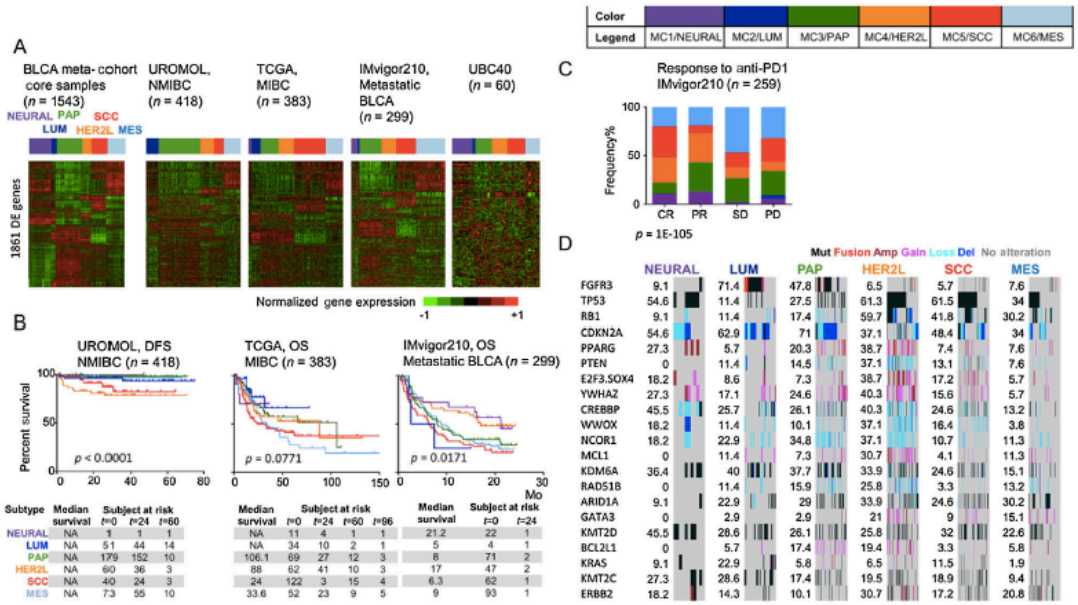

Fig. 3 – BOLD is reproducible in UROMOL, TCGA, and IMvigor210 cohorts. (A) Heatmap of 1861 most differentially expressed genes (red = high expression, green = low expression) across BOLD in core samples (silhouette width > 0.01) in BLCA meta-cohort, and in NMIBC cohort UROMOL, MIBC cohort TCGA, metastatic BLCA cohort IMvigor210, and cell lines UBC40. Color bars above heatmap show the inferred BOLD subtype on the different cohorts. (B) Kaplan-Meier analyses of OS and DFS (progression- and recurrence-free) in UROMOL (left), TCGA (middle), and IMvigor210 (right). (C) Frequency% (*y*-axis) plot of response to anti-PD1 (atezolizumab). Response is measured by RECIST v1.1 (*x*-axis). (D) Heatmap of BLCA significantly mutated genes and focal copy number aberrations differentially associated with subtypes. Copy number (*cn*) definition in log2 ratio: Amp, $cn > 1$; gain, $0.59 < cn \leq 1$; loss, $-1 \leq cn < -0.42$; del, $cn < -1$. The frequency% of altered genes in each subtype is given next to the heatmap.
The *p* values were computed by log-rank test (B) and ANOVA (C).
Color code: Purple = NEURAL; dark blue = LUM; green = PAP; orange = HER2L; red = SCC; light blue = MES; black = mutated; maroon = amp; pink = gain; light blue = loss; dark blue = del.
ANOVA = analysis of variance; Amp = copy number amplification; BLCA = bladder carcinoma; BOLD = bladder carcinoma subtypes of large meta-cohort database; CR = complete response; Del = copy number deletion; DFS = disease-free survival; HER2L = HER2-like; LUM = luminal-like; MES = mesenchymal-like; MIBC = muscle-invasive bladder cancer; Mut = mutated; NEURAL = neural-like; NMIBC = non-muscle-invasive bladder cancer; OS = overall survival; PAP = papillary-like; PD = progressive disease; PR = partial response; SCC = squamous-cell carcinoma-like; SD = stable disease; TCGA = The Cancer Genome Atlas; UBC 40 cell line = urothelial bladder cancer 40 cell line.

stage, low-grade, lower European Organisation for Research and Treatment of Cancer scores, smaller (<3 cm) tumors, and younger patients; SCC tended to progress during treatment (Supplementary Fig. 8D). Intriguingly, the observation that PAP had a good prognosis in NMIBC but comparable prognosis to that of other subtypes in MIBC was replicated in UROMOL, TCGA, and IMvigor210 cohorts (Fig. 3B). This suggests that PAP classification is more relevant in NMIBC, where PAP NMIBC and non-PAP NMIBC showed significantly different OS (Supplementary Fig. 8B; $p = 0.0022$). Nevertheless, we observed that SCC had the poorest outcome across NMIBC, MIBC, and metastatic BLCA. Similarly, LUM and MES both performed poorly in terms of survival. HER2L had a similar poor survival outcome in NMIBC and MIBC but relatively better prognosis in an anti-PD1-treated cohort in IMvigor210. This could be because HER2L is more likely to respond to anti-PD1 treatment (Fig. 3C). Higher mutation, copy number aberrations, and neoantigen load, thus, may predict the response to anti-PD1 treatment (Supplementary Fig. 9). In general, the clinical characterization of BOLD in our BLCA meta-cohort, UROMOL, TCGA, and IMvigor210 cohorts were concordant, indicating good reproducibility of our subtype identification.

Using TCGA data, we investigated the association of BOLD with significantly mutated genes, focal [11] and genome-wide copy number profiles (Fig. 3D; Supplementary Fig. 9C; Supplementary Table 16). Similar to previous reports, we observed that *FGFR3* fusion, mutation, and amplification were highly enriched in PAP, and that *TP53* mutation was enriched in HER2L and SCC. HER2L had more mutations, copy number aberrations, and neoantigen load (Supplementary Fig. 9A). Notably, PAP and LUM had 9q extensive deletions (Supplementary Fig. 9C), mimicking the low-risk HG1 NMIBC genomic subtype [17] but had different prognosis outcomes. In brief, BOLD exhibited diverse genetic and genomic alterations that may point to a potential targeted therapy.

We noticed that BLCA tumors harbor subtype-specific actionable mutations, aberrations, or pathway activations (Supplementary Tables 11 and 16): *FGFR3-TACC3* fusion in PAP; *ERBB2* amplification in HER2L and LUM (Supplementary

Table 16; Supplementary Fig. 10A; Supplementary data); *AXL* pathway in MES; AR pathway in MES and SCC; PD1 and CTLA4 pathways in MES and SCC; and *PPARG* fusion/amplification in HER2L. Of note, high *PPARG* and *MRE11* expressions have been linked to good outcome to bladder-preserving trimodality treatment (maximal transurethral resection, radiotherapy, and chemotherapy or immunotherapy) [41], suggesting HER2L could be a good candidate for trimodality treatment (Supplementary Fig. 10B). To explore a potential treatment strategy, we projected the BOLD signature to a BLCA cell line collection, UBC40 [42] (Supplementary Table 17), a patient-derived organoid collection GSE103990 [43] established from mainly Ta/T1 BLCA, and BLCA cell lines from COSMIC [44]. We correlated subtype enrichment scores with 50% growth inhibitory concentration (GI50) of different compounds. The epithelial-like PAP and LUM were more resistant than SCC (Supplementary Fig. 10C–E). MES, being stem-like, is expectedly resistant. HER2L, being genomically unstable, surprisingly shows no preferential sensitivity or resistance to any of the compounds tested (Supplementary data). In summary, BOLD subtypes have distinct molecular characteristics that are targetable, and the preliminary cell line-drug response analysis shows that subtypes have differential responses to compounds.

4. Discussion

Molecular subtyping holds great promise in understanding disease and in personalized therapeutics. In BLCA, an endeavor has been made to classify the disease into molecular subtypes to guide disease management [10,11,13–15,30,40]. However, most studies to date have been based on smaller cohort sizes (100–500 samples) even though >3000 BLCA samples are required to reliably detect gene mutations in 2% of samples [40]. Accordingly, more samples are needed to detect subtype differences with greater statistical power and to identify rare subtypes. This is exemplified by the TCGA, where only four gene expression subtypes were detected among 130 samples initially and later refined to five after expanding to 412 samples [10,11]. Here, we curated a database of >2400 samples and identified six molecular subtypes (denoted as BOLD). These six subtypes showed good concordance with previous reports, thus representing a convergence of findings. A recent meeting reached a consensus that there is a basal/SCC subtype; however, it remains unclear whether luminal/urobasal subtypes should be considered [19]. By amalgamating a large dataset, our findings not only affirm the basal/SCC subtype but also corroborate the existence of three luminal/epithelial-like subtypes (PAP, LUM, HER2L), a NEURAL subtype, and a claudin-low/stem-like MES subtype. Furthermore, our study showed that ~20% of NMIBCs display features of MIBC-like subtypes such as MES and SCC. Analysis of the meta-cohort also revealed that the rare but aggressive variant histologies of BLCA showed transcriptomic similarity with poor prognosis subtypes—SCC, MES, and HER2L. This resonates with the findings that NE BLCA has striking resemblance with UC [45], exhibiting similar mutational landscape and signature. However, a caveat of the rare histology analysis is the low number of samples for each variant ($n < 50$), and that the rare variants often co-existed with UC within a tumor lesion.

Molecular characterization of BOLD uncovered specific exploitable vulnerabilities. Notably, PAP NMIBC patients have significantly better survival outcomes and may, thus, require less frequent surveillance. HER2L, LUM, MES, and SCC are at high risk of progression and would, therefore, require more frequent monitoring and may be treated more aggressively. It is not surprising that BOLD displayed widely preferential responses. From a cell line-drug response analysis, MES was generally resistant to chemotherapy compounds, such as cisplatin and paclitaxel, agreeing with a previous report that claudin-low (resembles MES) tumors are less likely to respond to cisplatin-neoadjuvant chemotherapy [13]. While NEURAL, MES, and SCC had elevated PD1 and CTLA4 signaling, suggesting that they may be candidates for anti-PD(L)1 or anti-CTLA4 treatments; data from IMvigor210 show that the three subtypes were not significantly associated with complete response, with MES being the least beneficial. However, HER2L had a high tumor mutational burden and neoantigen load, which are associated or predicted with durable immune checkpoint inhibition response [8,9]. IMvigor210 data show that HER2L is more likely to be benefited from anti-PD(L)1 treatment. Interestingly, HER2L displayed elevated DNA-replication/cell-cycle signaling, lower hypoxia signaling (Supplementary Table 11), and at the same time high *PPARG* and *MRE11* expression (Fig. 1A; Supplementary Fig. 10B), suggesting that HER2L tumors may benefit from bladder-preserving trimodality therapy (maximal transurethral resection, followed by concurrent radiotherapy and chemotherapy/immunotherapy) [41,46]. However, BLCA is heterogeneous and unlikely to be solely dependent on one pathway. For example, MES and SCC, despite having high PD1, CTLA-4 signaling, also exhibited elevated angiogenesis, TGF-β signaling, and increased infiltration of immunosuppressive macrophage M2, which have been linked to lack of immunotherapy response [9]. Thus, a single-agent approach may not yield significant outcome improvement in these subtypes. Instead, combining immune checkpoint inhibition with an AXL inhibitor [47] in MES, an anti-TGF-β in MES and SCC [9], or an AR inhibitor in MES, and SCC may be viable treatment options [3]. Other targetable axes that could be explored include: (1) *FGFR3* amplification, activating mutations, and *FGFR3-TACC3* fusion in MIBC or metastatic BLCA of PAP subtype through the use of a pan-FGFR inhibitor [5]; TCGA luminal-papillary subtype, which resembling PAP, was shown to have promising activity to a pan-FGFR inhibitor Erdafitinib [48], suggesting the feasibility of targeting FGFR3 in PAP subtype, (2) ERBB2 amplification in HER2L and LUM via a HER2 inhibitor, (3) PPARG activating mutation, fusion in HER2L by a PPARG inhibitor [49], and (4) *PTGS2*-driven wound healing pathway in NEURAL, MES, and SCC via a COX2 inhibitor [50]. Supplementary Figure 11 summarizes the potential therapeutic framework of BOLD stratification.

As this study is based on curation and re-analysis of samples from different sources, the study is limited by the completeness, accuracy, or quality of the samples collected. More of the available studies were MIBC-focused, and thus, the prevalence and natural history of BLCA were not fully represented by the compiled meta-cohort. In addition, the main limitations of our study are the lack of clinical annotation among several publicly available BLCA cohorts. Therefore, while care has been taken to ensure that the analyses were not biased by samples without complete clinical annotation (Supplementary Tables 6 and 7), we cannot rule out the possibility of misdiagnosis, especially for Ta/T1 and CIS cases. However, we believe even such misdiagnosed or wrongly annotated cases are likely rare, and the effect of such cases within >2400 cohort should be minimal. Another limitation is that some genes were not available in the meta-cohort as the analysis required a comparison across different gene expression quantification technologies. However, the effect of missing genes should be negligible in regard to subtype prediction, as seen by the good molecular characteristic conformity of the BOLD classification with other published subtypes. Finally, the clinical relevance of these six molecular subtypes is based on survival data analysis. The therapeutic impact of these subtypes could not be assessed due to the unavailability of treatment-related data.

5. Conclusions

BLCA can be stratified into six molecular subtypes, each with distinct pathways and targetable vulnerability. These findings may have relevance in clinical practice. Therapeutic implications should be evaluated in prospective biomarker-driven clinical trials.

Author contributions: Tuan Zea Tan, Ruby Yun-Ju Huang, and Jean-Paul Thiery had full access to all the data in the study and take responsibility for the integrity of the data and the accuracy of the data analysis.

Study concept and design: T.Z. Tan, Thiery.
Acquisition of data: T.Z. Tan.
Analysis and interpretation of data: T.Z. Tan, Rouanne, K.T. Tan, Huang, Thiery.
Drafting of the manuscript: T.Z. Tan, Rouanne, Thiery.
Critical revision of the manuscript for important intellectual content: T.Z. Tan, Rouanne, K.T. Tan, Huang, Thiery.
Statistical analysis: T.Z. Tan.
Obtaining funding: Huang.
Administrative, technical, or material support: T.Z. Tan.
Supervision: Huang, Thiery.
Other: None.

Financial disclosures: Tuan Zea Tan, Ruby Yun-Ju Huang, and Jean-Paul Thiery certify that all conflicts of interest, including specific financial interests and relationships and affiliations relevant to the subject matter or materials discussed in the manuscript (eg, employment/affiliation, grants or funding, consultancies, honoraria, stock ownership or options, expert testimony, royalties, or patents filed, received, or pending), are the following: K.T. Tan is an employee of ACT Genomic. J.-P. Thiery is a consultant/advisory board member for Aim Biotech Singapore, ACT Genomic and CSO BioCheetah Ltd Singapore. No potential conflicts of interest were disclosed by the other authors.

Funding/Support and role of the sponsor: None.

Acknowledgments: This work is supported by National Research Foundation (NRF) Singapore and the Singapore Ministry of Education under its Research Centres of Excellence initiative to R.H.; National Medical Research Council (NMRC) under its Centre Grant scheme to National University Cancer Institute (NCIS) to R.H.

Appendix A. Supplementary data

Supplementary data associated with this article can be found, in the online version, at https://doi.org/10.1016/j.eururo.2018.08.027.

References

[1] Torre LA, Bray F, Siegel RL, Ferlay J, Lortet-Tieulent J, Jemal A. Global cancer statistics, 2012. CA Cancer J Clin 2015;65:87–108.
[2] Sanli O, Dobruch J, Knowles MA, et al. Bladder cancer. Nat Rev Dis Primers 2017;3:17022.
[3] Knowles MA, Hurst CD. Molecular biology of bladder cancer: new insights into pathogenesis and clinical diversity. Nat Rev Cancer 2015;15:25–41.
[4] Witjes JA, Lebret T, Comperat EM, et al. Updated 2016 EAU Guidelines on muscle-invasive and metastatic bladder cancer. Eur Urol 2017;71:462–75.
[5] Tabernero J, Bahleda R, Dienstmann R, et al. Phase I dose-escalation study of JNJ-42756493, an oral pan-fibroblast growth factor receptor inhibitor, in patients with advanced solid tumors. J Clin Oncol 2015;33:3401–8.
[6] Rouanne M, Loriot Y, Lebret T, Soria JC. Novel therapeutic targets in advanced urothelial carcinoma. Crit Rev Oncol Hematol 2016;98:106–15.
[7] Powles T, Eder JP, Fine GD, et al. MPDL3280A (anti-PD-L1) treatment leads to clinical activity in metastatic bladder cancer. Nature 2014;515:558–62.
[8] Rosenberg JE, Hoffman-Censits J, Powles T, et al. Atezolizumab in patients with locally advanced and metastatic urothelial carcinoma who have progressed following treatment with platinum-based chemotherapy: a single-arm, multicentre, phase 2 trial. Lancet 2016;387:1909–20.
[9] Mariathasan S, Turley SJ, Nickles D, et al. TGFbeta attenuates tumour response to PD-L1 blockade by contributing to exclusion of T cells. Nature 2018;554:544–8.
[10] Cancer Genome Atlas Research N. Comprehensive molecular characterization of urothelial bladder carcinoma. Nature 2014;507:315–22.
[11] Robertson AG, Kim J, Al-Ahmadie H, et al. Comprehensive molecular characterization of muscle-invasive bladder cancer. Cell 2017;171:540–56, e25.
[12] Rebouissou S, Bernard-Pierrot I, de Reynies A, et al. EGFR as a potential therapeutic target for a subset of muscle-invasive bladder cancers presenting a basal-like phenotype. Sci Transl Med 2014;6:244ra91.
[13] Seiler R, Ashab HAD, Erho N, et al. Impact of molecular subtypes in muscle-invasive bladder cancer on predicting response and survival after neoadjuvant chemotherapy. Eur Urol 2017;72:544–54.
[14] Sjodahl G, Lauss M, Lovgren K, et al. A molecular taxonomy for urothelial carcinoma. Clin Cancer Res 2012;18:3377–86.
[15] Choi W, Porten S, Kim S, et al. Identification of distinct basal and luminal subtypes of muscle-invasive bladder cancer with different sensitivities to frontline chemotherapy. Cancer Cell 2014;25:152–65.

[16] Aine M, Eriksson P, Liedberg F, Sjödahl G, Höglund M. Biological determinants of bladder cancer gene expression subtypes. Sci Rep 2015;5:10957.
[17] Hurst CD, Alder O, Platt FM, et al. Genomic subtypes of non-invasive bladder cancer with distinct metabolic profile and female gender bias in KDM6A mutation frequency. Cancer Cell 2017;32:701–15, e7.
[18] Aine M, Eriksson P, Liedberg F, Höglund M, Sjödahl G. On molecular classification of bladder cancer: out of one, many. Eur Urol 2015;68:921–3.
[19] Lerner SP, McConkey DJ, Hoadley KA, et al. Bladder cancer molecular taxonomy: summary from a consensus meeting. Bladder Cancer 2016;2:37–47.
[20] Choi W, Ochoa A, McConkey DJ, et al. Genetic alterations in the molecular subtypes of bladder cancer: illustration in the Cancer Genome Atlas Dataset. Eur Urol 2017;72:354–65.
[21] Sjodahl G, Eriksson P, Liedberg F, Höglund M. Molecular classification of urothelial carcinoma: global mRNA classification versus tumour-cell phenotype classification. J Pathol 2017;242:113–25.
[22] Ein-Dor L, Kela I, Getz G, Givol D, Domany E. Outcome signature genes in breast cancer: is there a unique set? Bioinformatics 2005;21:171–8.
[23] McConkey DJ, Choi W. Subtyping bladder cancers: biology vs bioinformatics. J Natl Cancer Inst 2018;110:439–40.
[24] George SL. Reducing patient eligibility criteria in cancer clinical trials. J Clin Oncol 1996;14:1364–70.
[25] Santos M, Martinez-Fernandez M, Duenas M, et al. In vivo disruption of an Rb-E2F-Ezh2 signaling loop causes bladder cancer. Cancer Res 2014;74:6565–77.
[26] Johnson WE, Li C, Rabinovic A. Adjusting batch effects in microarray expression data using empirical Bayes methods. Biostatistics 2007;8:118–27.
[27] Shabalin AA, Tjelmeland H, Fan C, Perou CM, Nobel AB. Merging two gene-expression studies via cross-platform normalization. Bioinformatics 2008;24:1154–60.
[28] Center BITGDA. Firehose stddata_2016_01_28 run. Broad Institute of MIT and Harvard; 2016.
[29] Wilkerson MD, Hayes DN. ConsensusClusterPlus: a class discovery tool with confidence assessments and item tracking. Bioinformatics 2010;26:1572–3.
[30] Damrauer JS, Hoadley KA, Chism DD, et al. Intrinsic subtypes of high-grade bladder cancer reflect the hallmarks of breast cancer biology. Proc Natl Acad Sci U S A 2014;111:3110–5.
[31] Tan TZ, Miow QH, Miki Y, et al. Epithelial-mesenchymal transition spectrum quantification and its efficacy in deciphering survival and drug responses of cancer patients. EMBO Mol Med 2014;6:1279–93.
[32] Newman AM, Liu CL, Green MR, et al. Robust enumeration of cell subsets from tissue expression profiles. Nat Methods 2015;12:453–7.
[33] Hedegaard J, Lamy P, Nordentoft I, et al. Comprehensive transcriptional analysis of early-stage urothelial carcinoma. Cancer Cell 2016;30:27–42.
[34] Mo Q, Nikolos F, Chen F, et al. Prognostic power of a tumor differentiation gene signature for bladder urothelial carcinomas. J Natl Cancer Inst 2018;110:448–59.
[35] Prat A, Parker JS, Karginova O, et al. Phenotypic and molecular characterization of the claudin-low intrinsic subtype of breast cancer. Breast Cancer Res 2010;12:R68.
[36] Dyrskjot L, Reinert T, Algaba F, et al. Prognostic impact of a 12-gene progression score in non-muscle-invasive bladder cancer: a prospective multicentre validation study. Eur Urol 2017;72:461–9.
[37] Dyrskjot L, Kruhoffer M, Thykjaer T, et al. Gene expression in the urinary bladder: a common carcinoma in situ gene expression signature exists disregarding histopathological classification. Cancer Res 2004;64:4040–8.
[38] Subramanian A, Tamayo P, Mootha VK, et al. Gene set enrichment analysis: a knowledge-based approach for interpreting genome-wide expression profiles. Proc Natl Acad Sci U S A 2005;102:15545–50.
[39] Hugo W, Zaretsky JM, Sun L, et al. Genomic and transcriptomic features of response to anti-PD-1 therapy in metastatic melanoma. Cell 2016;165:35–44.
[40] Hurst CD, Knowles MA. Bladder cancer: multi-omic profiling refines the molecular view. Nat Rev Clin Oncol 2018;15:203.
[41] Miyamoto DT, Gibb E, Mouw KW, et al. Genomic profiling of muscle invasive bladder cancer to predict response to bladder-sparing trimodality therapy. Genitourinary Cancers Symposium. San Francisco: ASCO; 2018,. http://ascopubs.org/doi/abs/10.1200/JCO.2018.36.6_suppl.513
[42] Lee JK, Havaleshko DM, Cho H, et al. A strategy for predicting the chemosensitivity of human cancers and its application to drug discovery. Proc Natl Acad Sci U S A 2007;104:13086–91.
[43] Lee SH, Hu W, Matulay JT, et al. Tumor evolution and drug response in patient-derived organoid models of bladder cancer. Cell 2018;173:515–28, e17.
[44] Yang W, Soares J, Greninger P, et al. Genomics of Drug Sensitivity in Cancer (GDSC): a resource for therapeutic biomarker discovery in cancer cells. Nucleic Acids Res 2013;41:D955–61.
[45] Shen P, Jing Y, Zhang R, et al. Comprehensive genomic profiling of neuroendocrine bladder cancer pinpoints molecular origin and potential therapeutics. Oncogene 2018;37:3039–44.
[46] Hoskin P. Use of molecular markers in bladder preservation. Genitourinary Cancers Symposium. San Francisco, CA: ASCO; 2018.
[47] Antony J, Tan TZ, Kelly Z, et al. The GAS6-AXL signaling network is a mesenchymal (Mes) molecular subtype-specific therapeutic target for ovarian cancer. Sci Signal 2016;9:ra97.
[48] Siefker-Radtke AO, Necchi A, Park SH, et al. First results from the primary analysis population of the phase 2 study of erdafitinib (ERDA; JNJ-42756493) in patients (pts) with metastatic or unresectable urothelial carcinoma (mUC) and FGFR alterations (FGFRalt). Chicago, IL: ASCO; 2018,. http://ascopubs.org/doi/abs/10.1200/JCO.2018.36.15_suppl.4503
[49] Goldstein JT, Berger AC, Shih J, et al. Genomic activation of PPARG reveals a candidate therapeutic axis in bladder cancer. Cancer Res 2017;77:6987–98.
[50] Kurtova AV, Xiao J, Mo Q, et al. Blocking PGE2-induced tumour repopulation abrogates bladder cancer chemoresistance. Nature 2015;517:209–13.

Contribution to other original articles

c-Met activation leads to the establishment of a TGFβ receptor regulatory network required for bladder cancer invasion.

Accepted for publication in Nature Communications, in press.

Wen Jing Sim[1*], Prasanna Vasudevan Iyengar[2,3*], Dilraj Lama[4], Sarah Lui Kit Leng[2], Hsien Chun Ng[1], Lior Haviv Gelibter[5], Eytan Domany[5], Dennis Kappei[2], Tuan Zea Tan[2,6], Azad Saie[7,8], Patrick William Jaynes[2], Chandra Shekhar Verma[4,9,10], Alan Prem Kumar[2,11,12,13] , Mathieu Rouanne[14,15], Hong Koo Ha[16], Camelia Radulescu[17], Peter ten Dijke[3], Pieter Johan Adam Eichhorn[2,11,18,19,#], Jean Paul Thiery[1,8,20,#]

Running title: Regulation of TbR activity by MET

Keywords: Bladder cancer invasion/ EMT/ c-MET/ TbR

Abstract

Treatment of muscle-invasive bladder cancer remains a major clinical challenge. Aberrant HGF/c-MET upregulation and activation is frequently observed in bladder cancer correlating with cancer progression and invasion. However, the precise mechanisms underlying HGF/c-MET mediated invasion in bladder cancer remains unknown. As part of a negative feedback loop SMAD7 binds to the E3 ligase SMURF2 targeting the TGFβ receptor for degradation. Under these conditions SMAD7 acts as a SMURF2 agonist by disrupting the intramolecular interactions within SMURF2. We demonstrate that HGF stimulates TGFβ signalling by inducing c-SRC-mediated phosphorylation of SMURF2 at two tyrosine residues impeding SMAD7 binding and enhancing SMURF2 C2-HECT domain interaction, resulting in SMURF2 inhibition and TGFβ receptor stabilization. This upregulation of the TGFβ pathway by HGF leads to TGFβ-mediated Epithelial-Mesenchymal Transition (EMT) and invasion. Using biologically relevant orthotopic mouse models we show that inhibition of TGFβ signalling completely prevents HGF induced bladder cancer invasion. Furthermore, we make a rationale for the use of combinatorial TGFβ receptor kinase and MEK inhibitors in the treatment of high-grade non-muscle-invasive bladder cancers or early stage muscle invasive bladder cancers.

PARP inhibition enhances tumor cell–intrinsic immunity in ERCC1-deficient non–small cell lung cancer

Roman M. Chabanon,[1,2,3,4] Gareth Muirhead,[3] Dragomir B. Krastev,[3,4] Julien Adam,[2] Daphné Morel,[1,2] Marlène Garrido,[2] Andrew Lamb,[5] Clémence Hénon,[1,2] Nicolas Dorvault,[2] Mathieu Rouanne,[1,6] Rebecca Marlow,[7] Ilirjana Bajrami,[3,4] Marta Llorca Cardeñosa,[3,4,8] Asha Konde,[3,4] Benjamin Besse,[1,9] Alan Ashworth,[10] Stephen J. Pettitt,[3,4] Syed Haider,[3] Aurélien Marabelle,[6,11] Andrew N.J. Tutt,[3,7] Jean-Charles Soria,[1] Christopher J. Lord,[3,4] and Sophie Postel-Vinay[1,2,11]

[1]Université Paris Saclay, Université Paris-Sud, Faculté de médicine, Le Kremlin Bicêtre, Paris, France. [2]ATIP-Avenir group, Inserm U981, Gustave Roussy, Villejuif, France. [3]The Breast Cancer Now Toby Robins Breast Cancer Research Centre and [4]CRUK Gene Function Laboratory, The Institute of Cancer Research, London, United Kingdom. [5]Sage Bionetworks, Seattle, Washington, USA. [6]Inserm U1015, Gustave Roussy, Villejuif, France. [7]The Breast Cancer Now Research Unit, King's College London, London, United Kingdom. [8]Biomedical Research Institute INCLIVA, Hospital Clinico Universitario Valencia, University of Valencia, Valencia, Spain. [9]Department of Medical Oncology, Gustave Roussy, Villejuif, France. [10]UCSF Helen Diller Family Comprehensive Cancer Center, San Francisco, California, USA. [11]Département d'Innovations Thérapeutiques et Essais Précoces (DITEP), Gustave Roussy, Villejuif, France.

The cyclic GMP-AMP synthase/stimulator of IFN genes (cGAS/STING) pathway detects cytosolic DNA to activate innate immune responses. Poly(ADP-ribose) polymerase inhibitors (PARPi) selectively target cancer cells with DNA repair deficiencies such as those caused by *BRCA1* mutations or *ERCC1* defects. Using isogenic cell lines and patient-derived samples, we showed that ERCC1-defective non–small cell lung cancer (NSCLC) cells exhibit an enhanced type I IFN transcriptomic signature and that low ERCC1 expression correlates with increased lymphocytic infiltration. We demonstrated that clinical PARPi, including olaparib and rucaparib, have cell-autonomous immunomodulatory properties in ERCC1-defective NSCLC and BRCA1-defective triple-negative breast cancer (TNBC) cells. Mechanistically, PARPi generated cytoplasmic chromatin fragments with characteristics of micronuclei; these were found to activate cGAS/STING, downstream type I IFN signaling, and CCL5 secretion. Importantly, these effects were suppressed in *PARP1*-null TNBC cells, suggesting that this phenotype resulted from an on-target effect of PARPi on PARP1. PARPi also potentiated IFN-γ–induced PD-L1 expression in NSCLC cell lines and in fresh patient tumor cells; this effect was enhanced in ERCC1-deficient contexts. Our data provide a preclinical rationale for using PARPi as immunomodulatory agents in appropriately molecularly selected populations.

Introduction

Immune checkpoint inhibitors (ICIs) have revolutionized the prognosis of several aggressive cancers, notably non–small cell lung cancer (NSCLC). Recent impressive results of large phase III trials in NSCLC have reported unprecedented improvements in overall survival and progression-free survival when anti–programmed death receptor 1 or anti–programmed death ligand 1 (anti–PD-[L]1) was used in first-line therapy (1, 2). Likewise, remarkable 5-year survival rates of 16% have recently been reported in this disease (3), highlighting the ability of these agents to provide long-term tumor control. Although these results are encouraging, they also reinforce the fact that still only a minority of patients receive long-term benefit. Better understanding of the determinants of response to ICIs and identification of rational combinations that would increase the proportion of patients benefiting from these therapies are therefore crucial.

Several factors have been associated with response to immunotherapy: tumor-related factors (e.g., cancer cell mutations), microenvironment-related factors (e.g., expression of immune checkpoints, lymphocytic infiltration, or IFN signatures), and host-related factors (e.g., microbiome) (4). Defects in the DNA damage response (DDR) in cancer cells are key determinants of cancer immunogenicity. Indeed, DDR defects result in genomic instability and increased tumor mutational burden (TMB), which has been linked — at least in some cases — to better outcome upon ICI treatment (5). The best illustrations of this are probably mismatch repair-deficient tumors (6) and *POLE/POLD1*-mutated endometrial carcinoma and glioblastoma (7, 8), which are highly sensitive to ICIs, likely due to their increased neoantigen repertoire. High TMB has also been correlated with better response to ICIs in melanoma (9) and NSCLC (2, 10, 11). Other DNA repair defects, such as *BRCA1/2* mutations, have been found to be enriched in ICI responders (12). However, a simple correlation among DNA repair defect–induced genomic instability, TMB, and response to ICIs cannot be claimed (5), as tumor heterogeneity (13) and other determinants of response also play a role that, importantly, seems to be independent from TMB in response to ICIs (14, 15).

Conflict of interest: SPV has received research funding from Merck KGaA for an unrelated project, as part of the funding for her research team. AA, CJL, and ANJT are named inventors on patents (US patent nos. 9611223, 8143241) describing the use of PARPi and stand to gain from their use as part of the Institute of the Cancer Research "Rewards to Inventor" scheme. JCS has been a full-time employee of Medimmune/AstraZeneca since September 2017. He has received consultancy fees from AstraZeneca, Roche, Sanofi, Servier, and Pierre Fabre. AM has received consultancy fees and honoraria from Roche/Genentech, Pfizer, Novartis, Lytix Biopharma, Bristol-Myers Squibb, and MSD.

Submitted: July 3, 2018; **Accepted:** December 18, 2018.
Reference information: *J Clin Invest*. 2019;129(3):1211–1228.
https://doi.org/10.1172/JCI123319.

World Journal of Urology
https://doi.org/10.1007/s00345-018-2332-5

TOPIC PAPER

Development of immunotherapy in bladder cancer: present and future on targeting PD(L)1 and CTLA-4 pathways

Mathieu Rouanne[1,2] · Mathieu Roumiguié[3,4] · Nadine Houédé[3,5,6] · Alexandra Masson-Lecomte[3,7] · Pierre Colin[3,8] · Géraldine Pignot[3,9] · Stéphane Larré[3,10] · Evanguelos Xylinas[3,11] · Morgan Rouprêt[3,12] · Yann Neuzillet[1,3]

Received: 2 March 2018 / Accepted: 8 May 2018

Abstract

Purpose Over the past 3 decades, no major treatment breakthrough has been reported for advanced bladder cancer. Recent Food and Drug Administration (FDA) approval of five immune checkpoint inhibitors in the management of advanced bladder cancer represent new therapeutic opportunities. This review examines the available data of the clinical trials leading to the approval of ICIs in the management of metastatic bladder cancer and the ongoing trials in advanced and localized settings.

Methods A literature search was performed on PubMed and ClinicalTrials.gov combining the MeSH terms: 'urothelial carcinoma' OR 'bladder cancer', and 'immunotherapy' OR 'CTLA-4' OR 'PD-1' OR 'PD-L1' OR 'atezolizumab' OR 'nivolumab' OR 'ipilimumab' OR 'pembrolizumab' OR 'avelumab' OR 'durvalumab' OR 'tremelimumab'. Prospectives studies evaluating anti-PD(L)1 and anti-CTLA-4 monoclonal antibodies were included.

Results Evidence-data related to early phase and phase III trials evaluating the 5 ICIs in the advanced urothelial carcinoma are detailed in this review. Anti-tumour activity of the 5 ICIs supporting the FDA approval in the second-line setting are reported. The activity of PD(L)1 inhibitors in the first-line setting in cisplatin-ineligible patients are also presented. Ongoing trials in earlier disease-states including non-muscle-invasive and muscle-invasive bladder cancer are discussed.

Conclusions Blocking the PD-1 negative immune receptor or its ligand, PD-L1, results in unprecedented rates of anti-tumour activity in patients with metastatic urothelial cancer. However, a large majority of patients do not respond to anti-PD(L)1 drugs monotherapy. Investigations exploring the potential value of predictive biomarkers, optimal combination and sequences are ongoing to improve such treatment strategies.

Keywords Bladder cancer · Urothelial cancer · Immunotherapy · Immune checkpoint inhibitors · PD-1 · PD-L1 · CTLA-4

✉ Mathieu Rouanne
rouanne.mathieu@gmail.com

1 Department of Urology, Hôpital Foch, Université Versailles-Saint-Quentin-en-Yvelines, Université Paris-Saclay, 40 Rue Worth, 92150 Suresnes, France

2 INSERM U1015, Gustave Roussy, Université Paris-Saclay, Villejuif, France

3 Comité de Cancérologie de l'Association Française d'Urologie (ccAFU), Bladder Cancer Group, Maison de l'Urologie, Paris, France

4 Department of Urology, Institut Universitaire du Cancer, Oncopole, Toulouse, France

5 Department of Medical Oncology, CHU de Nîmes, Nimes, France

6 INSERM U1194, Montpellier Cancer Research Institute, Université de Montpellier, Montpellier, France

7 Department of Urology, Hôpital Saint-Louis, Université Paris-Diderot, Paris, France

8 Department of Urology, Hôpital privé de la Louvière, Lille, France

9 Department of Urology, Institut Paoli-Calmettes, Marseille, France

10 Department of Urology, CHU de Reims, Reims, France

11 Department of Urology, CHU Bichat, Paris, France

12 Department of Urology, Hôpital La Pitié-Salpétrière, AP-HP, GRC n°5, ONCOTYPE-URO, Paris, France

Published online: 01 June 2018

Introduction

Cisplatin-based chemotherapies have been the gold standard of care for metastatic bladder cancer for more than 30 years and are still recommended by international guidelines as first-line treatment for advanced tumours that are known to be sensitive to platinum salts [1–4]. However, long-term responses are rare and relapses often occur within 3 months of the end of chemotherapy. Additionally, almost half of patients are not eligible for first-line cisplatin-containing chemotherapy. For these patients, there is no clear standard treatment, but carboplatin-based regimens or single agent therapies have been considered as acceptable alternatives, gemcitabine–carboplatin (GC) being considered, until recently, as the preferred combination according to European guidelines [2, 3]. As second-line therapy, only vinflunine has been approved in Europe, with overall survival (OS) of 6.9 months (5.7–8.0) in the intent to treat population [5, 6]. Taxanes have also been widely used, based on the results of phase II trials, in North American countries [7].

Recent advances in cancer research have highlighted the pivotal role of the immune system in controlling tumour initiation, growth and progression [8]. In bladder cancer and many other cancer types, intra-tumoural CD8+ T cells have been associated with a positive prognosis [9]. Cytotoxic T cells can attack tumour cells, either directly or indirectly, and provide long-term protection from relapse and progressive disease. Importantly, the process of T cell activation is tightly regulated by several signals to avoid collateral damage and auto-immunity [10, 11]. First, T cells specifically recognize tumour antigens via their T cell receptors (TCR). Second, following TCR engagement, activated T cells are regulated by multiple co-stimulatory and co-inhibitory receptors that are called immune checkpoints. Inflammatory cytokines including interleukin (IL)-12 and type I interferon (IFN) then act as a third signal supporting T cell activation [12]. Importantly, cancer cells can hijack the immune system and develop several mechanisms to avoid immune destruction. One of the key ways of establishing and maintaining immune escape is activation of co-inhibitory receptors of T cells such as programmed-death protein 1 (PD1) and cytotoxic T-lymphocyte-associated protein 4 (CTLA-4). Targeting these immune checkpoints to increase anti-tumour immunity is currently one of the most promising therapeutic strategies in urothelial carcinoma as well as in a large variety of other tumours (Fig. 1). In 2017, two molecules, pembrolizumab, an anti-PD1 antibody, and atezolizumab, an anti-PD-L1 antibody,

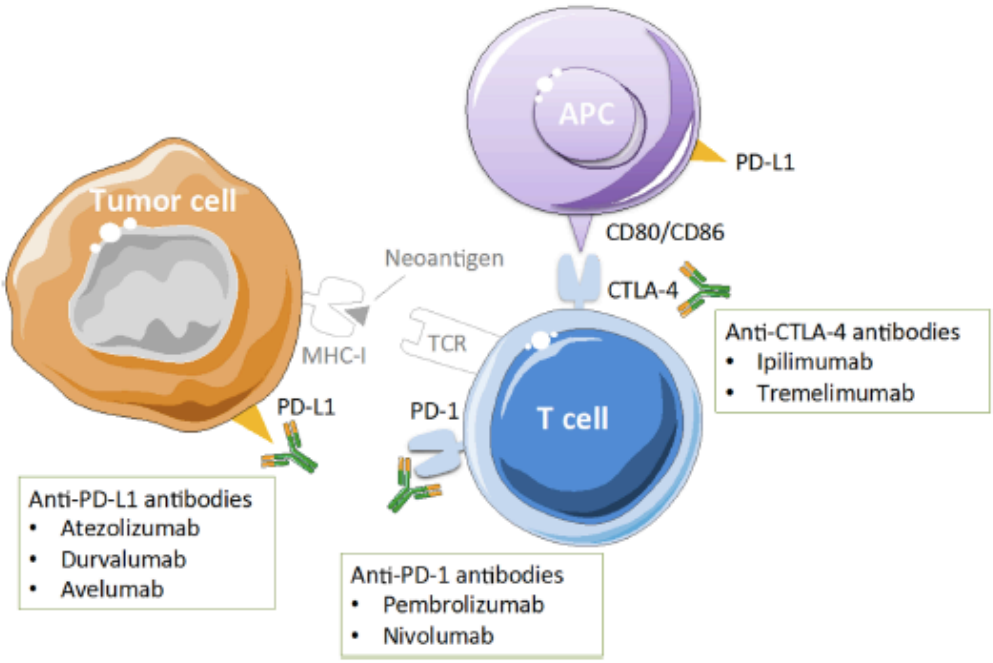

Fig. 1 Mechanisms of action of anti-PD(L)-1 and anti-CTLA-4 checkpoint inhibitors. *MHC-I* major histocompatibility complex type I, *TCR* T cell receptor, *APC* antigen presenting cell, *CD* cluster of differentiation, *PD-1* programmed cell death 1, *PD-L1* programmed cell death ligand 1, *CTLA-4* cytotoxic T lymphocyte-associated antigen-4

received US Food and Drug Administration (FDA) and European Medicines Agency (EMA) approval as first-line therapy for cisplatin-ineligible patients with advanced urothelial cancer. In addition, five ICIs including pembrolizumab, nivolumab, atezolizumab, durvalumab and avelumab, have recently been approved for the treatment of patients with advanced and metastatic urothelial carcinoma in the post-platinum setting (Fig. 2). Beyond single pathway blockade, several combinations with anti-PD(L)1 and anti-CTLA-4 inhibitors (i.e. ipilimumab and tremelimumab) are currently under evaluation, due to the potential synergistic effects of these drugs (Table 1).

These new drugs can induce a robust and durable response in a subset of patients with metastatic urothelial cancer. Monotherapy with immune checkpoint inhibitors (ICIs) has recently shown striking results in clinical trials, both as second- and first-line therapy for advanced bladder cancer [13]. Between May 2016 and May 2017, five anti-PD(L)1 antibodies were granted accelerated approval by the US Food and Drug Administration (FDA) and European Medicines Agency (EMA) to treat metastatic bladder cancer. In this review, the main results related to early phase and phase III clinical trials evaluating ICIs in advanced stages of urothelial cancer have been summarized. Anti-tumour activity of the 5 ICIs supporting the FDA approval in the second-line setting are reported. The activity of PD(L)1 inhibitors in the first-line setting in cisplatin-ineligible patients are described. Controversies regarding the potential biomarkers and toxicity profile of these treatments have been addressed. Finally, we discuss the ongoing trials in earlier disease-states including non-muscle-invasive (NMIBC) and muscle-invasive bladder cancer (MIBC).

Fig. 2 Timelines of FDA approval for anti-PD(L)-1 inhibitors in metastatic urothelial carcinoma

Table 1 PD(L)-1 and CTLA-4 immune checkpoint inhibitors used in advanced urothelial carcinoma

Drug/target	Company	Type	Dose	Approvals
PD-L1				
Atezolizumab	Roche/Genentech	IgG1	1200 mg IV q 3 we	Cisplatin-ineligible (1L)
Durvalumab	AstraZeneca/MedImmune	IgG1	10 mg/kg IV q 2 we	Post-platinum (2L)
Avelumab	Pfizer	IgG1	10 mg/kg IV q 2 we	Post-platinum (2L)
				Post-platinum (2L)
PD-1				
Pembrolizumab	Merck/MSD	IgG4	200 mg IV q 3 we	Cisplatin-ineligible (1L)
Nivolumab	BMS	IgG4	240 mg IV q 2 we	Post-platinum (2L)
				Post-platinum (2L)
CTLA-4				
Ipilimumab	BMS	IgG1	Ongoing (combo)	N/A
Tremelimumab	AstraZeneca/MedImmune	IgG2	Ongoing (combo)	N/A

Methods

A literature search was performed on PubMed and ClinicalTrials.gov combining the MeSH terms: 'urothelial carcinoma' OR 'bladder cancer', and 'immunotherapy' OR 'CTLA-4' OR 'PD-1' OR 'PD-L1' OR 'atezolizumab' OR 'nivolumab' OR 'ipilimumab' OR 'pembrolizumab' OR 'avelumab' OR 'durvalumab' OR 'tremelimumab'. Prospectives studies evaluating anti-PD(L)1 and anti-CTLA-4 monoclonal antibodies were included. The search dates queried were January 1, 2011, to December 1, 2017, and original articles of prospective studies and descriptions of ongoing studies pertaining to the use of immunotherapy regimens in urothelial carcinoma were reviewed. Review articles or letters or comments or editorials or communications were excluded from the search strategy. Inclusion criteria for prospective studies were as follows: (1) publication in a peer-reviewed journal; (2) proven diagnosis of bladder cancer in humans without restriction on TNM stage; (3) treatment efficacy and safety; (4) contribution of clinical or biological factors to the clinical response or resistance to treatment. No pre-specified sample size or follow-up period was used to determine study inclusion. Articles were excluded based on the following criteria: (1) laboratory studies in vitro or in vivo; (2) medico-economic studies and absence of key information such as hazard ratios and 95% confidence intervals. Two reviewers independently screened and retrieved the potentially relevant references. Articles were reviewed and extracted independently by all authors for article inclusion or exclusion. A flowchart of the process is presented in the supplementary data S1.

Results

Clinical results of ICIs in advanced urothelial carcinoma

Five ICIs are currently approved by the FDA for the treatment of metastatic urothelial carcinoma as second-line post platinum-based chemotherapy: atezolizumab [14, 15], durvalumab [16], avelumab [17], nivolumab [18] and pembrolizumab [19]. These approvals were mainly based on the results of phase I or phase II clinical trials summarized in Table 2. Surprisingly, substantial variations were observed in the objective response rates (ORRs) (from 15 to 21.1%) and OS (from 8.7 to 18.2 months in the durvalumab study) despite similar characteristics of the study populations with a similar median age of 67-year, as well as similar percentages of PS 0 status (30%), haemoglobin level < 10 g/dL (22%), visceral metastases (90%) and the presence of liver metastases in one-third of patients. Longer follow-up and

Table 2 Main results for immune checkpoint inhibitors as monotherapy in advanced urothelial carcinoma

	Clinical trial	Target	Phase	Overall survival (%)	Overall response rate (%)	Disease control (%)	Toxicity (%)
2nd line setting							
Nivolumab [1]	CheckMate 275 NCT02387996	PD-1	II	8.7 (6.05–NE*)	19.6 (15–24.9)	UN**	17 ≥ 3 (hepatic, GI)
Pembrolizumab [2]	KEYNOTE-045 NCT02256436	PD-1	III	10.3 (8.0–11.8)	21.1 (16.4–26.5)	UN**	15 ≥ G3 (pneumonitis, diarrhoea)
Atezolizumab [3, 4]	IMvigor210 NCT02108652	PD-L1	II	11.4 (9.0–NE*)	15 (11–20)	UN**	16 ≥ G3 (fatigue, anaemia, blood pressure)
	IMvigor 211 NCT02302807		III	8.6 (7.8–9.6)	16		
Durvalumab [5]	NCT01693562	PD-L1	I/II	18.2 (8.1–NE*)	17.8 (12.7–24)	36.6 (29.8–43.9)	6.8 ≥ G3 (AST, blood pressure)
Avelumab [6]	NCT01772004	PD-L1	Ib	13.7 (8.5–NE*)	18.2 (8.2–32.7)	52.3	6.8 ≥ G3 (PAlc, AST)
1st line setting							
Nivolumab [7]	CheckMate 032 NCT01928394	PD-1	I/II	9.7 (7.3–16.2)	24.4 (15.3–35.4)	UN**	10.3 ≥ G3 (pneumonitis, thrombocytopenia)
Pembrolizumab [8]	KEYNOTE-012	PD-1	Ib	13 (15–20)	26 (11–46)	UN**	15 ≥ G3 (myositis, hypercalcaemia)
Atezolizumab [9]	IMvigor210 NCT 02108652	PD-L1	II	15.9 (10.4–NE*)	23 (16–31)	30 (22–39)	8 ≥ G3 (rash)

*Not estimable, ** Unknown

in-depth analyses of these results are needed to understand these differences. Nevertheless, all these ICIs were given fast track FDA approval in the second-line setting within a few months of publication of these clinical trials. In the first-line setting, two ICIs have been developed for cisplatin-ineligible patients: pembrolizumab [20] and atezolizumab [21]. Again, the results of the corresponding trials showed spectacular OS ranging from 9.7 to 15.9 months, which was not really expected for such a population of patients with a usually poor prognosis. The unprecedented activity of these five ICIs explains the fast and unique mode of approval of these treatments by the FDA regardless of the disease stage (locally advanced or metastatic urothelial carcinoma) and whether chemotherapy was previously administered or not.

Toxicity profiles

Despite their spectacular activity, a non-negligible rate of severe treatment-related adverse events (AEs) was noted that varied from 6.8 to 17% (Table 2). These events were directly linked to the immune response and could occur early within a month after initiation of treatment. A wide range of side-effects was described, the most common being fatigue and skin toxicity, but any organ could be affected. Recommendations have, therefore been published to carefully monitor patients treated with ICIs [22].

Biomarkers of response

Although some patients will have a long-term response with ICIs, no more than 30% of patients will benefit from these therapies, independently of the inhibitor used (anti-PD-1 or -PDL-1). In some cases, tumour progression was noticed during treatment, leading to the death of patients [23, 24]. PDL-1 expression by tumour cells or T cells has been explored as a potential biomarker of tumour response, but controversial results have been obtained, probably due to differences in the immunohistochemistry assays that were used in the trials and/or the choice of cut-off value used to determine tumour positivity [25]. Indeed, while the IMvigor study demonstrated a higher response in patients with high PDL-1 expression in immune cells, durable responses have also been observed in patients with low expression of the ligand [14, 26]. Mutational load and molecular classification are two other biomarkers that are currently under investigation for their potential role in measuring the tumour response to ICIs [15].

Emergence of new immune targets

The optimized use of ICIs is still a question of debate and the results of the latest clinical trials have raised several questions that remain unanswered. For instance, when should these drugs be introduced? Should they be used as first-line therapy in patients who are eligible for a cisplatin-based regimen, in combination with chemotherapy, or as maintenance treatment following a response to cytotoxic agents? What would be the best combination to use: two ICIs (and which ones) or a combination of an ICI with chemotherapy eventually associated with targeted therapy? The best schedule of administration and the optimal individual dosing should also be determined, as well as the treatment duration for responder patients. Another important issue is to select the best predictive markers associated with the clinical response to each of these ICIs. It is already known that PD-L1 levels alone may not systematically predict response to anti-PD1/PD-L1 agents. Moreover, PD-L1 criteria may also need to be standardized across studies since the use of different antibodies to assess PD-L1 levels by immunochemistry and/or different positivity cut-offs may be the source of variation in interpretation of the results. Thus, other markers may need to be associated including tumour burden and factors that are associated with it such as the genes involved in DNA damage response, cell cycle control or APOBEC cytidine deaminases [27]. While numerous clinical trials are currently underway to address these different questions (Table 3), it has also been shown that it is possible to induce a cytotoxic T cell response by inhibiting targets other than PD-1 or CTLA-4. The JapicCTI-090980 phase I/II study investigating S-288310, a cancer vaccine composed of two HLA-A*24:02-restricted peptides derived from two tumour specific antigens (DEPDC1 and MPHOSPH1), is an example of such a promising approach [28]. This trial showed a 14.4-month OS in urothelial carcinoma naïve patients despite a relatively poor ORR (6.3%), but much better control of the disease in more than half of patients. These results are opening the way to further studies targeting the numerous other modulators of the immune system [29].

Ongoing clinical trials evaluating ICIs for MIBC

Carthon et al. carried out the first neoadjuvant clinical trial with the anti-CTLA-4 antibody ipilimumab in 12 patients with localized invasive bladder cancer [30]. Immune monitoring showed that anti CTLA-4 led to an increase in inducible co-stimulator CD4 + T cells in tumour tissue and peripheral blood. This has been thought of as a marker of T cell activation and a potential biomarker to monitor the immune response. To date, there are three major areas of clinical interest to evaluate ICIs in the localized MIBC setting (Table 4). First, in the neoadjuvant setting before radical cystectomy, several phase I/II trials are evaluating PD-1/PD-L1 antibodies alone or in combination with conventional chemotherapy. Primary endpoints include pathological response rate in the surgical specimen and evaluation of safety. In the NCT02451423 and NCT02845323

Table 3 Ongoing immunotherapeutic trials in advanced urothelial carcinoma

NCT number	Trial design	Clinical setting: phase (*n*)	Interventions	Primary endpoint	Secondary endpoints
Metastatic UTC					
Monotherapy					
02807636	Atezolizumab monotherapy and in combination with platinum-based chemotherapy	III (*n* = 1200)	Atezolizumab | carboplatin | gemcitabine | cisplatin	PFS|OS |AEs	
02527434	Tremelimumab	II (*n* = 64)	Tremelimumab monotherapy | biological: MEDI4736 monotherapy | biological: MEDI4736 + tremelimumab combination therapy	ORR | DoR |DCR | PFS | OS | BOR	
Combination therapy					
02925533	B-701 in combination with pembrolizumab	IB	B-701| pembrolizumab	Safety of B-701 in combination	Efficacy of B-701 in combination
02989 584		I/II (*n* = 30)	Atezolizumab | gemcitabine | cisplatin	Safety (DLT)	
03288545		I (*n* = 85)	Enfortumab vedotin | pembrolizumab | atezolizumab	Incidence of DLT	AEs
03123055		I (*n* = 48)	B-701 | pembrolizumab	FGFR3 expression safety and tolerability	Safety and tolerability
02437370		1 (*n* = 38)	Pembrolizumab |docetaxel | gemcitabine hydrochloride	Safety and tolerability of MK-3475 (pembrolizumab) in combination	Efficacy, programmed death (PD)-ligand (L)1 expression in archived tumour specimens—correlation with patient outcomes
02043665		I (*n* = 90)	Biological: CVA21	Response rate	
02619253		I/Ib (*n* = 42)	Pembrolizumab | vorinostat	Recommended phase II dose	Serious AEs |ORR |PFS
03093922		II (*n* = 31)	Atezolizumab | gemcitabine | cisplatin	ORR	
03324282		II (*n* = 90)	Avelumab | GC	Efficacy and safety	Specific immunological toxicity | DoR |PFS |OS | GC + avelumab efficacy according to expression of PD-L1 at the tumour site | GC + avelumab efficacy according to immune infiltrate populations at the tumour level and/or the tumour surroundings
Maintenance therapy					
02500121	Pembrolizumab as maintenance therapy after initial chemotherapy	II (*n* = 200)	Placebo | pembrolizumab	6-month PFS	Six-month PFS rates among the subsets of subjects with PD-L1 positive and PD-L1 negative tumours |OS
02603432	Study of avelumab in patients with locally advanced or metastatic urothelial cancer (JAVELIN Bladder 100)	3 (668)	Avelumab	OS	PFS | ORR | DoR

Table 3 (continued)

NCT number	Trial design	Clinical setting: phase (n)	Interventions	Primary endpoint	Secondary endpoints
Biomarker studies					
01198808	Tumour-specific T cell immunity in bladder cancer as prognostic marker	NA ($n=50$)	Non-interventional		Biospecimen retention: samples without DNA
03007719	[18F]F-AraG imaging + atezolizumab	II ($n=30$)	Drug: [18F]F-AraG (cohort 1) | radiation: PET/MRI scan (cohort 1) | Drug: [18F]F-AraG (cohort 2) | radiation: PET/MRI scan (cohort 2) | Drug: atezolizumab (cohort 1) | Drug: atezolizumab (cohort 2)	Change between pre and post-treatment SUV_{max}/change in SUV_{max}	
02553642	Relationship between tumour mutation burden and predicted neoantigen burden in patients treated with nivolumab or nivolumab plus ipilimumab (CA209-260)	II ($n=70$)	Nivolumab | nivolumab plus ipilimumab	RR | PD-L1 expression	
02546661	Open-label, randomised, multi-drug, biomarker-directed	Ib ($n=140$)	AZD4547 | durvalumab | olaparib | AZD1775 | vistusertib | AZD9150	AEs	
03263039	Biomarkers in urothelial cancer patients treated with pembrolizumab	II ($n=80$)	Pembrolizumab	Biomarkers in patients with clinical benefit | mechanisms of primary and acquired resistance | correlations between biomarkers and clinical activity	
03359239	Atezolizumab given in combination with a personalized vaccine	I ($n=15$)	Atezolizumab | PGV001 | poly ICLC | normal saline	Number of neoantigens | number of peptides synthesized | vaccine production time | proportion of consent to tissue acquisition phase | proportion of subjects eligible for the treatment phase | number of toxicities	ORR | DoR | Time to progression in adjuvant patients | OS
01282463	Ramucirumab or IMC-18F1 with docetaxel or docetaxel alone as second-line therapy	II ($n=148$)	Docetaxel | ramucirumab DP | IMC-18F1	PFS | ORR | DoR | number of participants with AEs | maximum concentration (C_{max}) | minimum concentration (C_{min}) | change in circulating levels of PlGF | change in circulating levels of VEGF-A | change in circulating levels of VEGF-B | change in circulating levels of VEGFR-1 | change in circulating levels of soluble VEGFR-2 | serum anti-ramucirumab antibody assessment | serum anti-18F1 antibody assessment	

Table 3 (continued)

NCT number	Trial design	Clinical setting; phase (n)	Interventions	Primary endpoint	Secondary endpoints
02331719	Combination of ACP-196 and pembrolizumab in subjects with platinum resistant urothelial bladder cancer	II (n=75)	Pembrolizumab | ACP-196	ORR	
01326871	ALT-801 in combination with cisplatin and gemcitabine in muscle invasive or metastatic urothelial cancer	I/II (n=90)	Cisplatin | gemcitabine | ALT-801	MTD and/or recommended dose | safety profile | clinical benefit	PFS | OS | pharmacokinetics and immunogenicity | tumour typing
02426125	Ramucirumab (LY3009806)+ docetaxel	III (n= 466)	Ramucirumab | docetaxel | placebo	PFS	OS | ORR | DCR | DoR | Quality of life questionnaire-C30 (EORTC QLQ-C30) | EuroQol 5-1 | pharmacokinetics

DFS disease-free survival, *OS* overall survival, *PFS* progression free survival, *AEs* adverse events, *ORR* objective response rate, *DoR* duration of response, *DCR* disease control rate, *BOR* best objective response, *DLT* dose-limiting toxicity, *SUV*$_{max}$ maximum Standardized uptake value, *RR* response rate, *MTD* maximum tolerated dose, *P1GF* placental growth factor, *VEGF-A* vascular endothelial growth factor-A, *VEGF-B* vascular endothelial growth factor-B, *VEGFR-1* vascular endothelial growth factor-1, *VEGFR-2* vascular endothelial growth factor-2

trials, changes in tumour infiltrating CD3+ and CD8+ T cell density are quantified after treatment with atezolizumab or nivolumab with or without urelumab, an agonist anti-CD137 antibody. The NCT02812420 trial is assessing the combination of durvalumab plus tremelimumab before radical cystectomy. Second, ICIs are being evaluated after cystectomy in the adjuvant setting. Phase III randomized trials (NCT03244384, NCT02450331, NCT02632409) evaluating PD-1/PD-L1 antibodies versus observation are reported in Table 3. The primary endpoints are disease-free survival (DFS) and/or OS in a large cohort of patients (640–800 patients). The final results will be available between 2019 and 2022. Finally, other trial designs are testing the combination of ICIs and radiation or chemoradiotherapy in localized MIBC. Radiation is widely known to induce tumour cell death through DNA damage. However, in preclinical studies, immunosuppressed mice before treatment required higher dose of radiation to control tumour growth. These data suggested that beyond the traditional effects of radiation as a DNA-damaging agent, the host immune system might also affect the therapeutic efficacy of radiation. Recent studies showed that radiation enhances many steps involved in the generation of antigen-specific immune responses, including inflammatory tumour-cell death, dendritic cell activation, antigen cross-presentation and cytotoxic T cell activation and proliferation. This effect has sparked interest in combining the process of killing tumour cells with ICIs [31–33]. Two phase II trials (NCT02621151, NCT02662062) are evaluating bladder preservation after combination therapy with cytotoxic chemotherapy, radiation therapy and pembrolizumab or nivolumab in patients with MIBC. Primary endpoints are safety and 2-year bladder-intact DFS rate. Among other ongoing trials, NCT02891161 is exploring maintenance therapy with durvalumab after primary treatment with radiation therapy and durvalumab. The primary endpoint is PFS and disease control rate. Assuming that the results of ongoing studies are positive, further trials will have to determine the best treatment strategy and the correct timing of such immunotherapeutic approaches (i.e. immune checkpoint blockade before, during or after radiotherapy).

Ongoing clinical trials evaluating ICIs for NMIBC

Eleven ongoing clinical trials are currently underway in the NMIBC setting (Table 5). Importantly, in the NMIBC setting, trials are investigating the intravesical administration of drugs. This treatment modality justifies the involvement of urologists in the development of such immunotherapeutic approaches. As the bladder immune microenvironment may be modified by previous intravesical BCG therapy, patients should be distinguished into three subgroups: patients with BCG-naïve, BCG-relapsing and BCG-unresponsive NMIBC. According to these subgroups, only two clinical

Table 4 Ongoing immunotherapeutic trials in muscle-invasive bladder cancer (MIBC)

NCT identifier	Clinical setting	Interventions and treatments	Trial design	Primary outcome	Secondary outcome
Adjuvant after radical cystectomy or chemoradiotherapy					
NCT03171025	Adjuvant localized MIBC following chemoradiation in bladder preservation management (n = 28)	Nivolumab following chemoradiation	Phase II Single arm	DFS at 2 years	Rate of salvage cystectomy Rate of cystoscopic control Rate of distant failure free survival OS Quality of life Safety
NCT03244384	Adjuvant localized and advanced MIBC (n = 739)	Pembrolizumab	Phase III randomized versus observation	DFS OS	DFS in PD-L1/PD-1 patients OS in PD-L1/PD-1 patients
NCT02450331	Adjuvant high risk MIBC after cystectomy (n = 700)	Atezolizumab	Phase III randomized versus observation	DFS	OS DFMS NUTRFS AEs QoL
NCT02632409	Adjuvant high risk MIBC after cystectomy (n = 640)	Nivolumab	Phase III randomized versus placebo	DFS	OS DFS NUTRFS
Bladder preservation management in combination with chemoradiotherapy					
NCT02662062	Localized MIBC bladder preservation management (n = 30)	Pembrolizumab Chemotherapy: cisplatin Radiation therapy 64 Gy	Phase II Single arm	Safety (AEs)	Rate of cystoscopic control Rate of salvage cystectomy Rate of metastatic disease
NCT02560636	Advanced MIBC bladder preservation management (n = 34)	Pembrolizumab Radiation therapy	Phase I Single arm	Safety (AEs), maximum tolerated dose combined with radiotherapy)	Rate of cystoscopic control Safety (AEs) OS PFS
NCT02621151	Localized MIBC bladder preservation management (n = 54)	Pembrolizumab IV Chemotherapy: gemcitabine (4 cycles) Radiation therapy (hypofractionated EBRT 52 Gy)	Phase II Single arm	DFS at 2 years	Safety (AEs) Complete response OS DFMS
NCT02891161	Localized MIBC (T2-4 N0-2 M0) bladder preservation management (n = 42)	Durvalumab IV Radiation therapy Durvalumab IV adjuvant	Phase Ib/II	Phase Ib: Safety (AEs) Phase II: DCR PFS	Complete remission OS Correlation between expression of PD-L1 and complete disease response
Neoadjuvant before radical cystectomy or chemoradiotherapy					
NCT03359239	Adjuvant (within 6 weeks) and neoadjuvant localized MIBC (n = 15)	Atezolizumab IV +PGV001	Phase I	Number of neoantigens Number of peptides synthesized Safety (AEs)	ORR DoR OS Adjuvant cohort: time to progression
NCT03212651 PANDORE	Neoadjuvant localized MIBC before cystectomy (n = 40)	Pembrolizumab IV	Phase II	Pathological complete response rate (PCR)	Not provided

Table 4 (continued)

NCT identifier	Clinical setting	Interventions and treatments	Trial design	Primary outcome	Secondary outcome
NCT02662309 ABACUS	Neoadjuvant localized MIBC before cystectomy ($n=85$)	Atezolizumab IV	Phase II	PCR Efficacy on immune parameters	Safety (AEs) Radiological response DFS OS
NCT02690558	Neoadjuvant localized MIBC before cystectomy ($n=30$)	Pembrolizumab IV Chemotherapy: gemcitabine + cisplatin	Phase II	Pathological down-staging (<pT2)	Safety (AEs) PCR DFS OS
NCT02812420	Neoadjuvant localized MIBC before cystectomy ($n=15$)	Durvalumab IV Tremelimumab IV	Phase I	Safety (AEs)	Immune and molecular changes in peripheral blood and tumour tissues
NCT02736266	Neoadjuvant localized MIBC before cystectomy ($n=90$)	Pembrolizumab IV	Phase II	PCR	Safety (AEs) Percentage of treatment-related delay in surgery
NCT02845323	Neoadjuvant localized MIBC in cisplatin-ineligible patients before cystectomy ($n=44$)	Nivolumab with or without urelumab IV	Phase II	Immune response (tumour infiltrating CD8+ T)	Safety Pathological down-staging (< pT2) PCR Prognostic value of tumour biopsy PD-1 and PD-L1 expression change in expression for pathologic response
NCT02365766	Neoadjuvant localized MIBC (T2-4aN0M0) before cystectomy ($n=81$)	Pembrolizumab IV Chemotherapy: gemcitabine + cisplatin	Phase Ib/II	Phase Ib: Safety (AEs) Phase II: PR)	Rate of radical cystectomy OS RFS
NCT03319745	Neoadjuvant localized MIBC before cystectomy ($n=81$)	Pembrolizumab IV	Phase II	Safety (AEs)	Signal of anti-cancer immunological activity and biomarkers
NCT03294304	Neoadjuvant localized MIBC before cystectomy ($n=41$)	Nivolumab IV Chemotherapy: gemcitabine + cisplatin	Phase II	PR down-staging to≤ pT1pN0	Safety (AEs) PFS
NCT03234153	Neoadjuvant localized MIBC before cystectomy ($n=68$)	Durvalumab IV Tremelimumab IV four cycles every 4 weeks	Phase II.	PR	Safety (AEs) RFS OS
NCT02989584	Neoadjuvant localized MIBC before cystectomy ($n=30$)	Atezolizumab IV Chemotherapy: gemcitabine + cisplatin	Phase II	Safety (AEs)	Not provided

DFS disease-free survival, *OS* overall survival, *PFS* progression free survival, *AEs* adverse events, *ORR* objective response rate, *DoR* duration of response, *NUTRFS* non urinary tract recurrence free survival, *QoL* quality of life, *DFMS* disease free metastasis, *IV* intravenous, *PCR* pathological response, *NUTRFS* non urinary tract recurrence free survival, *QoL* quality of life, *DFMS* disease free metastasis, *IV* intravenous, *PCR* pathological

Table 5 Ongoing immunotherapeutic trials in non-muscle-invasive bladder cancer (NMIBC)

NCT identifier	Clinical setting (*n*, cases)	Interventions and treatments	Trial design	Primary endpoint	Secondary endpoints
03167151	Intermediate risk recurrent NMIBC ($n=36$)	Intravesical or intravenous pembrolizumab	Randomized phase I/II with marker lesion: intravesical pembrolizumab + intravenous placebo vs. intravesical placebo + intravenous pembrolizumab	Safety and tolerability profile	CRR of marker lesion Recurrence interval PFS Expression of PD-L1, and PD-1 + infiltrating lymphocytes Gene expression signature TCR repertoire and clonality of infiltrating T cells Change in cytokines in blood and urine
02138734	High risk BCG- and chemotherapy naïve NMIBC ($n=81$)	Intravesical BCG ± ALT-803	Randomized phase I/II: intravesical BCG vs. intravesical BCG + ALT-803	MTD Safety and tolerability profile	CRR Plasma concentration–time profile of ALT-803 Change in cytokines in blood and urine Lymphocyte profile RFS, PFS, OS
02808143	BCG naïve high-risk NMIBC and BCG-relapsing NMIBC ($n=27$)	Intravesical pembrolizumab + intravesical BCG	Phase I dose-escalation study: intravesical pembrolizumab + intravesical BCG	MTD	Dose-limiting toxicities Safety profile Change in cytokines in blood and urine Expression of PD-L1, PD-L2 and PD-1 Lymphocyte profile Plasma and urine concentration-time profiles of pembrolizumab Response rate Progression rate
03317158	BCG-relapsing NMIBC ($n=186$ in phase I + II)	Intravenous durvalumab ± intravesical BCG and external beam radiation therapy	Randomized phase II: monotherapy vs. durvalumab + BCG vs. durvalumab + radiation	6-month RFS rate	24-month RFS rate Identify significant associations between 6- and 24-month RFS rates and baseline tumour immunohistochemistry staining patterns of PD-L1. Safety profile
03258593	BCG-relapsing NMIBC ($n=40$)	Intravenous durvalumab + oportuzumab	Phase I: intravenous durvalumab + oportuzumab	Safety and tolerability profile	Predictive biomarkers and biomarkers of the immune response Pharmacokinetics Correlation between urinary EpCAM and response to therapy Antitumor activity PD-L1 expression and PD-1 expressing T cells

Table 5 (continued)

NCT identifier	Clinical setting (*n*, cases)	Interventions and treatments	Trial design	Primary endpoint	Secondary endpoints
02792192	BCG-relapsing or BCG-unresponsive NMIBC or very high risk BCG-naïve NMIBC (*n* = 70)	Intravenous atezolizumab + intravesical BCG	Single arm phase I/II: intravenous Atezolizumab + Intravesical BCG with de-escalation dose study	Adverse events rate BCG DLT rate BCG MDT 6-month CRR	3-month CRR RFS PFS Time to cystectomy OS Plasma concentration–time profile of atezolizumab Anti-therapeutic antibody Response rates to atezolizumab
02625961	BCG-unresponsive NMIBC (*n* = 260)	Intravenous pembrolizumab	Single arm phase II: intravenous pembrolizumab	3-year CRR RFS	Duration of response
02844816	BCG-unresponsive NMIBC (*n* = 148)	Intravenous atezolizumab	Single arm phase II: intravenous atezolizumab monotherapy	CIS CRR at 25 weeks 18-month RFS	OS Bladder cancer specific survival Cystectomy-free survival Ta/T1 RFS Safety profile
03022825	BCG-unresponsive NMIBC (*n* = 100)	Intravesical BCG ± ALT-803	Single arm phase II: intravesical BCG + ALT-803	6-month CRR	12-, 18- and 24-month CRR 24-month PFS 24-month OS Time to cystectomy Safety profile Quality of life
03317158	BCG-unresponsive NMIBC (*n* = 186)	Intravenous durvalumab ± intravesical BCG and external beam radiation therapy	Randomized phase I: intravenous durvalumab monotherapy vs. intravenous durvalumab + intravesical BCG vs. intravenous durvalumab + radiation	Determine the recommended phase II doses	6-month RFS rate Safety profile
02901548	BCG-unresponsive CIS (*n* = 34)	Intravenous durvalumab	Single arm phase II: intravenous durvalumab monotherapy	6-month CRR	24-month CRR

MTD maximum tolerated dose, *DLT* dose-limiting toxicity, *CRR* complete response rate, *OS* overall survival, *RFS* relapse-free survival, *PFS* progression-free survival, *TCR* T cell receptor, *BCG* Bacillus Calmette-Guérin, *ALT* IL-15 superagonist complex, *CIS* carcinoma in situ

trials are related to the BCG-naïve NMIBC setting, namely NCT trials 02138734 and 02808143, which are investigating the maximum tolerated dose of intravesical treatment with BCG associated with ALT-803 and pembrolizumab, respectively. The combination of intravesical BCG and ALT-803 is also being studied in the NCT03022825 trial, which concerns patients with BCG-unresponsive NMIBC. Regarding ALT-803, previous reports of intravesical treatment in humans have led to its investigation in phase II trials. Conversely, one study investigating intravesical pembrolizumab is a phase I dose-escalation study. Data regarding pharmacokinetics and tolerance of new immunotherapy instillation are lacking and the results from these trials are eagerly awaited. Other trials are investigating new immunotherapy administrated by intravenous infusion, using doses previously employed in a metastatic setting.

Conclusions

Cisplatin-based chemotherapy has been the standard of care for locally advanced and metastatic urothelial carcinoma for the past 30 years. The striking results of anti-PD(L)1 agents in this clinical setting suggest that immunotherapy is changing the present and the future treatment of this disease. Ongoing trials are evaluating immune-checkpoint inhibitors in other setting including high-risk NMIBC and MIBC, in neo-adjuvant and adjuvant treatment, or as frontline therapy for cisplatin eligible and ineligible patients. However, a large majority of patients do not respond to anti-PD(L)1 drugs as monotherapy. Combination treatments are evaluating the efficacy of anti-PD(L)1 agents with anti-CTLA-4 drugs, chemotherapy and radiotherapy, targeted therapies or other immunomodulatory agents. The identification of robust biomarkers to predict the antitumor activity and drug toxicities remains crucial to improve the efficacy of such treatment strategies. Current research is actively exploring these gaps of knowledge to improve use of these drugs.

Acknowledgements Mathieu Rouanne is the recipient of a Scholarship Funding from the French Urological Association (Association Française d'Urologie)..

Compliance with ethical standards

Conflict of interest The authors declare no conflict of interest with the contents of this work.

References

1. Sternberg CN, de Mulder PH, Schornagel JH, Théodore C, Fossa SD, van Oosterom AT et al (2001) Randomized phase III trial of high-dose-intensity methotrexate, vinblastine, doxorubicin, and cisplatin (MVAC) chemotherapy and recombinant human granulocyte colony-stimulating factor versus classic MVAC in advanced urothelial tract tumors: European Organization for Research and Treatment of Cancer Protocol no. 30924. J Clin Oncol 15(19):2638–2646
2. Witjes AJ, Lebret T, Compérat EM, Cowan NC, De Santis M, Bruins HM et al (2017) Updated 2016 EAU guidelines on muscle-invasive and metastatic bladder cancer. Eur Urol 71:462–475
3. Roupret M, Neuzillet Y, Masson-Lecomte A, Colin P, Compérat E, Dubosq F et al (2016) CCAFU French national guidelines 2016–2018 on bladder cancer. Prog Urol 27(Suppl 1):S67–S91
4. Bellmunt J, Orsola A, Leow JJ, Wiegel T, De Santis M, Horwich A (2014) Bladder cancer: ESMO practice guidelines for diagnosis, treatment and follow-up. Ann Oncol 25(3):40–48
5. Dash A, Galsky MD, Vickers AJ, Serio AM, Koppie TM, Dalbagni G, Bochner BH (2006) Impact of renal impairment on eligibility for adjuvant cisplatin-based chemotherapy in patients with urothelial carcinoma of the bladder. Cancer 107:506–513
6. Bellmunt J, Théodore C, Demkov T, Komyakov B, Sengelov L, Daugaard G (2009) Phase III trial of vinflunine plus best supportive care compared with best supportive care alone after a platinum-containing regimen in patients with advanced transitional cell carcinoma of the urothelial tract. J Clin Oncol 20:4454–4461
7. Ortmann CA, Mazhar D (2013) Second-line systemic therapy for metastatic urothelial carcinoma of the bladder. Future Oncol 9:1637–1651
8. Schreiber RD, Old LJ, Smyth MJ (2011) Cancer immunoediting: integrating immunity's roles in cancer suppression and promotion. Science 25(331):1565–1570
9. Fridman WH, Zitvogel L, Sautès-Fridman C, Kroemer G (2017) The immune contexture in cancer prognosis and treatment. Nat Rev Clin Oncol 14:717–734
10. Chen DS, Mellman I (2017) Elements of cancer immunity and the cancer-immune set point. Nature 18(541):321–330
11. Sharma P, Hu-Lieskovan S, Wargo JA, Ribas A (2017) Primary, adaptive, and acquired resistance to cancer immunotherapy. Cell 9(168):707–723
12. Curtsinger JM, Mescher MF (2010) Inflammatory cytokines as a third signal for T cell activation. Curr Opin Immunol 22:333–340
13. Rouanne M, Loriot Y, Lebret T, Soria JC (2016) Novel therapeutic targets in advanced urothelial carcinoma. Crit Rev Oncol Hematol 98:106–115
14. Powles T, Durán I, van der Heijden MS, Loriot Y, Vogelzang NJ, De Giorgi U et al (2018) Atezolizumab versus chemotherapy in patients with platinum-treated locally advanced or metastatic urothelial carcinoma (IMvigor211): a multicentre, open-label, phase 3 randomised controlled trial. Lancet 391(10122):748–757. https://doi.org/10.1016/S0140-6736(17)33297-X
15. Rosenberg JE, Hoffman-Censits J, Powles T, van der Heijden MS, Balar AV, Necchi A et al (2016) Atezolizumab in patients with locally advanced and metastatic urothelial carcinoma who have progressed following treatment with platinum-based chemotherapy: a single-arm, multicentre, phase 2 trial. Lancet 387:1909–1920
16. Powles T, O'Donnell PH, Massard C, Arkenau HT, Friedlander TW, Hoimes CJ et al (2017) Efficacy and safety of durvalumab in locally advanced or metastatic urothelial carcinoma: updated results from a phase 1/2 open-label study. JAMA Oncol 3:e172411
17. Patel MR, Ellerton J, Infante JR, Agrawal M, Gordon M, Aljumaily R et al (2018) Avelumab in metastatic urothelial carcinoma after platinum failure (JAVELIN Solid Tumor): pooled results from two expansion cohorts of an open-label, phase 1 trial. Lancet Oncol 19:51–64
18. Sharma P, Retz M, Siefker-Radtke A, Baron A, Necchi A, Bedke J et al (2017) Nivolumab in metastatic urothelial carcinoma after

platinum therapy (CheckMate 275): a multicentre, single-arm, phase 2 trial. Lancet Oncol 18:312–322
19. Bellmunt J, de Wit R, Vaughn DJ, Fradet Y, Lee JL, Fong L et al (2017) Pembrolizumab as second-line therapy for advanced urothelial carcinoma. N Engl J Med 376:1015–1026
20. Balar AV, Galsky MD, Rosenberg JE, Powles T, Petrylak DP, Bellmunt J et al (2017) Atezolizumab as first-line treatment in cisplatin-ineligible patients with locally advanced and metastatic urothelial carcinoma: a single-arm, multicentre, phase 2 trial. Lancet 389:67–76
21. Balar AV, Castellano D, O'Donnell PH, Grivas P, Vuky J, Powles T et al (2017) First-line pembrolizumab in cisplatin-ineligible patients with locally advanced and unresectable or metastatic urothelial cancer (KEYNOTE-052): a multicentre, single-arm, phase 2 study. Lancet Oncol 18:1483–1492
22. Haanen JBAG, Carbonnel F, Robert C, Kerr KM, Peters S, Larkin J et al (2018) Management of toxicities from immunotherapy: ESMO Clinical Practice Guidelines for diagnosis, treatment and follow-up. Ann Oncol 28(Suppl 4):119–142
23. Champiat S, Dercle L, Ammari S, Massard C, Hollebecque A, Postel-Vinay S et al (2017) Hyperprogressive disease is a new pattern of progression in cancer patients treated by anti-PD-1/PD-L1. Clin Cancer Res 23:1920–1928
24. Kato S, Goodman A, Walavalkar V, Barkauskas DA, Sharabi A, Kurzrock R (2017) Hyperprogressors after immunotherapy: analysis of genomic alterations associated with accelerated growth rate. Clin Cancer Res 23:4242–4250
25. Wexel F, Vallo S, Roghmann F (2017) Do we have biomarkers to predict response to neoadjuvant and adjuvant chemotherapy and immunotherapy in bladder cancer? Transl Androl Urol 6:1067–1080
26. Powles T, Eder JP, Fine GD, Braiteh FS, Loriot Y, Cruz C et al (2014) MPDL3280A (anti-PD-L1) treatment leads to clinical activity in metastatic bladder cancer. Nature 515:558–562
27. Robertson AG, Kim J, Al-Ahmadie H, Bellmunt J, Guo G, Cherniack AD et al (2017) Comprehensive molecular characterization of muscle-invasive bladder cancer. Cell 171:540–556
28. Obara W, Eto M, Mimata H, Kohri K, Mitsuhata N, Miura I et al (2017) A phase I/II study of cancer peptide vaccine S-288310 in patients with advanced urothelial carcinoma of the bladder. Ann Oncol 28:798–803
29. Pardoll DM (2012) The blockade of immune checkpoints in cancer immunotherapy. Nat Rev Cancer 12:252–264
30. Carthon BC, Wolchok JD, Yuan J, Kamat A, Ng Tang DS, Sun J et al (2010) Preoperative CTLA-4 blockade: tolerability and immune monitoring in the setting of a presurgical clinical trial. Clin Cancer Res 16:2861–2871
31. Gough MJ, Crittenden MR (2009) Combination approaches to immunotherapy: the radiotherapy example. Immunotherapy 6:1025–1037
32. Formenti SC, Demaria S (2013) Combining radiotherapy and cancer immunotherapy: a paradigm shift. J Natl Cancer Inst 4:256–265
33. Tang C, Wang X, Soh H, Seyedin S, Cortez MA, Krishnan S et al (2014) Combining radiation and immunotherapy: a new systemic therapy for solid tumors? Cancer Immunol Res 9:831–838

EUROPEAN UROLOGY 75 (2019) e108–e109

available at www.sciencedirect.com
journal homepage: www.europeanurology.com

European Association of Urology

Letter to the Editor

Reply to Pontus Eriksson and Gottfrid Sjödahl's Letter to the Editor re: Tuan Zea Tan, Mathieu Rouanne, Kien Thiam Tan, Ruby Yun-Ju Huang, Jean-Paul Thiery. Molecular Subtypes of Urothelial Bladder Cancer: Results from a Meta-cohort Analysis of 2411 Tumors. Eur Urol 2019;75:423–32

We thank Eriksson and Sjödahl for their critical remarks on our bioinformatic analysis. We believe that our meta-cohort sheds light on bladder cancer (BC) subtypes through a comprehensive analysis of a unique data set of 2411 bladder tumors [1]. Notably, studying non-muscle-invasive BC (NMIBC) and muscle-invasive tumors allowed us to define a molecular portrait of potentially lethal, high-risk NMIBC. Therefore, our study – while imperfect – provides an important resource for the BC community.

Although we have already detailed the limitations of our analysis, Eriksson and Sjödahl pointed out three issues that we would like to address.

First, we agree that batch effects (BEs) cannot be eliminated completely, and BE removal is a nontrivial task [2]. We used principal component analysis and several metrics (Supplementary Fig. 2 [1]) to remove BEs due to major confounding factors. Notably, the same subtypes were found with each platform (Supplementary Fig. 5 [1]), suggesting that intrinsic biological differences were not compromised. No subtype found was exclusive to specific cohorts, platforms, or tissue sources (Supplementary Fig. 3 and Supplementary Table 4 [1]). Results from the Affymetrix and Illumina platforms were in good agreement. A similar strategy was successfully used to build the CSIOVDB ovarian cancer subtype database [3]. Importantly, subtype-specific associations were highly concordant with findings in independent BC gene expression subtype studies (Figs. 1–3 and Supplementary Figs. 5, 6, and 8 [1]). A large, uniformly processed, and well-annotated BC cohort (eg, TCGA [4] and UROMOL [5]) provides practitioners with an invaluable resource; however, BEs still exist even with these cohort types and must be acknowledged [6].

Second, the centroid provided (Supplementary Table 15 [1]) is the median-centered expression of differentially expressed genes in the meta-cohort; it is not a classifier. While application of a classifier to individual cohorts constituting the meta-cohort is valid, centroid-based classifiers require gene standardization with the training data before classification. This is because class imbalance or missing data in a cohort will distort the "high" or "low" expression levels and lead to classification variability [7]. If a reclassification uses the median-centered expression within a cohort, the subtype assignment assumes that all subtypes are present and are balanced in the cohort. This assumption may not be true. The consistency of subtype annotation also depends on tumor heterogeneity. Multiple subtype signatures within a tumor lesion exist, as seen in single-cell and multitumor region studies [8,9] and from our experience in ovarian cancer [10].

Third, we wish to stress that formalin-fixed, paraffin-embedded (FFPE) samples were not limited to the NEURAL subtype. NEURAL and fresh-frozen samples were not mutually exclusive (Supplementary Table 4 [1]); GSE39016 had more samples assigned as non-NEURAL. Importantly, another FFPE cohort, GSE87304, also had multiple subtypes, including NEURAL. Both NEURAL and LUM were enriched in published cancer subtypes identified using microarray and RNA sequencing data (Fig. 1 [1]), indicating that NEURAL and LUM are unlikely to be artifactual.

Importantly, we echo the call of Dyrskjot [11] that perhaps the most critical task now is to establish the clinical relevance of these molecular subtypes. The value of a subtype scheme lies in its biological and clinical relevance. Moving forward, basket trials and multi-omics big-data analyses at multiple centers are needed to determine subtype-specific therapeutic interventions. Consensus on the clinical relevance of these BC subtypes will hopefully become a reality.

Conflicts of interest: Jean-Paul Thiery is a consultant/advisory board member for Aim Biotech Singapore, ACT Genomic, and CSO BioCheetah Singapore. The remaining authors have nothing to disclose.

References

[1] Tan TZ, Rouanne M, Tan KT, et al. Molecular subtypes of urothelial bladder cancer: results from a meta-cohort analysis of 2411 tumors. Eur Urol 2019;75:423–32.

[2] Chen C, Grennan K, Badner J, et al. Removing batch effects in analysis of expression microarray data: an evaluation of six batch adjustment methods. PLoS One 2011;6:e81723.

DOIs of original articles: https://doi.org/10.1016/j.eururo.2018.11.049, https://doi.org/10.1016/j.eururo.2018.08.027.

https://doi.org/10.1016/j.eururo.2018.11.048

[3] Tan TZ, Yang H, Ye J, et al. CSIOVDB: a microarray gene expression database of epithelial ovarian cancer subtype. Oncotarget 2015;6:43843–52.
[4] Robertson AG, Kim J, Al-Ahmadie H, et al. Comprehensive molecular characterization of muscle-invasive bladder cancer. Cell 2017;171, 540–56.e25.
[5] Hedegaard J, Lamy P, Nordentoft I, et al. Comprehensive transcriptional analysis of early-stage urothelial carcinoma. Cancer Cell 2016;30:27–42.
[6] Leek JT, Scharpf RB, Bravo HC, et al. Tackling the widespread and critical impact of batch effects in high-throughput data. Nat Rev Genet 2010;11:733–9.
[7] Altman N, Krzywinski M. Clustering. Nat Methods 2017;14:545.
[8] Zhang X, Zhang M, Hou Y, et al. Single-cell analyses of transcriptional heterogeneity in squamous cell carcinoma of urinary bladder. Oncotarget 2016;7:66069–76.
[9] Thomsen MBH, Nordentoft I, Lamy P, et al. Comprehensive multiregional analysis of molecular heterogeneity in bladder cancer. Sci Rep 2017;7:11702.
[10] Tan TZ, Heong V, Ye J, et al. Decoding transcriptomic intra-tumour heterogeneity to guide personalised medicine in ovarian cancer. J Pathol. In press. https://doi.org/10.1002/path.5191.
[11] Dyrskjot L. Molecular subtypes of bladder cancer: academic exercise or clinical relevance? Eur Urol. In press. https://doi.org/10.1016/j.eururo.2018.09.006.

Tuan Zea Tan[a]
Mathieu Rouanne[b,c]
Ruby Yun-Ju Huang[a,d,e]
Jean-Paul Thiery[f,g,h,i,*]

[a]*Cancer Science Institute of Singapore, National University of Singapore, Center for Translational Medicine, Singapore*
[b]*Department of Urology, Hôpital Foch, Université Versailles-Saint-Quentin-en-Yvelines, Université Paris-Saclay, Suresnes, France*
[c]*INSERM Unit 1015, Laboratoire de Recherche Translationnelle en Immunothérapie, Gustave Roussy, Université Paris-Saclay, Villejuif, France*
[d]*Department of Obstetrics and Gynecology, National University Health System, Singapore*
[e]*Department of Anatomy, Yong Loo Lin School of Medicine, National University of Singapore, Singapore*
[f]*Department of Biochemistry, Yong Loo Lin School of Medicine, National University of Singapore, Singapore*
[g]*Guangzhou Institute of Biomedicine and Health, Chinese Academy of Science, Guangzhou, People's Republic of China*
[h]*CNRS Emeritus CNRS UMR 7057 Matter and Complex Systems, University Paris Denis Diderot, Paris, France*
[i]*INSERM UMR 1186, Integrative Tumor Immunology and Genetic Oncology, Gustave Roussy, Université Paris-Saclay, Villejuif, France*

*Corresponding author. Department of Biochemistry, Yong Loo Lin School of Medicine, National University of Singapore, 8 Medical Drive, 117597, Singapore.
E-mail address: bchtjp@nus.edu.sg (J.-P. Thiery).

November 23, 2018

European Journal of Nuclear Medicine and Molecular Imaging
https://doi.org/10.1007/s00259-019-04296-6

LETTER TO THE EDITOR

Comment on: Relationship between the expression of PD-1/PD-L1 and ^{18}F-FDG uptake in bladder cancer

Antoine Girard[1] · Mathieu Rouanne[2,3]

Received: 11 February 2019 / Accepted: 18 February 2019

Dear Sir,

The study by Chen et al. addresses an important question regarding the predictive value of ^{18}F-FDG uptake in assessing PD(L)-1 expression in bladder cancer [1]. Arguably, this innovative study is of major interest as multiple issues hamper the standardization of programmed cell death ligand-1 (PD-L1) scoring in tumour tissue. Recently, the Food and Drug Administration (FDA) issued a drug safety notification warning against the use of frontline single-agent immune checkpoint inhibitors in patients with urothelial carcinoma expressing low levels of PD-L1. In August 2018, PD-L1 status was incorporated into the labels for pembrolizumab and atezolizumab for existing frontline approvals for cisplatin-ineligible urothelial carcinoma. Therefore, this article shed light on a particularly relevant question from the clinical and scientific perspectives, but also raises technical issues regarding the method described.

First, the authors did not detail the staining protocol nor the antibody used to assess PD-L1 expression. Four PD-L1 assays have been approved by the FDA/European Medicines Agency (EMA) for use in urothelial carcinoma, including the Dako 28-8 and 22C3 and the Vantana SP142 and SP263 monoclonal antibodies [2]. Among these assays, divergent results have been reported in bladder cancer, leading to different PD-L1 expression detection rates, and thus providing different number of patients eligible for first-line treatment with immune checkpoint blockade [3]. The threshold of >1% for PD-L1 positivity was clearly defined by Chen et al. [1]. However, it remains unclear which PD-L1-stained cells were evaluated in their study (tumour cells, immune cells or both). The authors should have reported the PD-L1 score for each component of the tumour immune microenvironment. Indeed, variability in PD-L1 expression across the types of stained cells may lead to a variable relationship with ^{18}F-FDG uptake values.

Second, as immune checkpoint inhibitors are validated treatments in metastatic urothelial cancer, it would have been of interest to evaluate the correlation between ^{18}F-FDG uptake and PD-L1 expression in metastases rather than in the primary tumour. Indeed, PD-L1 expression in the primary tumour can easily be determined by endoscopic transurethral resection. Five immune checkpoint inhibitors have obtained accelerated approval by the FDA for the treatment of metastatic bladder cancer [4], and molecular and functional imaging is increasingly recognized as a reliable tool for cancer staging [5, 6]. Burgess et al. recently reported a discordance in the expression of PD-L1 immune cells between primary and metastatic urothelial carcinoma lesions [7]. Thus, the correlation between ^{18}F-FDG uptake and PD-1/PD-L1 expression in distant metastases may be more variable.

Third, non-muscle-invasive bladder cancer (NMIBC) represents more than 70% of bladder cancers at the time of diagnosis. NMIBCs are often detected as a subcentimetre thickening of the bladder wall. Approximately one third (13/38) of tumours analysed by Chen et al. were NMIBC disease [1]. In this situation, ^{18}F-FDG uptake for most of the tumours of stage pT1 or less may have been underestimated due to the partial volume effect. It is well known that this phenomenon leads to underestimation of uptake intensity in small or thin structures (i.e. approximately <8–12 mm depending on the full-width at half-maximum of the reconstructed image resolution) [8]. Tumour size (presumably in the great axis) was included in the multivariate analysis, but the thickness was not. In addition, stromal lymphocyte infiltration is associated with tumour invasion depth in bladder cancer of stage pT1,

✉ Antoine Girard
a.girard@rennes.unicancer.fr

[1] Department of Nuclear Medicine, Centre Eugène Marquis, Université Rennes 1, Rennes, France

[2] Department of Urology, Hôpital Foch, Université Versailles-Saint-Quentin-en-Yvelines, Université Paris-Saclay, Suresnes, France

[3] INSERM Unit 1015, Laboratoire de Recherche Translationnelle en Immunothérapie (LRTI), Gustave Roussy, Université Paris-Saclay, Villejuif, France

Published online: 01 March 2019

suggesting that immune infiltration is different between muscle-invasive and non-muscle-invasive tumours [9]. Indeed, most of the tumours of stage pT1 or less were negative for PD-1 and PD-L1, which may have biased the results.

Arguably, predicting and monitoring the response to immune checkpoint inhibitors will become key issues in the near future. Numerous phase III trials evaluating anti-PD(L)1 immune checkpoint inhibitors in the settings of both localized and advanced bladder cancer are ongoing. Metabolic and molecular imaging will have a major impact on patient management in the new era of cancer immunotherapy. The study reported by Chen et al. has taken the first step in a very promising direction [1].

Compliance with ethical standards

Conflicts of interest None.

Ethical approval This article does not describe any studies with human participants performed by any of the authors.

Publisher's note Springer Nature remains neutral with regard to jurisdictional claims in published maps and institutional affiliations.

References

1. Chen R, Zhou X, Liu J, Huang G. Relationship between the expression of PD-1/PD-L1 and 18F-FDG uptake in bladder cancer. Eur J Nucl Med Mol Imaging. 2019. https://doi.org/10.1007/s00259-018-4208-8.
2. Eckstein M, Erben P, Kriegmair MC, Worst TS, Weiß CA, Wirtz RM, et al. Performance of the Food and Drug Administration/EMA-approved programmed cell death ligand-1 assays in urothelial carcinoma with emphasis on therapy stratification for first-line use of atezolizumab and pembrolizumab. Eur J Cancer. 2019;106:234–43. https://doi.org/10.1016/j.ejca.2018.11.007.
3. Bellmunt J, Powles T, Vogelzang NJ. A review on the evolution of PD-1/PD-L1 immunotherapy for bladder cancer: the future is now. Cancer Treat Rev. 2017;54:58–67. https://doi.org/10.1016/j.ctrv.2017.01.007.
4. Rouanne M, Roumiguié M, Houédé N, Masson-Lecomte A, Colin P, Pignot G, et al. Development of immunotherapy in bladder cancer: present and future on targeting PD(L)1 and CTLA-4 pathways. World J Urol. 2018;36(11):1727–40. https://doi.org/10.1007/s00345-018-2332-5.
5. Girard A, Rouanne M, Taconet S, Radulescu C, Neuzillet Y, Girma A, et al. Integrated analysis of 18F-FDG PET/CT improves preoperative lymph node staging for patients with invasive bladder cancer. Eur Radiol. 2019. https://doi.org/10.1007/s00330-018-5959-0.
6. Öztürk H. Detecting metastatic bladder cancer using (18)F-fluorodeoxyglucose positron-emission tomography/computed tomography. Cancer Res Treat. 2015;47(4):834–43. https://doi.org/10.4143/crt.2014.157.
7. Burgess EF, Livasy C, Hartman A, Robinson MM, Symanowski J, Naso C, et al. Discordance of high PD-L1 expression in primary and metastatic urothelial carcinoma lesions. Urol Oncol. 2019. https://doi.org/10.1016/j.urolonc.2019.01.002.
8. Soret M, Bacharach SL, Buvat I. Partial-volume effect in PET tumor imaging. J Nucl Med. 2007;48(6):932–45.
9. Rouanne M, Betari R, Radulescu C, Goubar A, Signolle N, Neuzillet Y, et al. Stromal lymphocyte infiltration is associated with tumour invasion depth but is not prognostic in high-grade T1 bladder cancer. Eur J Cancer. 2019;108:111–9. https://doi.org/10.1016/j.ejca.2018.12.010.

Re: Differential Expression of PD-L1 in High Grade T1 vs Muscle Invasive Bladder Carcinoma and its Prognostic Implications

S. A. M. Wankowicz, L. Werner, A. Orsola, J. Novak, M. Bowden, T. K. Choueiri, I. de Torres, J. Morote, G. J. Freeman, S. Signoretti and J. Bellmunt

J Urol 2017; 198: 817–823.

To the Editor: This study addresses an important question regarding the prognostic value of PD-L1 expression in high grade T1 (HGT1) urothelial carcinoma of the bladder. Several phase I and II trials evaluating PD-1 or PD-L1 immune checkpoint inhibitors in this clinical setting are currently ongoing. However, few data regarding PD-L1 expression in high risk nonmuscle invasive bladder cancer have been specifically reported in independent retrospective cohorts. Therefore, this article sheds light on a particularly relevant question from a clinical and scientific perspective, and also raises technical issues regarding the method described.

The strengths of this article are the relatively large (140 patients) homogeneous cohort of primary HGT1 bladder cancer, the quality of the formalin fixed, paraffin embedded samples (initial HGT1 tumors with a visible, clearly identifiable and disease-free muscularis) and the long followup (median 7.4 years). We agree that the use of the same mouse monoclonal anti-PD-L1 antibody (405.9A11, developed in the laboratory of Gordon Freeman, Dana Farber Cancer Institute, Boston, Massachusetts) in the nonmuscle invasive and muscle invasive cohorts is a marker of reliability that allows comparison between samples. However, despite the high quality of this work, some additional issues need to be addressed.

The use of tissue microarray (TMA) calls for great caution regarding the large amount of heterogeneity observed in HGT1 bladder tumors. Actually the method used to build the TMA is unclear regarding the location of the selected areas in the tumor blocks. Have all 3 cores per sample been punched in the center of the tumor infiltrating the lamina propria? How are the

immune cell infiltrates in the tissue outside the tumor core accounted for? Since all bladder tumors have been initially endoscopically resected (and, therefore, cut into small pieces of tumor), selection of tumor areas is particularly challenging. Thus, the task of the pathologist is complex and should be detailed.

Furthermore, no correlation has been assessed for a subset of samples to determine the correlation of PD-L1 expression status in TMA cores and matched whole sections from the same tumors. This important step could have strengthened the reliability and reproducibility of the method used by the authors. In addition, no confirmatory analysis with other anti-PD-L1 antibodies has been performed for comparison. Altogether the tissue microarray technique may impede gathering unbiased information from the prognostic value of PD-L1 status regarding the heterogeneity of the immune response in the tissue. Prospective assessment of PD-L1 expression status on infiltrating immune cells in metastatic urothelial carcinoma has been determined in multiple clinical trials. There is still controversy surrounding whether higher levels of PD-L1 expression by immune and/or tumor cells in the tumor microenvironment could be predictive of higher response rates to anti-PD-1/PD-L1 therapy. As indicated by the authors, this discrepancy between studies may be explained by the substantial variability in performance of anti-PD-L1 antibodies (SP142, SP243, 22C3, 28-8, 73-10), in platform specificities (Ventana, Dako), in cutoff definitions among assays, in type of cells analyzed (immune cells or tumor cells) and also in quality of tissue sample (formalin fixed, paraffin embedded vs fresh frozen).

Arguably future efforts are essential to harmonize and validate the use of anti-PD-L1 antibodies as a potential prognostic or predictive biomarker in urothelial carcinoma. Such efforts are currently ongoing in other tumor types (eg lung cancer) and should also be a central issue for uropathologists in the near future.

Respectfully,

Mathieu Rouanne, Thierry Lebret, Camélia Radulescu and Julien Adam
Departments of Urology and Pathology
Foch Hospital
University of Paris-Saclay
Suresnes
and INSERM Unit U981 and Department of Pathology
Institute Gustave Roussy
University of Paris-Saclay
Villejuif
France
e-mail: rouanne.mathieu@gmail.com

Poster presentations

- **American Society of Clinical Oncology Genito-Urinary Symposium ASCO-GU 2018**, San Francisco, CA, USA.

  Association of stromal lymphocyte infiltration with tumor invasion depth and high-grade T1 bladder cancer. Mathieu Rouanne, Reem Betari, Camélia Radulescu, Nicolas Signolle, Yves Allory, Aurelien Marabelle, Julien Adam, Thierry Lebret.

- **United States and Canadian Academy of Pathology (USCAP) 107th Annual Meetings 2018**, Vancouver, BC, Canada.

  Plasmocytoïd variant of bladder cancer: immune and molecular pathologic profiling. Myriam Kossai, Camelia Radulescu, Julien Adam, Nicolas Signolle, Mathilde Sibony, Yves Allory, Mathieu Rouanne.

- **13ème Journées Scientifiques de l'Ecole Docotorale de Cancérologie 2017,** Roscoff, France.

  Exploring the changing immune landscape in primary high-grade T1 bladder cancer. Mathieu Rouanne

Manuscripts in preparation

- **HLA-I downregulation together with epithelial-mesenchymal transition is a mechanism of tumor escape to intravesical BCG immunotherapy in non-muscle invasive bladder cancers.** *Original article*

  Mathieu Rouanne PhD results presented in this manuscript

- **Comparison of immune profiling by flow cytometry, immunohistochemistry and NanoString gene expression in urothelial carcinoma of the bladder.** *Original article*

  Mathieu Rouanne, Julien Adam, Camélia Radulescu, Nicolas Signolle, Séverine Mouraud, Thierry Lebret, Aurélien Marabelle.

- **Comparison of morphological TILs assessment, CD8 and CD3 immunohistochemical quantitative analysis in urothelial carcinoma of the bladder.** *Original article*

  Julien Adam, Audrey Perret, Camélia Radulescu, Nicolas Signolle, Yves Allory, Thierry Lebret, Aurélien Marabelle, Mathieu Rouanne.

- **Plasmocytoïd variant of bladder cancer: immune and molecular pathologic profiling.** *Original article*

  Myriam Kossai, Camelia Radulescu, Julien Adam, Nicolas Signolle, Mathilde Sibony, Yves Allory, Mathieu Rouanne.

- **Theranostic value of the immune contexture in urothelial cancers.**

  Review article

  Mathieu Rouanne, Anna Schneider, Julien Adam, Aurélien Marabelle.

- **Rationale and outcomes of neo-adjuvant immunotherapy in bladder cancer.**

  Invited review, European Urology Oncology

  Mathieu Rouanne, Thomas Powles.

Translational research projects

- **A pilot study to assess the concordance of genomic alterations between urine and tissue to develop precision medicine-based immunotherapy approaches in high-risk NMIBC patients.**

  Mathieu Rouanne (PI) ; Yves Allory (Scientific coordinator)

  Collaboration between Hôpital Foch & Institut Curie.

- **Exploring the changing genomic and immune landscape in high-risk NMIBC.**

  Mathieu Rouanne (PI) ; Aurélien Marabelle (co-PI)

  Collaboration between Hôpital Foch, Gustave Roussy & Columbia University.

- **Artificial Intelligence in bladder cancer: radiomics machine-learning signature for lymph node staging in urothelial carcinoma of the bladder.**

  Antoine Girard (PI) ; Mathieu Rouanne (co-PI) ; Laurent Dercle (Scientific coordinator)

  Collaboration between Hôpital Foch, Rennes CLCC & Columbia University.

Titre: Mécanismes de résistance au BCG dans le cancer de la vessie

Keywords: BCG ; instillations endo-vésicales ; carcinome urothélial de la vessie ; échappement tumoral

Le cancer de la vessie est le 9ème cancer le plus fréquent au monde avec 435 000 nouveaux cas diagnostiqués chaque année et 165 000 décès par an. Au diagnostic, 70-80% des cancers de la vessie sont tumeurs superficielles n'infiltrant pas le muscle vésical (TVNIM). Depuis près de 40 ans, les instillations intra-vésicales de bacille de Calmette-Guérin (BCG) sont le traitement de référence des TVNIM ayant un risque élevé de progression (T1, carcinome in situ, Ta haut grade). Malgré un traitement bien conduit, le risque de récidive est d'environ 50%, et le risque progression vers une tumeur infiltrant le muscle est estimé entre 20% et 30% dans les 5 ans. Entre 10% et 15% des patients développent des métastases de leur carcinome urothélial. Aujourd'hui, aucun biomarqueur ne permet de prédire la réponse au BCG, ni l'évolution métastatique de la maladie. La cystectomie totale reste le traitement de référence en cas de non-réponse au BCG. Plusieurs essais cliniques évaluent des traitements immuno-modulateurs ciblant les récepteurs des points de contrôle immunitaires PD1, PD-L1 en 2° ligne de traitement après échec du BCG. Les instillations endo-vésicales d'interferon de type I, de virus oncolytique ou d'agonistes de STING sont des stratégies thérapeutiques en cours d'évaluation. L'objectif de ce travail était d'étudier les mécanismes de résistance intrinsèque des cellules tumorales exposées au BCG afin d'identifier de nouvelles cibles thérapeutiques.

Title: Mechanisms of resistance to BCG immunotherapy in bladder cancer.

Keywords: BCG; intravesical instillations; urothelial carcinoma of the bladder; tumor escape

Bladder cancer is a heterogeneous disease that displays invasive and non-invasive histological features, and a wide spectrum of molecular alterations and subtypes. Treatment of non-invasive tumors with high-risk features (carcinoma in situ, high-grade Ta, T1) includes trans-urethral resection of the tumor, followed by intravesical instillations of bacillus Calmette-Guérin (BCG). Despite a multitude of evidence for anti-tumor efficacy, 50% of patients with high-risk NMIBC develop tumor recurrence and 20-30% disease progression. Ultimately, 10-15% of patients die of metastatic disease. New therapeutic strategies are currently in clinical development to treat BCG-unresponsive tumors including antagonistic antibodies directed against the T-cell immune checkpoints PD-1, PD-L1 and CTLA-4, but also recombinant adenovirus interferon α (Ad-IFNα/Syn3), oncolytic virus and STING agonists. Although recent studies have identified potential immune parameters that could impact clinical response, mechanisms of tumor resistance to BCG immunotherapy remain poorly understood. Additionally, tumor heterogeneity and plasticity of cancer cells undermine our attempts to precise dynamics of immune escape under selective pressure. How cancer cells evade to the anti-tumor immune response, and whether cancer cells acquire intrinsic undesirable characteristics upon BCG exposure remain unknown. Altogether, this highlights the crucial need to better understand the mechanisms of tumor resistance that occur during BCG immunotherapy in order to identify new targetable pathways and treatment strategies.